This is to certify that the
thesis entitled

BIOMECHANICAL RESPONSE OF TISSUES TO VARIOUS BLUNT IMPACT ORIENTATIONS ON THE KNEE

presented by

ERIC G. MEYER

has been accepted towards fulfillment
of the requirements for the

MS degree in ENGINEERING MECHANICS

Roger C Haut
Major Professor's Signature

08/03/04
Date

BIOMECHANICAL RESPONSE OF TISSUES TO VARIOUS BLUNT IMPACT ORIENTATIONS ON THE KNEE

By

Eric G. Meyer

A THESIS

Submitted to
Michigan State University
in partial fulfillment of the requirements
for the degree of

MASTER OF SCIENCE

Department of Mechanical Engineering

2004

ABSTRACT

BIOMECHANICAL RESPONSE OF TISSUES TO VARIOUS BLUNT IMPACT ORIENTATIONS ON THE KNEE

By: Eric G. Meyer

Osteoarthritis (OA) is a chronic degenerative joint disease affecting a large percentage of older people. Post-traumatic OA has been demonstrated to occur following a ligament injury or a single blunt impact to a diarthrodial joint. Lower extremity injuries are a frequent outcome from automotive accidents. The automotive knee injury criterion is based on data for bone fracture in cadaver experiments. The current study combines human cadaver data and a chronic post-traumatic animal model to investigate blunt impacts on the patello-femoral (PF) and tibio-femoral (TF) joints. In Chapter 2, the role of the impact direction on PF joint response was investigated. Many automotive occupants sit with their legs slightly abducted and this orientation can significantly reduce fracture tolerance and change the orientation of patella fractures. Chapter 3 documents that compressive load axially in the tibia on an unconstrained knee will cause the tibia to displace anteriorly with respect to the femur and produce ACL rupture. These data may demonstrate one mechanism for non-contact ACL injuries to occur. Chapter 4 investigates this effect further by documenting the effect an axial tibia load has on the stiffness response of the knee to an anterior knee impact. This combined loading scenario reduces the amount of shear displacement between the tibia and femur. Finally, Chapter 5 documents accelerated subchondral bone changes in rabbits at 12 weeks, following a single blunt impact of approximately 50% of the fracture force. The data presented in this thesis may be applicable to injury prediction and the development of a new knee for the anthropomorphic dummy used in automotive crashes.

ACKNOWLEDGEMENTS

I would like to thank my mentor Dr. Roger Haut for his expertise, leadership, support and dedication throughout my research at the Orthopeadic Biomechanics Laboratories (OBL). I would also like to acknowledge Dr. G. Thomas Mase and Dr. Thomas J. Pence for their excellence in teaching and for serving on my committee. I would also like to thank Clifford Becket, Jane Walsh and Jean Atkinson for their hard work, knowledge and willingness to help me. Finally, I would like to acknowledge everyone who worked along side me at OBL; Dan Phillips, Eric Clack, Steve Rundell, Micheal Sinnott, Eugene Kepich, Joanne Ewen, and Anthony Meram and to everyone involved in MSU's Chapter of the Biomedical Engineering Society for their help and friendship.

Most of all I would like to thank my wife, Susan Meyer and my parents, Kevin and Marcia Meyer for their unwavering love and support of me throughout my academic career and life.

TABLE OF CONTENTS

RESEARCH PUBLICATIONS

PEER REVIEWED MANUSCRIPTS

1. Meyer EG, Haut RC. The Effect of Knee Impact Angle on Tolerance to Rigid Impacts. Stapp Car Crash Conference (2003)
2. Meyer EG, Haut RC. Excessive Compression of the Human Tibio-Femoral Joint Causes ACL Rupture before Bone Fracture. Journal of Biomechanics (In Review)
3. Meyer EG, Sinnott MT, Jayaraman , Haut RC. The Effect of Biaxial Impact on the 90° Flexed Human Knee Joint Stability and Injury Tolerance. Stapp Car Crash Conference (In Preparation)
4. Kirsch J, Dejardin L, Meyer E, Decamp C, Haut R. Effect of Intramedullary Pin-plate Combination on the Mechanical Properties of Pantarsal Arthrodesis; A Comparitive in Vitro Analysis in Dogs. American Journal of Veterinary Research (In Press)
5. Von Pfeil D, Dejardin L, Meyer E, Weerts R, Decamp C, Haut R. Biomechanical Comparison of an Interlocking Nail and a Plate-Rod Combination; An in vitro analysis in a canine fracture model. American Journal of Veterinary Research (In Preparation)
6. Wertheimer S, Hansen M, Le L, Meyer E, Haut R. Comparison of 3.5 mm and 4.0 mm Cortical Syndesmotic Screw Pull Out Strength. (In Preparation)

PEER REVIEWED ABSTRACTS

1. Haut R, Jayaraman V, Sevensma E, Meyer E. Anterior Cruciate Ligament Rupture Due to Compression of the Human Tibiofemoral Joint. Orthopaedic Research Society (2003)
2. Kirsch J, Dejardin L, Meyer E, Decamp C, Haut R. Mechanical evaluation of canine pantarsal arthrodesis. American College of Veterinary Surgeons (2003)
3. Von Pfeil D, Dejardin L, Meyer E, Weerts R, Decamp C, Haut R. Biomechanical Comparison of an Interlocking Nail and a Plate-Rod Combination; An in vitro analysis in a canine fracture model. Veterinary Orthopedic Society (2004)
4. Meyer E, Meram A, Haut R. Single Mechanical Impact Produces Post-traumatic Bone Injury in Tissues of the Rabbit Knee. Orthopaedic Research Society (In Preparation)

LIST OF FIGURES

LIST OF TABLES

INTRODUCTION

Treatments for medical conditions have become increasingly sophisticated and powerful in the last century. These breakthroughs have increased life expectancy, quality of life and allow people to do things at increased age that never would have been possible a century ago. However, with increased age our population also becomes more susceptible to other health problems, especially arthritis, diabetes and cancer. The common thread among these diseases is that there currently is no cure. In fact, in many ways we do not even understand the basic science behind what causes these diseases or their progression.

Nearly 50% of Americans over the age of 65 have some form of arthritis (CDC Fact Sheets, 1997) with total costs of the disease approximately $80 billion per year. Osteoarthritis (OA), or degenerative joint disease, is the most common musculoskeletal disease and the most common form of arthritis affecting 20.7 million people in the USA alone (1999). From the patient's perspective this disease is characterized by diarthrodial joint pain and tenderness, loss of range of motion and localized inflammation around the affected joint. Since the main function of diarthroidial joints is to allow body movement and locomotion, this disease has grave consequences for a patient's quality of life. The most commonly affected diarthrodial joints are the knee (Figure 1.1), hip, shoulder and fingers. The knee and hip are both necessary for locomotion so OA often renders people unable to stand or walk without intense pain.

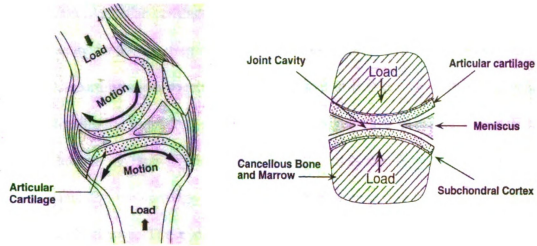

Figure 1.1. Anatomical features of diarthrodial joints such as the knee.

Diarthrodial joints allow movement by transferring forces between muscles and bones with very little friction, while also providing cushioning and distributing the forces over larger areas. Articular cartilage (AC) is a soft, near frictionless material that covers the ends of bones in diarthrodial joints and accomplishes these functions. This material is a form of connective tissue and is primarily composed of cells (chondrocytes), fiberous matrix (collagen), a ground substance (proteoglycans) and interstitial fluid (mostly water). The solid phase (chondrocytes, collagen and proteoglycans) accounts for 15-30 % of the wet weight of AC. The remaining 70-85% of the weight is water that pressurizes the cartilage. Proteoglycans have a negative charge that attracts electrolyte ions, this creates an osmotic gradient between the intercellular and the extracellular fluid. Collage fibers provide the structural support for the surface tension that is developed by the pressurized cartilage. As the cartilage is loaded and compressed during normal activities, fluid is squeezed out, similar to squeezing a sponge. There is a frictional component to this fluid flow that helps the cartilage respond appropriately depending on the level of

compression. Articular cartilage is nonvascular (no blood supply), so the fluid flow is also important for transporting nutrients and waste products into and out of the cartilage.

Osteoarthritis is a degenerative disease that affects the cartilage and subchondral bone of diarthrodial joints. It is characterized by irregular loss of cartilage in areas of high load, sclerosis of subchondral bone (SB), subchondral cysts and osteophytes. Biomechanically, the cartilage material properties, such as the tensile, compressive and shear moduli change. The hydraulic permeability of the cartilage also changes due to degradation of the collagen, causing increased water content and excessive swelling. Additionally, the SB thickness and stiffness change as it undergoes remodeling due to changing stress levels. The progression of this disease involves chronic fragmentation of the cartilage surfaces and remodeling of SB. Clinical diagnosis of osteoarthritis comes only when a significant reduction of the joint space is seen radiographically (Figure 1.2) (Hamerman, 1989), although MRI is proving to be a useful tool in diagnosing OA at an earlier point (Hodgson et al 1992).

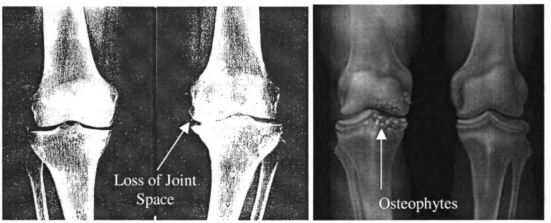

Figure 1.2. Radiographic diagnosis of OA by loss of joint space. Loss of joint space is due to wearing away of the AC and typically associated with osteopyhtes of the bone.

The initiation and progression of OA are not fully understood. In many patients the disease is due to a lifetime of high stresses in a particular joint from an occupation or recreational activity (Dieppe et al 1992). A significantly higher percentage of patients with ligament tears or sprains go on to develop OA as a result of the change in the way forces are transferred through the joint after an injury. There is also the possibility of a single mechanical insult initiating the disease process, especially if there is bone fracture or soft tissue damage near the articulating surfaces (Chapchal et al. 1978, Davis et al. 1989, Nagel et al. 1976, Volpin et al. 1990). Association between end stage OA from one particular cause have been difficult due to the long incubation time before chronic changes occur and radiographic evidence appears, typically at least 10-20 years (Wright 1990).

There are two theories for how OA initiation and progression occur (Figure 1.3). The first is that fissures and damage of the AC occur due to a mechanical insult thus changing the material properties and its ability to adequately absorb and transmit loads. This changes the stresses seen by the SB and initiates bone remodeling. The remodeled SB has increased stiffness that damages the overlying cartilage and the cycle continues. The other theory involves a similar cycle, except the mechanical insult causes trauma initially to the SB in the form of occult microcracks or "bone bruises". These cracks initiate remodeling of the SB, which in turn damages the AC by increasing the stresses seen in the overlying tissue, and the chronic degradation cycle begins (Vellet et al. 1991).

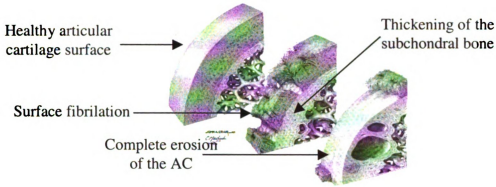

Figure 1.3. Osteoarthritis disease progression from healthy to end stage.

Since this process is still not clearly understood there is a lot of research currently under way in this area. Many investigators are focusing on new ways of diagnosing degenerative joint disease earlier, while others are looking for possible treatments or interventions for patients that are already in the degenerative cycle. There is also a group of researchers investigating causes, such as a single blunt impact, and ways of preventing these injuries in the first place.

Knee Anatomy

The knee is a synovial joint in the leg where three bones, the femur, tibia and patella, meet (Figure 1.4). The femur and tibia are two long bones in constant contact that rotate relative to each other (similar to a hinge) in order to produce knee flexion. The femur has two articulating surfaces, the medial and lateral condyles that are in contact with the medial and lateral tibial plateaus. The patella, or kneecap, is a sesamoid bone that rests on the anterior articulating surface of the femur to protect the knee and act as a lever for transferring muscle forces between the upper and lower leg.

The knee has two fibrocartilage pads, the medial and lateral menisci between the femur and tibia, in addition to the AC on each bone's articulating surface. There is a fibrous capsule of many ligaments and tendons that hold the joint together, as well as

keep the synovial fluid in a "closed system". The knee joint is made up of medial and lateral collateral ligaments and the patellar ligament and quadriceps tendon that support the patella. The anterior cruciate ligament (ACL) and posterior cruciate ligament (PCL) are two ligaments on the interior of the knee joint that prevent anterior and posterior motion of the tibia relative to the femur.

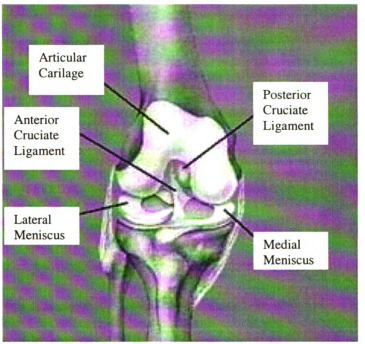

Figure 1.4. Anatomical structures of the knee.

The major muscle groups that produce knee flexion and extension are the hamstrings and quadriceps, respectively (Figure 1.5). The hamstrings are really four individual muscles that originate along the edges of the pelvis and insert at the tibia/fibula. The quadriceps also encompasses four muscles that originate on the pelvic girdle and insert into the patella and reach the tibial tuberocity via the patellar ligament. Muscle force plays an important role in the stability of the knee by assisting the knee ligaments in constraining the joint.

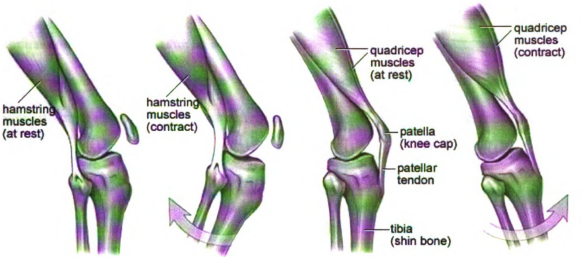

Figure 1.5. Knee muscle groups and their motion effect.

Knee Injuries

In addition to OA, the knee is susceptible to many other acute injuries caused by blunt impact from a fall, an automotive accident, sports or work related circumstances, or any number of other possibilities. High severity injuries include gross bone fracture and ligament trauma such as sprains, dislocation, rupture or avulsion. Two types of acute injury scenarios will be investigated in the current study; automotive accidents primarily producing bone fracture and sports related ligament injuries. The most common injuries from frontal automotive crashes are patellar or femoral fractures, while the most common sports injury is an ACL tear.

Automotive Trauma Literature Review

Automobile accident injuries are the cause of a significant percentage of societal cost from medical spending, lost workdays and reduced quality of life. In the United States alone 3.2% of annual medical costs are for injuries that result from motor vehicle

collisions, second only to cancer (Miller et al. 1998). Another study estimates these annual costs at $21.5 billion (Miller et al. 1995).

Lower extremity injuries can be the cause of permanent disability and impairment (States 1986), and are a frequent outcome of automotive accidents (Fildes et al. 1997). These injuries have been shown to comprise a significant percentage of the costs associated with motor vehicle trauma. MacKenzie et al. (1988) document that 40% of the automotive trauma costs in Maryland are from lower extremity injuries. Luchter and Walz (1995) find that 27.8% of the injuries in the 1993 National Accident Sampling System (NASS) database are for the lower extremity, making it the most frequently injured body region.

Many studies show the most commonly injured lower extremity region is the knee (Hartemann et al. 1977 and Bourrett et al. 1977, Fildes et al. 1997 Atkinson and Atkinson 2000). Atkinson and Atkinson (2000) document that for the years 1979-1995 approximately 25% of all injuries recorded in the NASS database are to the lower extremity and 10% are knee injuries. The knee injury rates remain relatively constant over this period even with the addition of mandatory seat belt laws and airbags. Most of these knee injuries are rated Abbreviated Injury Scale (AIS) 1 (Fildes et al. 1997 and Atkinson and Atkinson 2000), but even these "mild" injuries have significant costs associated with them, between approximately $1,400 and $2,500 per injury (Hendrie et al. 1994 and Miller et al. 1995). For more serious knee injuries (AIS 2-4), fracture is the most common, however sprains, ligament avulsions and ruptures, contusions and dislocations are also documented. These more serious knee injuries result in 40 or more lost workdays, 40-50% of the time, however may not have been the only injury sustained.

Patella fractures are shown to be the most common knee injury rated AIS 2-3 with femur fractures occurring slightly less frequently (Atkinson and Atkinson 2000). In the years 1993-1995 these fractures account for 2.4 and 2.2, out of every 1000 injuries respectively. Together with tibial plateau fractures they account for between 25-50% of all knee injuries. Tendon and ligament injuries combined accounted for approximately 25% of all knee injuries.

Knee fractures occur in accidents with a change of velocity of less than 45 kmph 90% of the time and with zero intrusion 61% of the time (Fildes 1997). Fractures were due to contact with the steering column or instrument panel in most cases. Nagel and States (1977) suggest major injury to the knee does not occur when the knee contacts smoothly contoured sheet metal, only rigid structures. Deformable knee bolsters have been commonly used in recent model cars, but are not standardized or regulated. Additionally, it has been shown that even with a deformable interface that protects against gross bone fracture there is still the possibility of causing microscopic damage to the subchondral bone (Atkinson and Haut 2001). These "bone bruises" have been shown to occur at much lower loads than knee fracture. Since most knee injuries occur to people 11-40 years old there is plenty of time for a chronic disease to progress as a result of these microfractures.

Fracture Experiments

The earliest biomechanical impact studies on the knee were for seated fresh and embalmed cadavers with either sled (Figure 1.6) or pendulum drop impactors (Patrick et al. 1965, Powell et al. 1975 and Cooke and Nagel 1991) or a pneumatic cylinder (Melvin et al. 1975). These studies used rigid and padded interfaces on 90° flexed knees and

documented fractures for a wide range of loads between approximately 7.3 kN and 21.0 kN. Rigid impactors result in transverse fractures of the patella, split fractures of the femoral condyles, and mid-femoral shaft fractures in 84%, 44%, and 25% of cases, respectively. Padding reduces fracture to the patella by 65%, to the femoral condyles

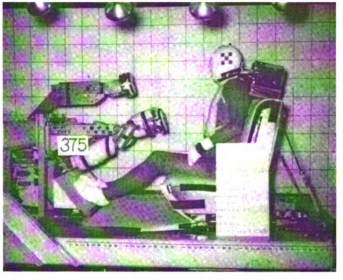

Figure 1.6. Cadaver sled test producing blunt impact to the knee (Patrick et al. 1975).

by 14%, and to the femoral shaft by 6% (Viano et al., 1980). Additional data was collected in the Melvin et al. and Powell et al. studies from strain gages attached to the femoral shaft. The bending moments in the femur were recorded during axial and off-axis impacts to the knee. These studies serve as the basis for the current automotive knee injury criterion of 10 kN in the femur during a 30 mph full frontal crash into a rigid barrier. However, in the time since these first studies were reported there has been more information collected about knee fracture mechanisms with a wide range of variables.

Recent studies have used isolated fresh human cadaver knees to investigate many of the factors important in predicting knee fracture (Figure 1.7). These experiments document many of the details that were overlooked by the preliminary knee impact studies.

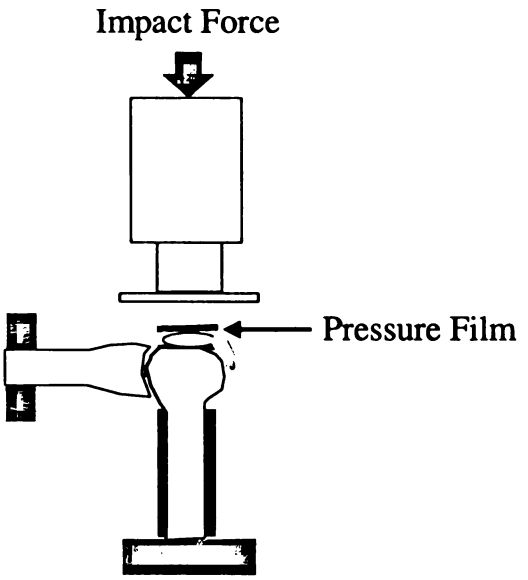

Figure 1.7. Isolated knee impact of the patello-femoral joint.

Impacts have typically been applied in one of two directions, either aligned with the axis of the femur or aligned with the axis of the tibia. Impacts along the axis of the femur mainly affect the patello-femoral (PF) joint, but depending on the contact area may also cause shear loading of the tibia with respect to the femur. These impacts simulate the knee impacting the dashboard or knee bolster in an automotive accident. Tibia axis impacts affect the tibio-femoral (TF) joint and are meant to simulate intrusion of the floor-pan applying a force through the ankle up into the knee.

Recent rigid impacts studies for the PF joint at 90° flexion have shown the force required for fracture to be between 4.5 and 8.5 kN (Table 1.1). This research is mostly on aged cadavers, due to availability constraints, but is comparable to many studies that are also used aged cadavers. A study by Atkinson et al. (1997) documents a significant relationship between the geometry of the cartilage surface and the peak load at fracture. As the area of cartilage decreased relative to the area of bone there was a significant decrease in the peak load at fracture. They did not find any significant trends between

peak load and age, sex, height or weight. Other studies, on the other hand, document that the strength of cortical bone decreases with specimen age (Burstein et al. 1976, Yamada 1970).

Study	Peak Load (kN)	Number of Specimens	Injuries			Age (yrs.)	Time to Peak (ms)
			Pat Fx	Fem Fx	Occult		
Atkinson and Haut, 2001a	4.7 (1.6)	6	6	0	5	69 (12)	4.7 (1.6)
Atkinson and Haut, 2001b	5.5 (1.8)	6	6	0	5	-	3.4 (1.1)
Ewers et al., 2000	4.6 (1.0)	6	3	0	4	75 (13)	4.9 (0.9)
	4.5 (1.2)	6	1	0	3	75 (13)	54 (3)
Atkinson et al., 1997	5.0 (1.5)	6	3	1	4	65 (12)	4.1 (0.5)
Haut and Atkinson, 1995	6.7 (2.1)	10	8	1	3	77 (7)	5
	6.7 (1.7)	10	7	2	5	48 (9)	5
Haut, 1989	8.5 (3.0)	8	4	4	-	72 (11)	9.4 (1.2)
Powell et al., 1975	11.2 (2.4)	4	4	0	-	58 (14)	-
Melvin et al., 1975	19.9 (3.3)	3	3*	-	-	65 (14)	4.7 (1.9)

Table 1.1. Previous results for rigid impacts to the PF joint in a 90° flexed knee.

Atkinson and Haut (2001a) investigated the effect of knee flexion angle on patello-femoral impacts (Table 1.2). They documented an increase in fracture tolerance with increasing flexion angle. Impacts at knee flexion of 60° resulted in patella fracture at a peak load of 2.9 kN, while 120° flexion impacts resulted in femur and patella fracture at a significantly different load of 6.4 kN (Table 1.2). This study also found that the location of the injuries changed depending on flexion angle. Impacts at 60° flexion caused injuries located near the distal edge of the patella, while 90° flexion injuries were located centrally on the patella and 120° injuries were near the proximal edge of the patella.

Another study by Atkinson and Haut (2001b) investigated the role of impact interface on fracture load with a range of flexion angles. Rigid and deformable (3.3 MPa crush strength honeycomb material) interfaces were used on paired specimens. Generally, the deformable interfaces increased the peak load for fracture. However, this effect was only statistically significant at 120° flexion. This study verified the results of the previous

flexion angle study by also documenting a significant increase in fracture tolerance with increased flexion angle. Other studies have also investigated the effect of deformable interfaces on fracture load (Atkinson et al., 1997, Hayashi et al., 1996). They also show that significant increases in fracture load can be achieved with a deformable interface and document a relationship between the stiffness of the interfaces and peak load at fracture. To protect the knee against fracture the stiffness interface was suggested by Hayashi et al. (1996) to have ultimate crush strength of approximately 90 psi.

Knee Flexion Angle (deg)	Peak Load (N)	Fem Fx.	Pat Fx.	Tib Fx.	Horz. OC	Vert OC	Cart Fiss
60 Rigid (2001a)	2.9 (0.9)	0	6	0	2	5	4
90 Rigid (2001a)	4.7 (1.6)	0	6	0	3	5	3
120 Rigid (2001a)	6.4 (1.9)	2	4	0	2	5	1
60 Sub Fx. Rigid (2001a)	2.4 (0.9)	0	3	0	2	2	5
90 Sub Fx. Rigid (2001a)	3.8 (1.5)	0	2	0	2	4	3
120 Sub Fx. Rigid (2001a)	5.4 (1.7)	0	0	0	2	3	4
60 Rigid (2001b)	4.3 (0.9)	0	6	0	1	4	3
90 Rigid (2001b)	5.5 (1.8)	0	6	0	1	5	1
120 Rigid (2001b)	5.8 (1.4)	3	3	2	1	1	3
60 Deform (2001b)	3.7 (2.0)	0	2	0	2	2	4
90 Deform (2001b)	5.0 (1.4)	0	1	0	1	5	2
120 Deform (2001b)	8.3 (1.2)	2	0	0	2	2	0

Table 1.2. Previous injury results from PF impacts at various knee flexion angles with rigid and deformable interfaces.

Many recent studies on the PF joint during blunt knee impact have used pressure film to document the contact and load distributions (Atkinson and Haut, 2001; Atkinson and Haut, 2001; Ewers et al., 2000; Atkinson et al., 1997; Atkinson and Haut, 1995; Haut, 1989). Atkinson and Haut (1995) document that the average pressures and contact areas on the interior surfaces of the knee are slightly higher on the lateral versus the medial patellar facet. The contact area is highest at 90° knee flexion (Atkinson and Haut, 2001 and Atkinson and Haut, 2001). Other studies also document that the patello-femoral

contact pressures and areas are reduced with addition of a padded interface (Haut, 1989; Atkinson et al., 1997; Atkinson and Haut 2001).

Viano et al. (1978) investigated the effect of loading the knee through different anatomical regions. Frontal impacts were applied to the knee (including the patella and tibial tuberocity) and the tibia (near and below the tibial tuberocity) (Figure 1.8). The authors document PCL rupture and avulsion for knee impacts at approximately 7 kN of load. Tibial impacts produce fractures of the tibia and fibula at approximately 5 kN. Additional experiments on isolated knee joints in the Viano et al. study showed that PCL rupture occurs at approximately 2.25 cm of posterior tibial displacement and approximately 2.5 kN of load.

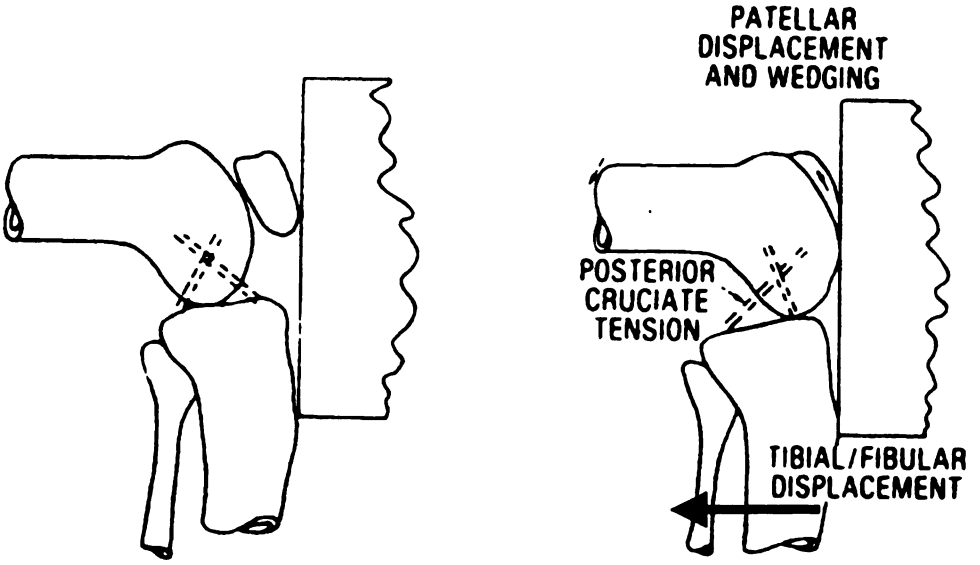

Figure 1.8. Frontal impact to a human knee joint flexed 90° (Viano 1978).

The effect of an axial tibia load has recently been studied using two impact protocols. Constrained experiments on the TF joint do not allow anterior-posterior (AP) or medial-lateral (ML) motion of the tibia with respect to the femur. These experiments result in fracture to the medial and lateral tibial plateau, medial femoral condyle and

femoral notch at 8.0 ±1.8 kN (Banglmaier et al. 1999). Other previous studies (Hirsch and Sullivan, 1965 and Kennedy and Baily, 1968) also constrained the TF joint and document a similar mean fracture load of approximately 8 kN. Recently a study by Jayaraman et al. (2001) documents the effect of TF joint constraint on knees at various flexion angles (60-120°). An interesting result occurred for unconstrained knees at all flexion angles, instead of bone fracture 14 of 16 knees failed by ACL ruptures. The authors hypothesize that this result was due to an inherent tilt of 8-15° in the tibial plateau (Figure 1.9). ACL rupture occurs at a load of 4.9 ± 2.1 kN which is statistically less than the load to cause fracture of bone in the constrained knees. The study also documents that during unconstrained TF compression the femur moves medially with respect to the tibia and the tibia rotates internally. Additionally for constrained joints the load to prevent motion of the femur relative to the tibia is 1.2 ±0.5 kN. This may be the tensile load in the PCL prior to rupture in unconstrained experiments.

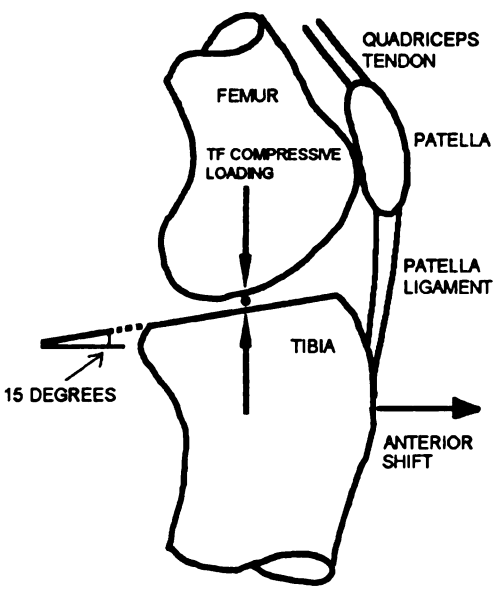

Figure 1.9. Tilt of the tibial plateau and resultant anterior displacement of the tibia.

These investigations have led to the following generalizations to predict traumatic injury to the knee. Axial femoral loading through the patella will most often produce patella fracture at approximately 6 kN for rigid impacts. However for padded impacts the load tolerance increases and the most commonly injured site is the femoral condyle (Atkinson 1997). Axial loading of the tibia will produce fracture in the medial and lateral tibial plateau, femoral condyle and femoral notch at approximately 8 kN, when the femur is constrained from translating relative to the tibia. For unconstrained tibio-femoral loading the most common injury is mid-substance tear of the ACL at approximately 6 kN. Shear loading of 2.5 kN between the tibia and femur results in PCL tears or avulsions at approximately 2.25 cm of relative displacement.

Knee fracture is easily documented during experiments and by clinicians after real world automotive accidents. Therefore a knee injury criterion based on fracture is the most obvious choice. However, many of these fracture studies also document other injuries that are not as obvious as gross fracture. Additionally, lower extremity trauma causes acute pain followed by a chronic disease process that can lead to an end-stage disease such as osteoarthritis (States 1986). Subtle damage to cartilage and subchondral bone can occur without radiographic evidence of bone fracture (Pritsch et al. 1984). Recent studies have focused on identifying occult bone trauma (Figure 1.10) and relating it to clinical findings. These radiographically occult injuries to the bone, otherwise referred to as occult fractures or bone bruises, may account for patient pain (Kapelov 1993). However, a direct association between mechanical insult and disease has been difficult because visible evidence of the disease may not show up for years (Wright 1990).

Figure 1.10. Bone bruise in the lateral femoral condyle.

Subfracture Experiments

Biomechanical impact studies, attempting to document subfracture injuries, have not had the luxury of being able to rely on human cadaver experiments. Since the nature of many of these injuries is their chronic progression, it is necessary to use an *in vivo* animal model that can document these long-term changes. This animal data must then be combined with human cadaver experiments to create useful information about automotive tolerances to chronic disease. Additional problems arise because of the controversy over the mechanisms of the chronic disease process. Recent studies have shown that impact can cause damage to both the cartilage and bone without gross fracture. Long-term studies with a rabbit model have further shown decreasing mechanical properties of cartilage and increased thickness of the subchondral bone over time (Newberry et al. 1996, Ewers et al. 2000). These studies have gone on to explore ways that the rate of disease progression is increased or decreased, by exercise or pharmaceutical treatment, so that early diagnosis of the initial injuries could prevent or delay an end-stage disease.

Histological methods are a common way of documenting subfracture injuries such as occult bone microcracking and cartilage fissuring (Figure 1.11). These studies use semi-quantitative scoring to analyze the condition of tissue as a result of impact and chronic degradation. Occult injuries such as subchondral bone microcracks are documented in a number of impact studies with and without gross fracture of bone (Ewers et al., 2000; Newberry and Haut, 1996; Haut and Atkinson, 1995). High rate impacts cause more microcracks than low rate impacts (Ewers et al., 2000). This microcracking is hypothesized to cause chronic subchondral bone thickening and remodeling post impact.

Cartilage fissures have been documented as a result from blunt impact. The number of fissures and their depth are related to the applied impact load. They have also been shown to increase over time post impact in a rabbit model (Haut 1989). Haut documents that at fracture up to 60% of the patello-femoral contact area exceeds 25 MPa. This level of pressure was previously shown to cause cartilage fissures in an *in vitro* explant model (Repo and Finlay 1977).

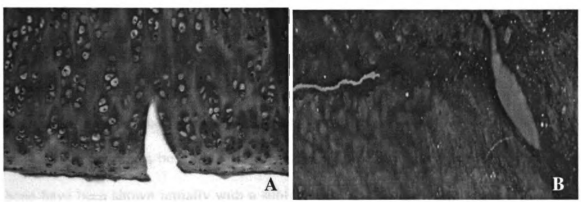

Figure 1.11. Surface fissure of the AC (A) and an occult microcrack at the tidemark (B).

The mechanical properties of cartilage have also been documented through the use of indentation testing with a cylindrical indenter (Figure 1.12). The instantaneous

(Gu) and relaxed (Gr) shear moduli are obtained from this method. Recent studies have shown that within 12 months post impact cartilage undergoes significant mechanical softening (Newberry et al. 1997, Ewers et al. 2000).

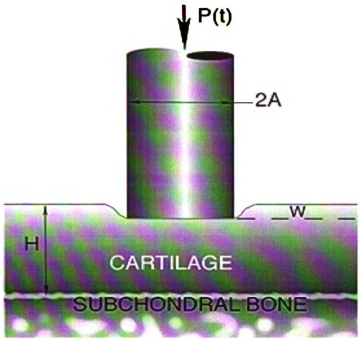

Figure 1.12. Indentation test to measure the mechanical properties of cartilage.

These investigations have led to the following generalizations about subfracture injuries. Impacts on human knees can result in occult microcracks of the subchondral bone before gross bone fracture. These microcracks may be precursors to gross bone fracture since they occur in the same regions where fractures typically occur. Deformable interfaces protect against gross fracture but microfractures still occur for stiffer interfaces. In animal experiments both fissures of the cartilage and microcracks of the underlying bone have been shown initially with a subfracture impact. At one year the stiffness and mechanical properties of the cartilage decrease and the subchondral bone thickness increases.

References

Atkinson PJ, Haut RC. (1995) Subfracture insult to the human cadaver patellofemoral joint produces occult injury. J Orthop Res 13: 936-944.

Atkinson PJ, Garcia JJ, Altiero NJ, Haut RC. (1997) The Influence of Impact Interface on Human Knee Injury: Implications for Instrument Panel Design and the Lower Extremity Injury Criterion, Stapp Conf Proc 41: 167-180.

Atkinson T, Atkinson P. (2000) Knee injuries in motor vehicle collisions: A study of the National Accident Sampling System database for the years 1979-1995. Accid Anal Prev 32 (6): 786.

Atkinson P, Haut R.C. (2001a) Impact responses of the flexed human knee using a deformable impact interface. J Biomech Egr 123 (3): 205-211.

Atkinson PJ, Haut RC. (2001b) Injuries produced by blunt trauma to the human patellofemoral joint vary with flexion angle of the knee. J Orthop Res 19(5): 827-833.

Banglmaier R, Dvoracek-Driksna D, Oniang'o T, Haut R. Axial compressive load response of the 90° flexed human tibiofemoral joint. Stapp Conf Proc 42: 127-140.

Bourrett P, Corbelli S, Cavallero C. (1977) Injury Agents and Impact Mechanisms in Frontal Crashes in about 350 Field Accidents. Stapp Conf Proc 21: 215-258.

Chapchal G. (1978) Posttraumatic Osteoartritis After Injury of the Knee and Hip Joint. Reconstr Surg Trauma 16: 87-94.

Cooke FW, Nagel DA. (1991) Biomechanical Analysis of Knee Impact. Stapp Conf Proc 13: 117-133.

Davis M, Ettinger W, Neuhaus J, Cho S, Hauck W. (1989) The Association of Knee Injury and Obesity with Unilateral and Bilateral Osteoarthritis of the Knee. Am J Epidemiology 130: 278-288.

Dieppe P, Cushnaghan J, McAlindon T. (1992) Epidemiology, Clinical Course and Outcome of Knee Osteoarthritis. *Articular Cart and Osteoarthritis* Raven Press Ltd, NY: 617-627.

Ewers BJ, Jayaraman V, Banglmaier R, Haut R. (2000) The effect of loading rate on the degree of acute injury and chronic conditions in the knee after blunt impact. Stapp Conf Proc 44: 299-314.

Fildes B, Lane L, Vulcan P, Seyer K. (1997) Lower Limb Injuries to Passenger Car Occupants. Accid Anal Prev 29: 789-795.

Hartemann F, Thomas C, Henry C, Foret-Bruno JY, Faverjon G, Tarriere C, Got C, Patel A. (1977) Belted or Not Belted: The Only Difference Between Two Matched Samples of 200 Car Occupants. Stapp Conf Proc 21: 97-150.

Haut RC. (1989) Contact Pressures in the Patello-Femoral Joint During Impact Loading on the Human Flexed Knee. J Orthop Res 7: 272-280.

Haut RC, Atkinson PJ. (1995) Insult to the Human Cadaver Patello-Femoral Joint: Effects of Age on Fracture Tolerance and Occult Injury. Stapp Car Crash J 39: 281-294.

Hayashi S, Choi HY, Levin RS, Yang KH, King AI. (1996) Experimental and Analytical Study of Knee Fracture Mechanisms in a Frontal Knee Impact. Stapp Car Crash J 40: 160-171.

Hendrie D, Rosman D, Harris A. (1994) Hospital inpatient costs resulting from road crashes in Western Australia. Aust J Public Health 18: 380–388.

Hirsch G, Sullivan L. (1965) Experimental Knee Joint Fractures. Acta Orthop Scand 36: 391-399.

Hodgson RJ, Carpenter TA, Hall LD. (1992) Magnetic Resonance Imaging of Osteoarthritis. *Articular Cart and Osteoarthritis* Raven Press Ltd, NY: 629-667.

Jayaraman VM, Sevensma ET, Kitagawa M, Haut RC. (2001) Effects of Anterior-Posterior Constraint on Injury Patterns in the Human Knee During Tibial-Femoral Joint Loading from Axial Forces Through the Tibia. Stapp Car Crash J 45: 449-468.

Kapelov R, Teresi L, Bradley WG, Bucciarelli NR, Murakami DM, Mullin WJ, Jordan JE. (1993) Bone Contusions of the Knee; Increased Lesion Detection with Fast Spin-echo MR Imaging with Spectroscope Fat Saturation. Radiology 189: 901-904.

Kennedy, J.C., Bailey, W.H., 1968. Experimental tibial-plateau fractures: studies of the mechanism and a classification. J Bone Jt Surg 50(A): 1522-1534.

Luchter S, Walz MC. (1995) Long-term Consequences of Head Injury. J Neurotrauma 12: 281-298.

MacKenzie E, Siegel J, Shapiro S. (1988) Functional Recovery and Medical Costs of Trauma: An Analysis by Type and Severity of Injury. J Trauma 28: 281-298.

Melvin J, Stalnaker R, Alem N, Benson J, Mohan D. (1975) Impact response and tolerance of the lower extremities. Stapp Conf Proc 19: 543-559.

Miller TR, Martin PG, Crandell JR. (1995) Cost of Lower Limb Injuries in Highway Crashes. Proc ICPLEI: 47-57.

Miller M, Osborne J, Gordon W, Hinkin D, Brinker M. (1998) The Natural History of Bone Bruises: A Prospective Study of Magnetic Resonance Imaging: Detected Trabecular Microfractures in Patients with Isolated Medial Collateral Ligament Injuries. Am J Sports Med 26: 15-19.

Nagel D, States J. (1977) Dashboard and bumper knee-will arthritis develop? AAAM 21: 272-278.

Newberry WN, Haut RC. (1996) The Effects of Subfracture Impact Loading on the Patello-Femoral Joint in a Rabbit Model. Stapp Car Crash J 40: 149-159.

Patrick L, Kroell C, Mertz H. (1965) Forces on the human body in simulated crashes. Stapp Conf Proc 9: 237-259.

Powell W, Ojala S, Advani S, Martin R. (1975) Cadaver femur responses to longitudinal impacts. Stapp Conf Proc 19: 561-579.

Pritsch M, Comba D, Frank G, Horoszowski H. (1984) Articular Cartilage Fractures of the Knee. J Sports Med 24: 299-302.

Repo R, Finlay J, (1977) Survival of Articular Cartilage After Controlled Impact. J Bone Jt Surg 59A: 1068-1076.

States JD. (1986) Adult Occupant Injuries of the Lower Limb. Proc Symp Biomech: 97-107.

Viano DC, Culver CC, Haut RC, Melvin JW, Bender M, Culver RH, Levine RS. (1978) Bolster Impacts to the Knee and Tibia of Human Cadavers and an Anthropomorphic Dummy. Stapp Conf Proc 22: 403-428.

Viano DC, Stalnaker RL. (1980) Mechanisms of Femoral Fracture. J Biomech 13: 701-715.

Vellet AD, Marks PH, Fowler PJ, Munro TG. (1991) Occult Post-Traumatic Osteochondral Lesions of the Knee: Prevalence, Classification and Short-term Sequelae Evaluated with MR Imaging. Radiology 178: 271-276.

Volpin G, Dowd G, Stein H, Bently G. (1990) Degenerative Arthritis After Intra-articular Fractures of the Knee: Long Term Results. J Bone Jt Surg 72: 634-638.

Wright V. (1990) Post-traumatic osteoarthritis- A medico-legal minefield. J Rheum 29: 474-478.

CHAPTER TWO

THE EFFECT OF IMPACT ANGLE ON KNEE TOLERENCE TO RIGID IMPACTS

ABSTRACT

While the number of deaths from vehicle accidents is declining, probably because of mandatory seat belt laws and air bags, a high frequency of lower extremity injuries from frontal crashes still occurs. For the years 1979-1995 the National Accident Sampling System (NASS) indicates that knee injuries (AIS 1-4) occur in approximately 10% of cases. Patella and femur fractures are the most frequent knee injuries. Current literature suggests that knee fractures occur in seated cadavers for knee impact forces of 7.3 to 21.0 kN. Experimental data shown in a study by Melvin et al. (1975) further suggests that fracture tolerance of the knee may be reduced for an impact directed obliquely to the axis of the femur. The current study hypothesized that the patella is more vulnerable to fracture from an oblique versus an axial impact (directed along the femoral axis), and that the fracture pattern would vary with impact direction. Isolated, 90° flexed, paired human knee joints (73 ± 16.9 years) were impacted at sequentially higher loads either axially or obliquely from the medial aspect with a rigid interface on the patella. The peak load at fracture for each case was recorded, and a detailed description of the fracture pattern was documented. For axial impacts all nine knees failed by linear and comminuted patella fracture with an average peak load of 5.9 ± 1.4 kN. Seven of nine obliquely impacted knees also failed by linear and comminuted patella fracture with a significantly lower peak load of 3.5 ± 1.4 kN. The peak load data from fracture experiments for all knees showed a strong correlation with age and direction of the

impact. Additionally, the fracture pattern for the axial impacts was generally oriented along a horizontal plane on the patella, while the fractures for oblique impacts were generally oriented along a vertical plane. In two oblique experiments patella fracture did not occur, as the patella dislocated at a load of 3.4 ± 0.2 kN. In one of these cases the medial aspect of the patello-femoral joint capsule was visibly torn, and in the other case surface damage was noted on the articular cartilage covering the lateral femoral condyle. In addition to the acute injuries described in this study, these data may suggest a potential for chronic diseases of the knee in cases where similar injuries are produced. Clinical studies have shown an increased risk of osteoarthritis in patients suffering patella fractures and damage to joint cartilage. Also, acute dislocation of the patella may cause soft tissue injury of the knee leading to chronic mal-tracking of the patella. These data may be particularly relevant in cases where occupants sit with abducted lower limbs prior to a frontal crash.

INTRODUCTION

Traumatic injury is the third leading cause of death in the U.S. Only heart disease and cancer exceed the frequency of traumatic death each year [Rice et al., 1989]. Motor vehicle injuries rank second to cancer in total societal cost, accounting for 3.2% of annual medical costs in the U.S. [Miller et al., 1998]. Overall, while the number of deaths from vehicle accidents is declining, probably because of mandatory seat belt laws and air bags, a high frequency of lower extremity injuries still occurs [Dischinger et al., 1992]. A recent study of the 1979-1995 National Accident Sampling System (NASS) indicates that knee injuries constitute approximately 10% of all injuries (AIS, abbreviated injury scale, 1-4) recorded each year in frontal crashes [Atkinson & Atkinson, 2000]. This study further suggests that the knee impact scenario for the years 1979-1995 remained relatively constant, as the knee injury rates showed little variation from year to year. For the years 1993-1995 approximately 26% of the total knee injuries were categorized as AIS 2 or 3 type injuries (bone fracture and severe soft tissue trauma). Additionally these more descriptive knee injury codes show that patella and femur fractures are the most frequent injuries.

The automotive trauma literature suggests that femur force does a good job separating human cadaver injury from non-injury of the knee-thigh-hip for axial (directed along the axis of the femur) impacts onto the knee [Morgan et al., 1990]. Early experiments using seated unembalmed human cadavers document the blunt impact response of the knee-thigh-hip complex using rigid and lightly padded interfaces. These studies show that the fracture force ranges from approximately 7.3 kN to approximately

21.0 kN [Melvin et al., 1975; Patrick et al., 1965; Powell et al., 1975]. A large percentage of the fractures represented in this database occur in the supracondylar region of the femur or in the patella. Recent experiments, using the isolated knee joint preparation, also document supracondylar femur fractures and patella fractures following repetitive, axial impact loads on the anterior surface of the patella with rigid impact interfaces [Atkinson & Haut, 2001b]. In these studies loads producing bone fracture range from 4.3 to 5.8 kN for the isolated human knee joint flexed 60, 90 or 120 degrees (angle between femur and tibia, where 180° refers to a straight, fully extended leg). For each flexion angle of the knee the study documents horizontal (a medial-lateral oriented fracture plane) fractures of the patella. In a few cases comminuted patella fractures are also noted with 90 and 120 degrees of knee flexion. As was typical in the 1970's studies that established impact tolerance forces for the human knee-thigh-hip during axial blunt impact to the knee, the Atkinson et al. study was conducted with aged cadaver specimens [70.4±14 years]. While the driving population is likely less aged than the above group of specimens, another study using the isolated human knee preparation and a rigid impact interface documents that fracture loads do not significantly vary with specimen age [Atkinson et al., 1998a].

Chronic experiments using a small animal model, the Flemish Giant rabbit, also show that axial (directed along the femoral axis) blunt impacts on the knee are less damaging to retropatellar cartilage than impacts directed obliquely (from the medial aspect with respect to the femoral axis) on the patella [Ewers et al., 2002]. The study using this animal model motivated a question about the role of impact direction on fracture tolerance of the human knee. One early study using the seated human cadaver

also investigated medial oblique impacts on the knee versus axial impacts [Powell et al., 1975]. In this study, while the oblique impacts generated strains on the femur suggesting a curved beam effect and the axial impacts suggested a beam-column effect, the authors did not specifically address how impact direction affects the femur or patella fracture load. On the other hand, Melvin et al., 1975 investigated the impact fracture responses of the human cadaver knee-thigh-hip complex for axial and oblique (medial-directed) impacts on the knee with a rigid impact interface covered with a 1" thick foam pad (Figure 2.1). Fractures were noted at 18.4 ± 2.0 kN (n=5) for axial impacts on the knee. In contrast, patella fractures were noted in 2 cases at 8.1 and 10.5 kN for oblique impacts (11° of hip abduction).

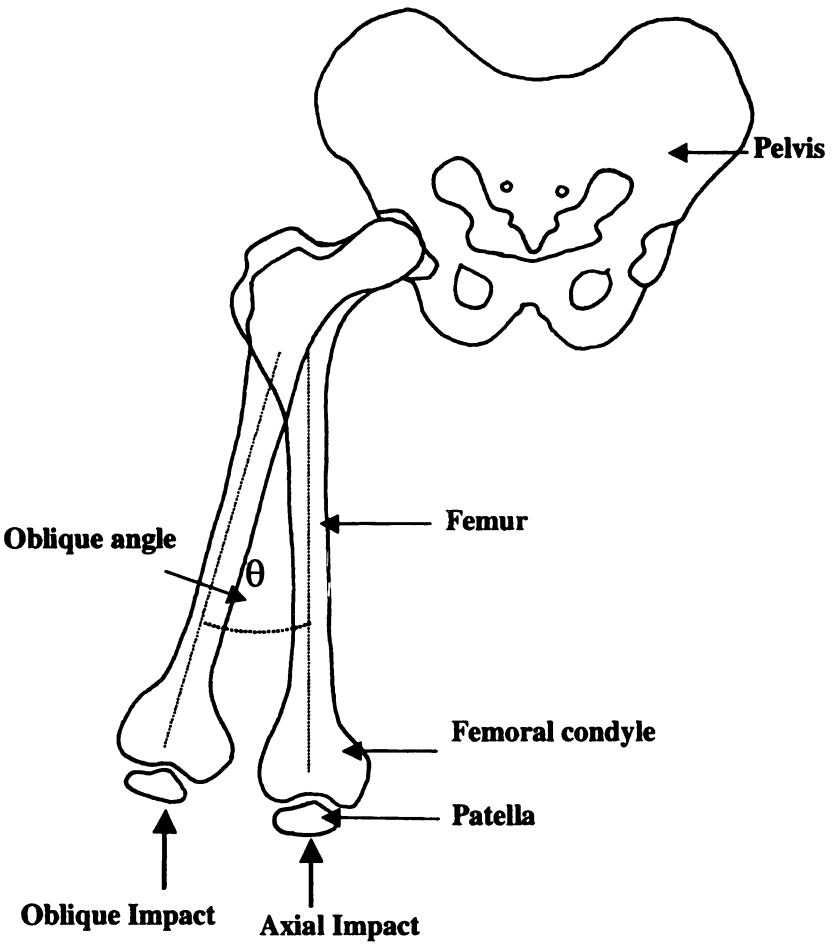

Figure 2.1. Axial and oblique impact loading direction of the knee-thigh-hip complex from Melvin et al., 1975.

These data may suggest a reduced fracture tolerance of the human patella for oblique versus axial impacts on the knee. Melvin et al., 1975 furthermore show a "typical" supracondylar femur fracture and a fractured patella. The patella fracture plane is interestingly vertical (inferior to superior oriented) rather than horizontal (medial to lateral oriented), as has been previously shown in studies using the isolated knee preparation for axial impacts on the patella [Atkinson et al., 1997, Atkinson & Haut, 2001b].

Therefore the following questions were asked: 1) Is the patella more vulnerable to fracture from an oblique (medial directed with respect to the femoral axis) versus an axial (directed along the femoral axis) impact? 2) Does the fracture pattern depend on direction of the blunt impact on the knee? The objectives of the current study were therefore to document the peak loads for fracture and fracture patterns on the human patella for a rigid interface impacting axially and obliquely (from the medial direction) with respect to the axis of the femur.

METHODS

Blunt impact was delivered to pairs of knee joints from nine human cadavers aged 73 ± 16.9 years. The limbs were procured from university sources (see Acknowledgment) and stored at -20°C until testing. The joints were selected from donors with no known knee injuries or signs of surgical intervention during a postmortem evaluation. Twenty-four hours prior to testing, the joints were thawed to room temperature. The preparations were sectioned 15 cm superiorly and inferiorly to the knee joint. Superficial muscle tissues were excised from each preparation leaving the articular joint capsule and the

quadriceps tendon-patella-patellar ligament complex intact (Figure 2.2). The femur was cleaned with alcohol and potted in a 6.3 cm diameter, 10 cm deep cylindrical aluminum sleeve with room temperature curing epoxy (Fibre Strand #6371, Martin Senour Co., Cleveland, OH). This allowed approximately 5 cm of the femur to be exposed beyond the potting material. The test specimens were mounted in the fixture with 90° of knee flexion. The angle was established by aligning the femur and tibia visually with a 90° square tool. A special clamp was designed to attach the quadriceps tendon to a pneumatic cylinder (Model #D-48349-A-6, Bimba Manufacturing Co., Monee, IL). The pneumatic cylinder was pressurized prior to each experiment to generate 1.3 kN of force in the quadriceps tendon. The quadriceps tendon force was applied in both the axial and oblique impacts to simulate an in vivo muscle force, and help keep the patella in the femoral groove for oblique impacts. One knee from each pair was randomly selected for axial (directed along the femoral axis) impact, while the contralateral knee from each pair was impacted at an oblique angle (15° or 30°) medially with respect to the femoral axis (Figure 2.3). A servo-controlled hydraulic testing machine (Model 1331 retrofitted with 8500 plus digital electronics, Instron Corp., Canton, MA) was programmed to load the anterior surface of the patella with a haversine waveform that generated a peak load in 50 ms. The 50 ms time to peak approximated the time to reach peak load (20 to 60 ms) documented for a Hybrid III midsize male dummy during a typical automotive crash simulation [Rupp et al., 2002]. A repetitive, increasing load protocol was followed where test 1 corresponded to an input load of 1 kN and tests 2, 3, 4, 5 and 6 corresponded to programmed input loads of 3, 5, 7, 9, and 11 kN, respectively. Specimen # 03-328L test 1 was carried out with an input load of 7 kN, due to a mechanical problem. Test 1 on the

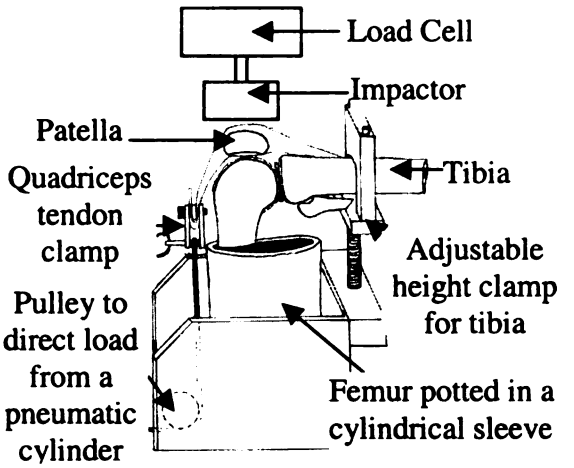

Figure 2.2. Isolated human knee joint flexed 90° with impact loading on the patella. A tension of 1.3 kN was applied to the quadriceps tendon immediately prior to the impact load.

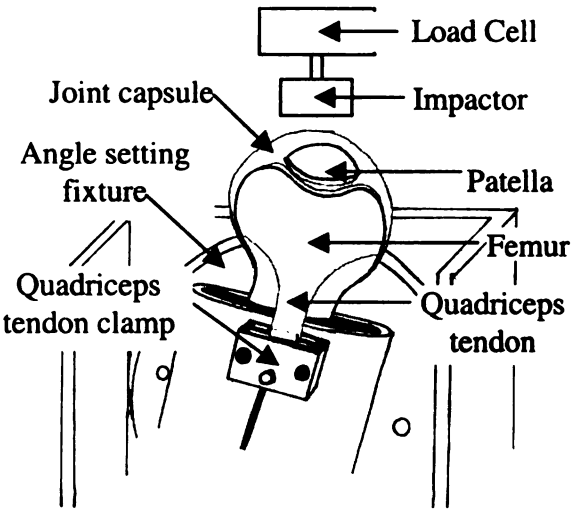

Figure 2.3. Oblique orientation of the knee joint preparation with respect to the femoral axis.

contra-lateral limb, #03-328R, was performed with an input of 5 kN and test 2 at 7 kN. All impacts were delivered with a rigid interface (aluminum, 5 cm diameter) that was attached to the hydraulic actuator of the testing machine. A 2500 lb. (11.1 kN) load transducer (Model #10101a-2500, Instron Corp. Canton, MA) was attached behind the interface. After each impact in the repetitive series of experiments, the specimen was examined for gross fracture of bone or dislocation of the patella by visual inspection and palpation of the retropatellar surface under the quadriceps tendon. The anterior surface of the patella was also visually inspected, and the location of the patella at the end of the loading was documented. Experimental data (load and displacement) from the testing machine were collected at 1000 Hz and recorded on a personal computer with a 16-bit analog/digital board (model DAS 1600; Computer Boards, Mansfield, MA, U.S.A.).

Prior to each sequential test, pressure sensitive film (Prescale, Fuji Film Ltd., Tokyo, Japan) was inserted into the patello-femoral joint to measure the magnitude and distribution of contact pressures generated in the joint during impact. Low (0-10 MPa)

and medium (10-50 MPa) range pressure films were stacked together and sealed between two sheets of polyethylene (0.04 mm thick) to prevent exposure of the film to body fluids [Atkinson et al., 1998b]. The film packets were inserted into the patello-femoral joint under the quadriceps tendon, without disturbing the medial and lateral aspects of the articular capsule. A new pressure film packet was placed in the joint immediately prior to each test in the sequence. A film packet was also placed on the anterior surface of the patella to record the magnitude and distribution of contact pressures between the rigid interface and the knee. The film was digitally scanned (ScanMaker E6, Microtek International Inc., Redondo Beach, CA), and the pressure distributions were quantified using commercial software (PhotoStyler, Aldus Corporation, Seattle, WA). The image resolution was set at 150 dpi, and the film data was converted to a gray scale (NIH Image, version 1.6). The gray scale values were converted to pressures using a previously established methodology [Atkinson et al., 1998b]. Briefly, calibration tests were performed on the low and medium stacked film packets while sandwiched between two polished stainless steel plates. A haversine, displacement-controlled, waveform was used to generate calibration loads in approximately 50 ms, using the servo-hydraulic testing machine. This provided a dynamic calibration for the film packets. As described by Atkinson et al. (1998b), the stacking order of the film and the rate of loading are important factors in the measurement of contact pressures using this film.

Each joint was grossly examined following the failure experiment. The medial and lateral capsules were carefully probed in an attempt to view any gross ruptures of the capsule, especially adjacent to the patella. Injuries were photographed. Thereafter, the medial and lateral capsules were carefully cut to fully expose the retropatellar surface and femoral

condyles. These articular surfaces were wiped with India ink in order to help visualize surface lesions on the articular cartilage. Photographs recorded any surface defects and damage.

The means and standard deviations for peak load, the corresponding displacement and time to peak load were documented for each experiment, and the pressure film contact area and average pressure were determined for each impact direction in the fracture experiments. Statistical comparisons of these values for the axial and oblique impact directions were performed with paired Student's t-tests. Statistical significance was determined for $p < 0.05$ in these experiments. Additionally, in the sub-fracture experiments joint stiffness was computed as the slope of a linear regression line through the load-displacement data for three load regions in tests 1, 2 and 3 on each specimen. The stiffness of the test fixture was also documented by loading it directly in the testing machine. The fixture stiffness was documented to be 5 to14 times higher than that of the joint for oblique and axial impacts, respectively. In post-processing of the load deflection data, the fixture deflection at each load was subtracted from the data to determine the stiffness of the knee joint itself. The means and standard deviations of the 3 load-range stiffnesses were determined for each experiment. These data were statistically compared with a one-way ANOVA and Student-Newman-Keuls post-hoc tests. Regression analyses (univariate and multivariate) were used to determine the relationships, if any, between peak loads for bone fracture and specimen age.

RESULTS

The output load-time response curves for the axial and oblique experiments were skewed haversines with a longer unloading than loading time (Figure 2.4). The time to

peak was 54 ± 8 ms for all experiments. While the time to peak load was typically less for fracture experiments (47 ± 8 ms for axial, 48 ± 9 ms for oblique) versus non-fracture experiments (53 ± 4 ms for axial, 60 ± 7 ms for oblique), there were no statistically significant differences in the time to peak load between axial and oblique experiments for the fracture or the non-fracture experiments (Tables 2.1 and 2.2).

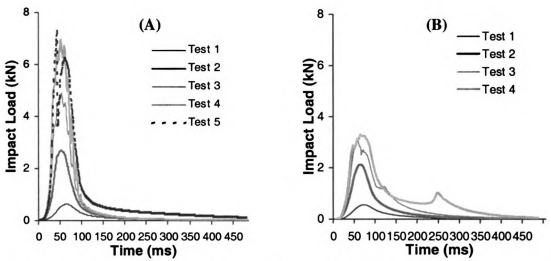

Figure 2.4. Representative load-time curves for sequential impacts on a specimen (03-017) for axial (A) and oblique (B) directed loadings.

The impact responses of the isolated knee in the oblique experiments generally indicated more specimen compliance than for the axial impacts. The overall shapes of the load-displacement responses for axial and oblique experiments were nonlinear (Figure 2.5). The impact responses did not vary significantly between sequential tests on the same specimen, except for an increase in peak load. The repeatability of sequential tests on the same limb was documented by a comparison of the average slopes of these curves for various load ranges (Figure 2.6). The response curves were divided into three load ranges that corresponded to the loads developed in tests 1, 2 and 3 on each specimen. In the lowest load range (0 – 630 N) the average slope (patello-femoral joint stiffness) for

test 1 (433 ± 164 N/mm) was not different from that generated in test 2 (490 ± 198 N/mm) or test 3 (418 ± 176 N/mm) for the axial impacts on all specimens (Figure 2.7). Similarly, the slope of the response curves in the second load range (630 N - 2440 N) computed from test 2 (893 ± 275 N/mm) was not different from that generated in test 3 (1015 ± 224 N/mm) for the specimens.

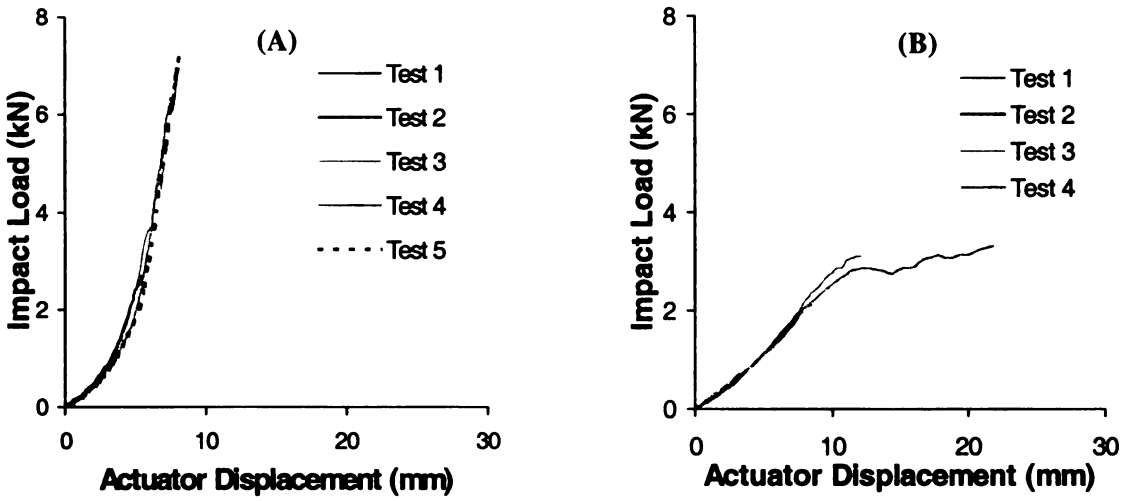

Figure 2.5: Representative load-actuator displacement curves for sequential impacts on a specimen (03-017) for axial (A) and oblique (B) directed experiments. In this experiment patellar fracture occurred for the axial loading while on the contralateral limb a medial oblique impact dislocated the patella.

Table 2.1: Biomechanical data for axial impacts. The fracture experiment is the last entry for each specimen.

Specimen ID	Sex (Age)	Impact Number	Peak Load (kN)	Displacement (mm)	Time to Peak (ms)	Injury Comments
02-687R	Male (94)	1	0.74	2.24	56	Femoral Condyle Fracture
		2	2.44	5.23	53	Linear Patella Fracture
		3	4.01	8.76	56	
		4	4.41	7.87	40	
02-698L	Female (88)	1	0.74	2.24	57	Comminuted Patella Fracture
		2	2.59	5.18	51	
		3	3.94	7.02	48	
		4	5.49	11.22	51	
03-035R	Female (85)	1	0.76	2.11	56	Comminuted Patella Fracture
		2	2.69	4.71	51	
		3	4.38	7.57	61	
		4	4.25	5.31	38	
03-048L	Female (82)	1	0.85	2.84	54	Linear Patella Fracture
		2	2.59	3.83	51	
		3	4.33	7.11	53	
		4	5.05	10.44	52	
02-686L	Female (81)	1	0.85	1.53	54	Femoral Condyle Fracture
		2	2.70	3.50	52	Comminuted Patella Fracture
		3	4.33	6.75	49	
		4	5.04	5.64	36	
03-328L	Female (64)	1	5.71	17.89	54	Linear Patella Fracture
03-017L	Male (60)	1	0.63	2.84	64	Comminuted Patella Fracture
		2	2.69	5.52	51	
		3	4.90	7.04	53	
		4	6.96	8.22	50	
		5	7.29	13.34	43	
03-383L	Female (60)	1	0.76	2.93	57	Linear Patella Fracture
		2	2.80	5.45	53	
		3	4.95	7.47	50	
		4	5.79	10.31	53	
		5	7.76	14.14	56	
03-369R	Male (43)	1	0.82	1.79	57	Linear Patella Fracture
		2	2.76	3.43	53	
		3	4.89	4.43	47	
		4	6.24	5.19	54	
		5	7.26	5.90	46	
		6	7.99	8.10	53	
Fracture Average			5.89*	10.44	47	
Fracture Standard Deviation			1.43	4.18	8	

* Significantly different than oblique.

Table 2.2: Biomechanical data for oblique impacts. The fracture or dislocation experiment is the last entry for each specimen.

Specimen ID	Sex (Age)	Impact Number	Peak Load (kN)	Displacement (mm)	Time to Peak (ms)	Injury Comments
02-687L	Male (94)	1	0.77	2.17	57	Linear Patella Fracture
		2	2.34	5.67	57	
		3	2.80	6.14	37	
02-698R	Female (88)	1	0.55	2.82	64	Linear Patella Fracture
		2	1.97	8.61	57	
		3	2.68	11.14	48	
03-035L	Female (85)	1	0.62	2.66	63	Comminuted Patella Fracture
		2	2.46	6.27	54	
		3	3.75	8.68	45	
		4	3.75	9.88	39	
03-048R	Female (82)	1	0.54	2.84	64	Linear Patella Fracture
		2	1.90	8.74	60	
		3	2.02	8.14	38	
02-686R	Female (81)	1	0.56	2.95	66	Linear Patella Fracture
		2	1.87	8.96	57	
		3	2.99	15.40	62	
		4	3.24	18.30	52	
03-328R	Female (64)	1	1.77	10.16	44	Gross Dislocation of Patella
		2	3.59	30.43	54	Torn Medial Capsule
03-017R	Male (60)	1	0.55	3.09	66	Gross Dislocation of Patella
		2	2.13	8.48	61	Cartilage Fissures on Lateral
		3	3.11	12.00	51	Femoral Condyle
		4	3.30	21.80	57	
03-383R	Female (60)	1	0.44	3.10	68	Comminuted Patella Fracture
(Angle at 15 degrees)		2	1.50	12.98	67	
		3	3.51	17.27	61	
03-369L	Male (43)	1	0.19	1.29	70	Comminuted Patella Fracture
(Angle at 15 degrees)		2	2.24	5.81	57	
		3	4.15	7.68	57	
		4	5.73	10.13	56	
		5	6.26	20.48	49	
Fracture Average			3.47*	13.05	48	
Fracture Standard Deviation			1.36	5.57	9	

* Significantly different than axial.

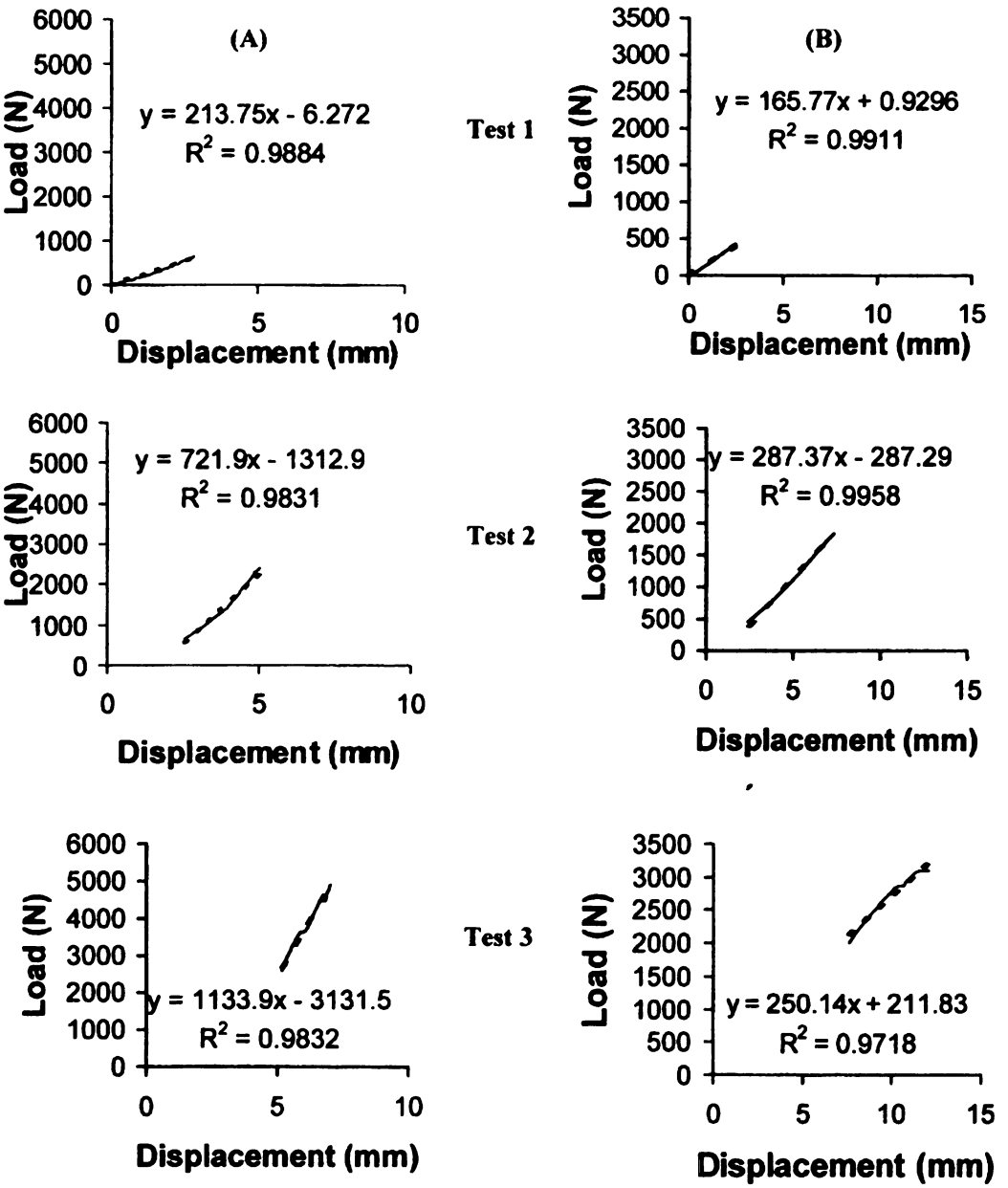

Figure 2.6. Representative load versus displacement plots of a specimen (03-017) for axial (A) and oblique (B) tests 1, 2 and 3 in their respective load ranges

The data for the first and second load ranges (tests 1 and 2) helped validate, on average, the repeatability of sequential load response data on the limbs. The oblique impacts also had slopes that were similar for each load range in these repeated tests. For the lowest range of loading (0 –440 N) the slopes were 223 ± 56 N/mm, 219 ± 27 N/mm and 199 ± 51 N/mm in tests 1, 2 and 3 on these specimens, respectively. These data verified that the

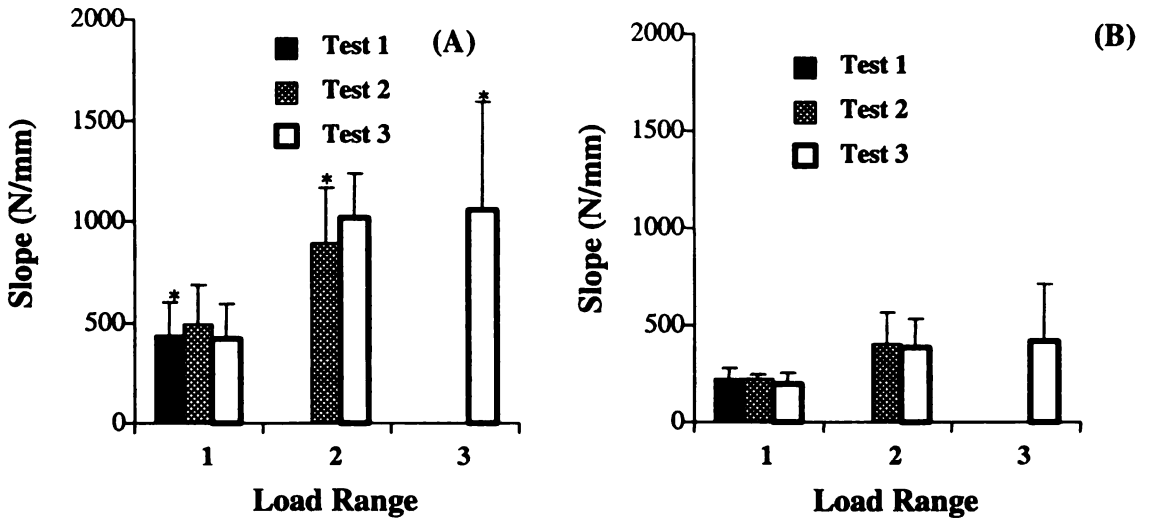

Figure 2.7. Bar graph of linear regression slopes for axial (A) and oblique (B) tests 1, 2 and 3. * Significantly different than oblique.

responses of the knee preparation did not vary, on average, between repeated tests on the limbs in the low range of loading. For the second range of loading (440 N – 1840 N) the slopes were 400 ± 162 N/mm and 386 ± 142 N/mm for tests 2 and 3, respectively. A comparison of the data for the axial and oblique impacts showed a significant difference in the average slopes of the response curves for load range 1 ($p = 0.007$) and load range 2 ($p < 0.001$), with the axial responses having a higher slope (stiffer) than that for oblique impacts. The slope of the highest load range from test 3 on the specimens was also different (greater) for axial (above 2440 N) (1055 ± 537 N/mm) versus oblique (above 1840 N) (415 ± 301 N/mm) impacts ($p = 0.003$). These data also showed that while the load-displacement responses of the knee for axial and oblique impacts were nonlinear, the slopes of these curves for the various load ranges indicated more dramatic changes at in stiffness for the sequentially higher load experiments in the axial than for the oblique impacts. The contact pressures within the patello-femoral joint were documented using Fuji film in this study for tests 3 and 4 on each specimen (Table 2.3).

Table 2.3: Pressure film data from medial and lateral facets of the patella and the anterior surface of the patella. * Significantly different than medial.

Joint Orientation	Test Number	Average Pressure (MPa)			Contact Area (mm^2)		
		Medial	Lateral	Anterior	Medial	Lateral	Anterior
Axial	3	16.1 (3.2)	18.1 (4.8)	16.4 (1.9)	115.6 (55.2)	209.8 (49.7)	182.3 (72.0)
Oblique	3	14.2 (6.3)	22.0 (3.7)*	18.2 (3.6)	19.2 (14.8)	219.5 (73.8)*	156.6 (68.7)
Axial	4	18.1 (4.9)	21.3 (5.2)	18.5 (3.2)	145.7 (84.3)	242.1 (52.8)	250.3 (92.2)
Oblique	4	12.8 (7.6)	24.2 (3.0)*	19.1 (2.9)	14.6 (14.7)	302.4 (66.9)*	315.1 (164.9)

Generally the pressure distributions were smooth with little or no apparent creasing of the film, which would indicate artificially high areas of contact pressure (Figure 2.8). The average pressure on the lateral facet significantly exceeded that on the medial facet for the oblique impacts (test 3 $p = 0.007$ and test 4 $p = 0.016$), but no differences in average

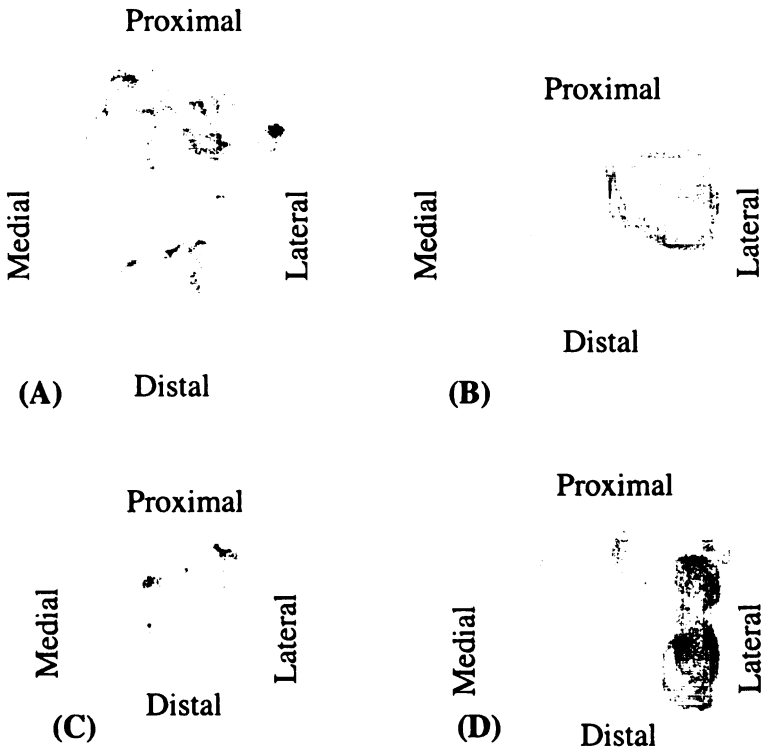

Figure 2.8. Representative pressure distributions of a direct impact (03-048L, test 4) on the anterior surface (A) and retropatellar surface (B) and an oblique impact (03-048R, test 3) on the anterior surface (C) and retropatellar surface (D).

pressure were measured on the medial versus the lateral facet for the axial impacts (Figure 2.9). Additionally, the lateral patello-femoral joint contact area was significantly higher than the medial contact area in test 3 ($p < 0.001$) and test 4 ($p = 0.001$) of the oblique impacts and test 3 ($p = 0.033$) of the axial impacts, but was not significant in test 4 ($p = 0.051$) for the axial experiment. There was also a significant difference in the medial contact areas for the axial and oblique impacts (test 3 $p = 0.004$ and test 4 $p = 0.010$). The peak loads carried by the lateral patellar facet, based on the pressure

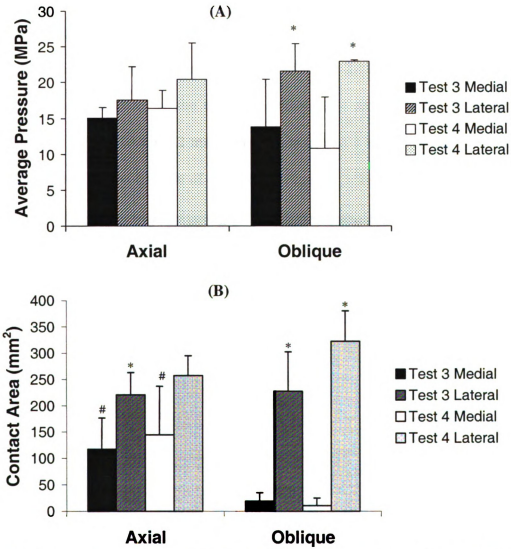

Figure 2.9. Bar graph of retropatellar surface average pressure (A) and contact area (B) for tests 3 and 4.
* Significantly different than medial side. # Significantly different than oblique.

film data, were significantly higher than those on the medial facet for oblique (test 3 p = 0.011 and test 4 p=0.022) experiments, and axial (test 3 p< 0.001 and test 4 p=0.002) experiments. The average pressure and contact area recorded from the anterior surface of the patella were not different for axial versus oblique impacts.

As mentioned previously, gross injury of the knee joint occurred on or after test 4 for most specimens (Table 2.1 and 2.2). Fracture of the patella for axial impacts was evident in each case (Figure 2.10A). In two cases the injury was associated with split fracture of the femoral condyles. Linear fractures were oriented horizontally across the patella in five axial directed experiments. Fracture of the patella resulted in significant comminution in four cases of axial impact (Figure 2.11A). The peak load and corresponding displacement of the hydraulic actuator for axial impacts on the patella were 5.9 ± 1.4 kN and 10.4 ± 4.2 mm, respectively (Table 2.1). Seven of nine obliquely impacted knees exhibited fracture of the patella (Figure 2.11B). In contrast to the axially

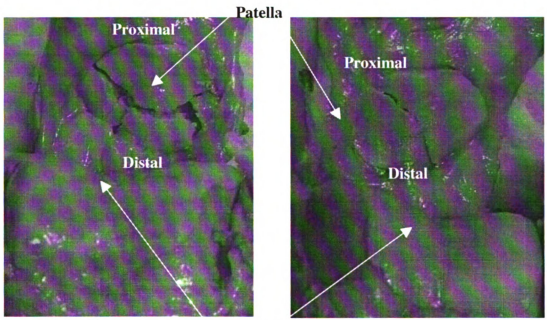

Figure 2.10. Representative photograph of patella fractures on paired human knees (02-698). Horizontal oriented and comminuted fracture for axial impact (A), and vertical oriented fracture for oblique impact (B).

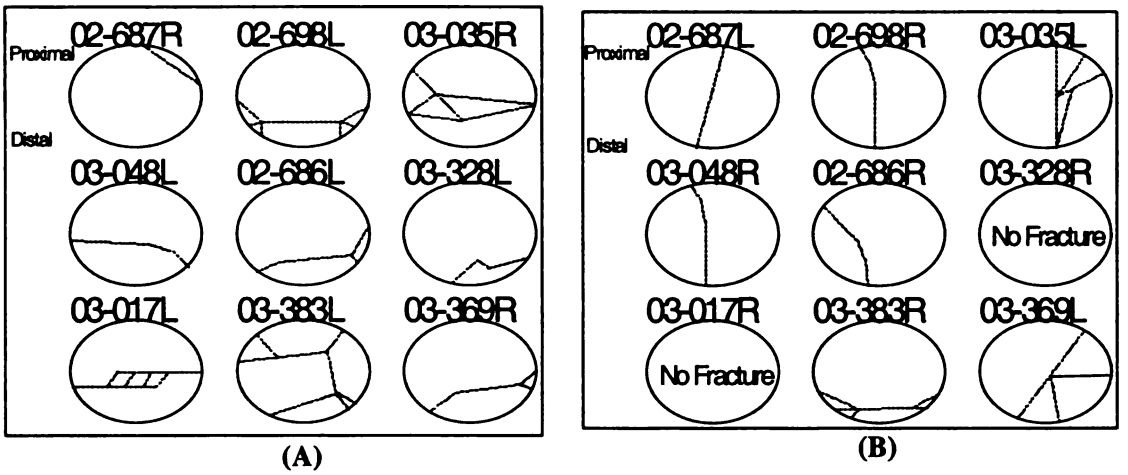

Figure 2.11. Schematic representations of the fracture patterns on the retropatellar surface for each axial (A) and oblique (B) directed impact. Fractures consisted of linear and comminuted patterns.

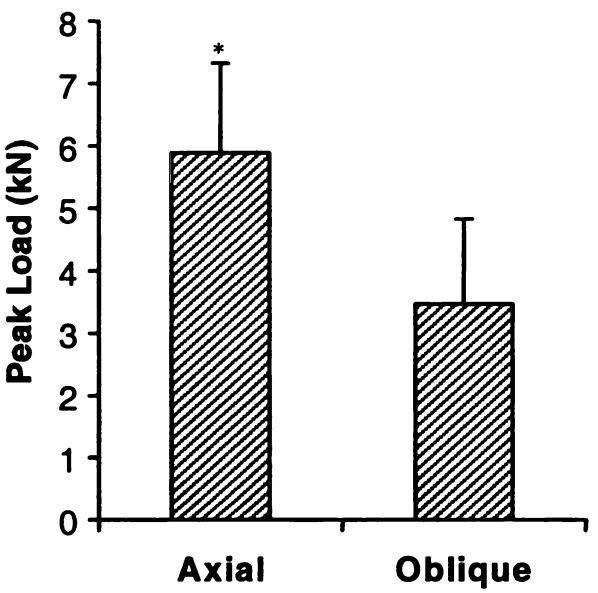

Figure 2.12. Bar graph of peak loads generated in axial versus oblique impacts.
* Significantly different than oblique.

directed impacts on the patella, the fracture patterns for the oblique impacts generally appeared to be oriented more vertically on the patella (Figure 2.10b). In three cases patella fractures were comminuted. In oblique experiments for cases of patella fracture the peak load and actuator displacement were 3.5 ± 1.4 kN and 13.1 ± 5. 6 mm, respectively (Table 2.2). The peak loads generated in axial and oblique fracture experiments were significantly different ($p = 0.008$) (Figure 2.12). Patella fracture did not occur in two oblique experiments. Rather, the patella dislocated

at a load of 3.4 ± 0.2 kN and an actuator displacement of 26.1 ± 6.1 mm. In one specimen (03-328R) the retinaculum (articular capsule) was separated at the medial border of the patella (Figure 2.13A). During this traumatic event the hydraulic actuator displaced approximately 30 mm, compared to 13.1 ± 5.6 mm in fracture experiments, as the patella was dislocated laterally out of the femoral groove between the condyles. The dislocation was visually evident during the experiment. In a second specimen (03-017) the patella was again dislocated laterally without a visible fracture. The actuator displacement at peak load in this second case was approximately 22 mm (Figure 2.5B), as the patella was dislocated laterally from the femoral groove. In this case of patellar dislocation a surface lesion was noted on the articular cartilage covering the lateral femoral condyle (Figure 2.13B). This articular surface could not be entirely viewed prior to the experiment because of the intact nature of the joint capsule. Because of the pristine appearance of this cartilaginous surface, the injury was suspected to be due to abnormal loading on the cartilage during acute dislocation of the patella.

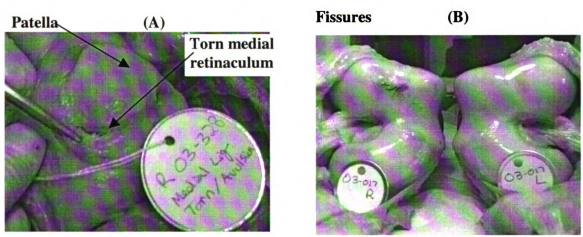

Figure 2.13. Specimen 03-328 showing a torn medial retinaculum from an oblique impact (A). Specimen 03-017 showing an articular cartilage surface lesion from an oblique impact (B).

The current experiments were conducted on specimens 43 to 94 years of age. Because of the large variation in specimen age, the peak load data were examined for a dependence on specimen age (Figure 2.14). Univariate regression analyses of peak load for fracture cases versus specimen age indicated a significant correlation for the axial and oblique (without 15° impact data) experimental data. The correlation coefficient (R^2) was lower for oblique (0.436) than for the axial impacts (0.823). A multivariate linear regression analysis of these data, using age (43-94 years) and direction (0 = axial and 1 = 30° oblique) generated the following expression (where age and direction were significant predictors, $p < 0.001$ and $p = 0.002$, respectively):

$$\text{Peak load} = 11536.6 - 77.4*\text{Age} - 1520.7*\text{Direction} \qquad (2.1)$$

This more general expression also fit the experimental data well (Figure 2.14). The univaritate and multivariate predictions were based on only the 30° oblique data, but the equations appeared to predict the 15° data for the youngest specimen within less than 10% of the peak load for fracture.

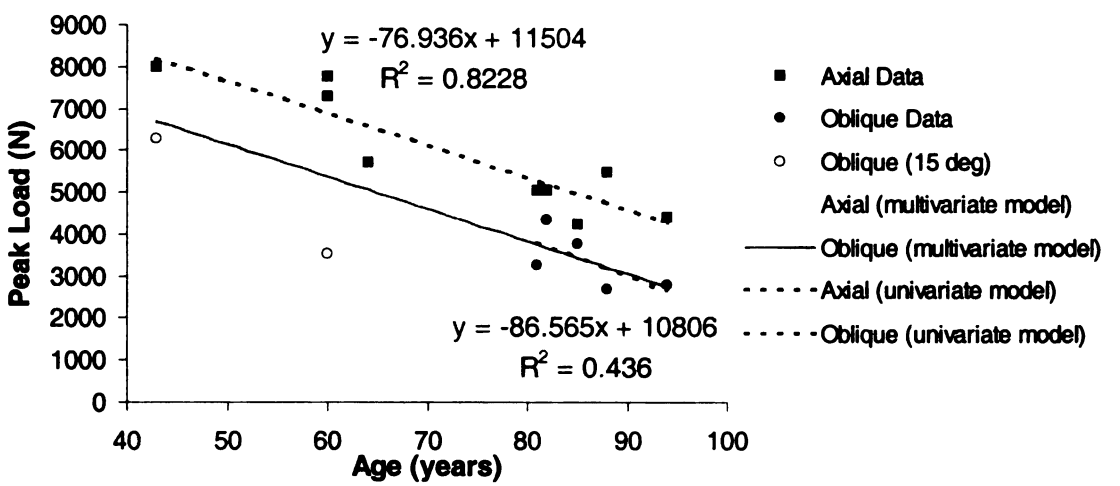

Figure 2.14. Fracture load-age plot for axial and oblique directions with univariate and multivariate linear regression lines.

DISCUSSION

The objective of this study was to document peak loads generated on the human patello-femoral joint during fracture experiments and the fracture patterns on the patella for rigid interface impacts with a 90° flexed knee. The experiments involved impact of one specimen from a pair of isolated cadaver knees with an axial (directed along the axis of the femur) patellar impact. The opposite knee was impacted with the same interface, but the impact was directed obliquely (15° and 30° medial) to the femoral axis. While most previous studies have focused on axial loading of the knee-thigh-hip complex, experimental data documented in Melvin et al., 1975 suggest that the peak load in a bone fracture experiment may be reduced and the patellar fracture pattern may be altered for an oblique versus an axial directed impact on the knee. In the current study, the peak load generated during fracture of the patella was significantly reduced from 5.9 ± 1.4 kN for axial impacts to 3.5 ± 1.3 kN for oblique impacts. Furthermore, in cases of patella fracture these surfaces were generally oriented vertical (inferior to superior) for oblique impacts and horizontal (medial to lateral) for axial directed impacts.

The failure loads in the current study were considered conservative measures for tolerance of the human knee to blunt impact because the study involved only rigid impact interfaces, the use of isolated joints, aged specimens with unknown tissue properties and a repeated impact protocol. These factors may influence the failure loads. The experimental results showed that the load-actuator displacement curves did not significantly vary between repeated tests on the same specimen, suggesting that joint tissue integrity may have remained high prior to gross failure. The experimental protocol was also to perform oblique experiments at 30° with respect to the axis of the femur.

However, after experiments on two of the younger specimens resulted in acute dislocations of the patella, the angle of impact was reduced to 15° for the two youngest specimens. The purpose of this change in protocol was to increase the probability of bone fracture versus patellar dislocation.

The experimental data generated in the current investigation using axial directed impacts on the patella compared well with previous experiments from this laboratory for axial impacts on the isolated human knee. Previous studies show that the load to produce linear horizontal or comminuted fracture of the patella with a rigid interface for the 90° flexed joint is 5.5 ± 1.8 kN [Atkinson and Haut, 2001a] and 4.7 ± 1.6 kN [Atkinson and Haut, 2001b] for specimens ages 70.4 ± 14 years and 69 ± 16 years, respectively, versus 5.9 ± 1.4 in the current study using specimens aged 73 ± 16.9 years.

The data in the current study, for an age range of 43 to 94 years, showed a correlation of peak loads in axial and oblique fracture experiments with specimen age. An earlier study indicates that for specimens ranging in age from 34-85 years, peak loads in fracture experiments were not dependent on specimen age [Atkinson and Haut, 1998a]. While the number of specimens in each study was different (15 in the 1998a study and 9 in the current study) and the range of specimen ages was different, neither factor was believed to fully explain discrepancies in the two studies. Another difference in the studies was the rate of loading. The earlier study by Atkinson and Haut (1998a) used a 4.8 kg free flight impact missile with a rigid interface that delivered repetitive impacts at sequentially higher energy until visible fracture of bone. The peak load was reached in 5.0 ± 2.6 ms, which contrasts with 48 ± 9 ms in the current study. Another previous study by this laboratory suggests that the number of occult microcracks in the subchondral bone

underlying retropatellar cartilage increases with the rate of loading on the knee [Ewers et al., 2000]. Since the same study shows fractured patellae for the high rate of loading versus none at the same load for a low rate of loading, the possibility may exist that peak load in patella fracture experiments could vary with specimen age more significantly in experiments using low versus high rates of loading on the knee. In fact, previous studies by others typically use low rates of loading and document that the strength of cortical bone decreases with specimen age [Burstein et al., 1976; Yamada, 1970]. These literature data would support data generated in the current study, which also suggested a decrease in peak load generated in patella fracture experiments with increased specimen age. The suggestion that a fracture load-age correlation for rigid impacts on the human patella may depend on the rate of impact loading would require validation in future studies. This type of experimental data may be particularly relevant in the future as the driving population tends to become more aged.

Another limitation of the current study was the use of only a rigid impact interface. The primary reason for using this interface was to establish basic impact data for the knee that could be compared with previous studies by this laboratory [Atkinson et al., 1995; 1997; 1998a; 1998b; 1999; 2001a; 2001b; Ewers et al., 2000] and early studies by others using the seated human cadaver [Melvin et al., 1975; Patrick et al., 1965; Powell et al., 1975]. The fracture load data are not to be interpreted as directly relevant to impact interactions of the knee with deformable interfaces. A recent study, for example, using a deformable interface (3.3 MPa crush strength aluminum material, Hexcel) documents significantly greater peak loads in patella fracture experiments with a deformable versus a rigid interface condition on the 90° flexed, isolated human joint

preparation described in the current study (Atkinson and Haut, 2001a). While for the same impact energy more gross fractures and occult microcracks underlying retropatellar cartilage are evident for rigid than for deformable interfaces, similar patella fracture patterns are evident for these axial directed impacts on the knee. The occult microcracks are found in areas of high patello-femoral contact pressure, and they are currently hypothesized to be precursors of gross fracture of bone in the patella (Atkinson and Haut, 2001b).

Another previous study from this laboratory also shows that the location of the horizontal linear fractures from axial directed impacts on the knee coincides with the orientation and location of the largest principal tensile stresses developed in the subchondral plate for a 3-D non-contact, impact model of the human patella [Atkinson and Haut, 1999]. The 3-D model applied patello-femoral contact pressures on the retropatellar surface and fixed the anterior surface of the patella in the area of interface contact. The study suggests that occult microcracks in the subchondral bone and the subsequent gross fracture of the patella results from excessive tensile stresses developed in the bone underlying retropatellar cartilage by the impact loading. It was also interesting to note that horizontal fractures of the patella from axial impacts in the current study were typically located more distally than described in previous studies [Atkinson and Haut, 1995; Atkinson and Haut, 1999]. The effect may be due to localized tensile stresses developed in the patella near the insertion of the patellar tendon. These stresses did not exist in previous studies because those experiments avoided using load in the quadriceps tendon during impact experiments and model simulations. In the current study a 1.3 kN load was applied to the quadriceps tendon immediately prior to impacting the

knee and during impact on the knee. The major reason for applying a quadriceps force in the current study was to help keep the patella in the femoral groove for the oblique impacts. Therefore, the protocol also had to be used in the axial directed impacts on contralateral limbs of each specimen. The 1.3 kN level of quadriceps force applied during blunt impact to the knee was not intended to represent the maximum force that could be generated by this muscle. Rather, this level was chosen to be relevant to a normal physiological condition. In fact, the maximum in vivo quadriceps force is documented to be approximately 3.9 kN for a group of 12 healthy male subjects from an early hallmark study [Lindahl et al., 1969]. The quadriceps muscle force, on the other hand, developed during extension of the knee from 90° to 60° of flexion is approximately 30% of the maximum force [Lieb and Perry, 1968]. Hence, a quadriceps force of 1.3 kN was chosen for the current study. Microdamages have also previously been documented near the insertion of the patellar tendon for axial patello-femoral impact studies with a canine model [Thompson et al., 1991]. In the canine study "step-off" fractures of the subchondral bone plate underlying retropatellar cartilage are evident, even without superficial damage of retropatellar cartilage. Such microfractures may be precursors of the gross bone fractures observed in the patella for the current study using the human cadaver. These data may also suggest that high levels of in vivo quadriceps muscle tension, that could approach maximal prior to or during a crash, may put the patella at greater risk of fracture.

Another limitation of the current study was the implementation of a repetitive impact protocol to increase the force input levels on the knee until gross fracture of bone. One reason for employing this methodology was to compare the current results with

those from previous studies of this laboratory [Atkinson et al., 1995; 1997; 1998a; 1998b; 1999; 2001a; 2001b; Ewers et al., 2000]. While single versus multiple impacts were not conducted previously on the human patello-femoral joint, a study was performed on the isolated human tibio-femoral joint at 90° flexion [Banglmaier et al., 1999]. The study showed that repetitive impact testing results in tibio-femoral bone fracture for peak loads of 8.0 ± 1.8 kN. In contrast, single impact experiments on contralateral limbs results in a 33% frequency of fracture for peak loads of 5.8 ±1.5 kN. As expected, single impact subfracture experiments also show occult microcracks in subchondral bone underlying tibial and femoral cartilage surfaces. Hence, the repeated impact test data of the current study were very likely conservative measures of the fracture tolerance of the human patella under a single impact scenario. On the other hand, occult microcracks may have been equally produced in the oblique and the axial impacts, so the objective of the current study was likely not compromised by this experimental protocol.

An axial versus oblique knee impact study has also been conducted using a small animal model, the Flemish Giant rabbit [Ewers et al., 2002]. The study shows that one-year following an oblique directed impact to the medial aspect of the patella, retropatellar cartilage is mechanically softened and has numerous superficial lesions (fissures). In contrast, following axial impact experiments with the same applied load on the patella, few superficial lesions are noted and the retropatellar cartilage is not softened. The effect is hypothesized due to a reduction in the level of shear stresses developed in the superficial layer of retropatellar cartilage in axial versus oblique experiments [Li et al., 1995]. These lower shear stresses in the retropatellar cartilage for axial versus medial impacted knees are suggested to be the result of a more uniform distribution of contact

pressure across the medial and lateral patellar facets for the axial experiments, which contrasts with a significantly higher level of contact pressure on the lateral versus the medial facet in oblique (medial-directed) impacts. The contact pressure distributions shown for oblique and axial directed impacts on the patella for the rabbit model compare well with data from the current study using the human cadaver knee. Since the current study was conducted on aged cadavers, that typically have significantly degraded retropatellar cartilage compared to the rabbit model, it was difficult to assess any differences in the extent of impact-induced fissuring of cartilage in axial versus oblique experiments. In one experiment, however, a distinct surface fissure was noted on the lateral femoral condyle after acute dislocation of the patella during an oblique impact. It was unknown, however, which impact generated this defect. Similarities of these data with the animal model data may suggest a significant chronic problem could exist following oblique versus the axial directed impacts on the knee following even a subfracture load on the patella. Acute subfracture injuries, however, would have to be investigated in future experiments.

The current study was also limited by the use of human cadaver specimens, as the potential effects of acute trauma could not be studied in a chronic setting. In fact, the study of Thompson et al. (1991) using the canine model indicates that "step-off" fractures of the subchondral bone plate heal after 1-year, but the overlying cartilage repairs with fibrocartilage versus normal hyaline cartilage. While these data may suggest occult microfractures themselves are not clinically relevant, the long-term durability of the fibrocartilaginous repair tissue in the joint is questionable. Correspondingly, clinical studies also suggest a high percentage of patients suffering gross patella fractures tend

towards development of a chronic osteoarthritis in the patello-femoral joint [Robinson and States, 1978; Nummi, 1971]. This potential chronic problem may put the oblique impacted trauma patient at a greater risk of disease. Another concern for this trauma patient is the potential for chronic disease of the knee following an acute dislocation of the patella via an oblique impact, such as that shown in 2 of 9 specimens from the current study. Numerous clinical investigations have described acute damage to the medial retinaculum (capsule) following dislocations of the patella caused by excessive twisting, valgus stress or direct blows to the knee [Burks et al., 1998]. This type of injury was grossly visualized in one current experiment, 03-328. Clinical studies have associated acute dislocation of the patella with damage to the medial patello-femoral ligament in approximately 60-90% of cases [Sallay et al., 1996; Ahmed and Duncan, 2000; Nomura et al., 2002]. While injury to the medial retinaculum could lead to chronic mal-tracking of the patella and a subsequent chronic disease, early diagnosis of this soft tissue injury and its surgical repair could restore normal tracking of the patella and minimize the potential for chronic joint disease [Sandmeier et al., 2000]. On the other hand, clinical dislocations of the patella are also associated with chondral and osteochondral lesions of the patella and the lateral femoral condyle, as was observed in one specimen from the current study [Sallay et al., 1996; Ahmed and Duncan, 2000]. These injuries have also been associated with articular cartilage degeneration reminiscent of early-stage osteoarthritis [Johnson et al., 1998]. While the current study suggested that oblique loading of the patella in an automobile crash might increase the potential for patella fractures or dislocations, the frequency of oblique versus axial loading in field accidents was not investigated in the current study. The current study involved experiments at 15° and 30° oblique to the

femoral axis. Melvin et al., 1975 performed experiments at 25° oblique to the axis of the femur and had difficulty producing patella fracture except in two cases. Interestingly in the NASS database, accidents that occur between 11 o'clock and 1 o'clock are all categorized as frontal. This range of vehicle impact directions coincides with ± 30° for the extremes of a frontal crash classification. Thus, the occupant may impact the automotive interior obliquely in a "NASS frontal" crash. On the other hand, in 12 o'clock frontal crashes the occupant may also impact the instrument panel, or other surfaces, obliquely. An early report by Schneider et al., 1983 indicates an abduction angle of the occupant lower extremity for a "standardized normal driving posture" of mid-size males at approximately 8°. This "splay angle" was measured in a simulated, vehicle-seating package for a range of vehicles from that period. A standardized posture had to be developed because they noted "occupant seating is very atypical". In contrast, a more recent unpublished report suggests automobile drivers can sit with knees significantly abducted under normal driving conditions [Reynolds, 1996]. In this study 39 drivers were filmed during 2-hour highway drives in a mid-size sedan. Surface markers were placed on the lateral epicondyle of the right knee and the right hip at the greater trochanter. Locations of these markers were recorded with four video cameras during the drives. The abduction angle was calculated in the horizontal plane, from a line between these two points and a reference line perpendicular to the seat. The drivers abducted (rotated the lower extremity laterally) 10-30° (Figure 2.15), with the degree of abduction greater for taller males and greater for males than females. These data may suggest that even in the event of a 12 o'clock frontal crash, automobile drivers may contact the instrument panel or steering column with abducted lower

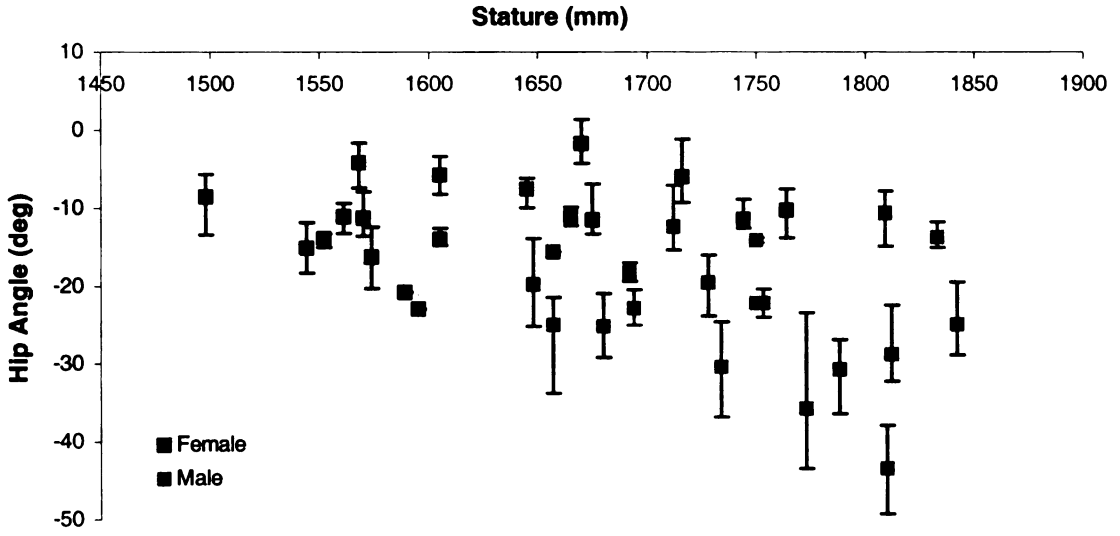

Figure 2.15. An abduction angle-stature plot for male and female drivers in a two-hour automobile trip (H. Reynolds, ERL LLC). Data collected with each change in position. The plot shows the mean and range of leg "splay" angles of the lower extremity during the drives.

extremities. So, the oblique impact direction may be a more typical scenario in field accidents than an axial impact on the knee. This could predispose the occupant to patella fracture or even acute patellar dislocation. Currently, this soft tissue injury is not specifically documented in the NASS database. A documentation of patella fracture orientation from field accidents may be helpful for reconstruction studies, since oblique versus axial experiments showed a difference in the patterns of patella fracture in the current study. These data may help in the analysis of injury causations in field accidents.

This study examined the peak loads on the human knee generated during fracture of the patella with a rigid interface. As impact interfaces in current automobiles are typically deformable, the current data is not directly applicable to this setting. However, these data do expand on the current database that is used to establish fracture tolerance criteria for the lower extremity.

CONCLUSION

The study showed that the patella was more vulnerable to fracture with a rigid interface when the knee was impacted oblique versus axially with respect to the femoral axis. Furthermore, while axial impacts resulted in horizontal linear or comminuted patella fractures, oblique impacts (15° - 30° medial to the femoral axis) resulted in fractures whose surfaces were oriented vertically across the patella. In two cases of oblique impact on the knee the patella dislocated laterally prior to fracture. Soft tissue injuries were noted in both cases. In the oblique and axial experiments, peak loads were also correlated inversely with specimen age in the current study.

Since clinical studies often show an association of patella fractures and dislocations with the onset of chronic disease in the knee, these trauma patients appear to be more at risk from oblique than axial impacts on the knee. Yet, the current study only involved rigid impact interfaces that are not similar to current automobile interiors. The direct relevance of oblique versus axial impact loads on the knee to the automobile occupant will ultimately need to be determined using more deformable impact interfaces in future studies.

ACKNOWLEDGMENTS

This study was supported by a grant from the Centers for Disease Control and Prevention (R49/CCR503607). Its contents are solely the responsibility of the authors and do not necessarily represent the official views of the Centers for Disease Control and Prevention. We also thank Mr. R.S. Wade, Director of the Anatomical Services Division /

State Anatomy Board, University of Maryland for help in procuring human test specimens for this research project.

REFERENCES

Ahmed AM, Duncan NA. (2000) Correlation of patellar tracking pattern with trochlear and retropatellar surface topographies. J Biomech Egr 122 (6): 652-660.

Atkinson PJ, Haut RC. (1995) Subfracture insult to the human cadaver patellofemoral joint produces occult injury. J Orthop Res 13: 936-944.

Atkinson PJ, Garcia JJ, Altiero NJ, Haut RC. (1997) The Influence of Impact Interface on Human Knee Injury: Implications for Instrument Panel Design and the Lower Extremity Injury Criterion, Stapp Conf Proc 41: 167-180.

Atkinson PJ, Mackenzie CM, Haut RC. (1998a) Patellofemoral joint fracture load prediction using physical and pathological parameters. SAE 67-73.

Atkinson PJ, Newberry WN, Atkinson TS, Haut RC. (1998b) A method to increase the sensitive range of pressure sensitive film. J Biomech 31: 855-859.

Atkinson PJ, Haut R.C. (1999) Occult injuries in the subchondral plate are precursors to gross fracture in an experimenal model of impact injury in the human knee. 45th Orthopaedic Research Society Meeting.

Atkinson P, Haut R.C. (2001a) Impact responses of the flexed human knee using a deformable impact interface. Journal of Biomechanical Engineering 123 (3): 205-211.

Atkinson PJ, Haut RC. (2001b) Injuries produced by blunt trauma to the human patellofemoral joint vary with flexion angle of the knee. J Orthop Res 19(5): 827-833.

Atkinson T, Atkinson P. (2000) Knee injuries in motor vehicle collisions: A study of the National Accident Sampling System database for the years 1979-1995. Accid Anal Prev 32 (6): 786.

Banglmaier R, Dvoracek-Driksna D, Oniang'o T, Haut R. Axial compressive load response of the 90° flexed human tibiofemoral joint. Stapp Conf Proc 1999; 42 127-140.

Burks RT, Desio SM, Bachus KN, Tyson L, Springer K. (1998) Biomechanical evaluation of lateral patellar dislocations. Am J Knee Surg 11 (1): 24-31.

Burstein AH, Reilly DT, Martens M. (1976) Aging of bone tissue: Mechanical properties. J Bone Jt Surg 58-A (1): 82-86.

Dischinger P, Cushing B, Kerns T (1992) Lower extremity fractures in motor vehicle collisions: Influence of direction, impact and seatbelt use. 36th AAAM Conf: 319-326.

Ewers BJ, Jayaraman V, Banglmaier R, Haut R. (2000) The effect of loading rate on the degree of acute injury and chronic conditions in the knee after blunt impact. Stapp Conf Proc 44: 299-314.

Ewers BJ, Weaver BT, Haut RC. (2002) Impact orientation can significantly affect the outcome of a blunt impact to the rabbit patellofemoral joint. J Biomech 35: 1591-1598.

Johnson DL, Urban WP, Caborn DNM, Vanarthos WJ, Carlson CS. (1998) Articular cartilage changes seen with magnetic resonance imaging-detected bone bruises associated with acute anterior cruciate ligament rupture. Am J Sports Med 26: 409-414.

Li X, Haut RC, Altiero NJ. (1995) An analytic model to study blunt impact response of the rabbit P-F joint. J Biomech Egr 117: 485-491.

Lieb F, Perry J. (1968) Quadriceps function. An anatomical and mechanical study using amputated limbs. J Bone Jt Surg 50A: 1535

Lindahl O, Movin A, Ringqvist I. (1969) Knee extension. Measurement of the isometric force in different positions of the knee-joint. Acta Orthop Scand 40 (1): 79-85

Melvin J, Stalnaker R, Alem N, Benson J, Mohan D. (1975) Impact response and tolerance of the lower extremities. Stapp Conf Proc 19: 543-559.

Miller T, Martin P, Crandell JR (1995) Cost of lower limb injuries in highway crashes. Proc Inter Conf Pelvic Lower Extremity Inj: 47-57.

Morgan RM, Eppinger RH, Marcus JH, Nichols H. (1990) Human cadaver and hybrid III responses. Inter Conf Biomech Impacts.

Nomura E, Horiuchi Y, Inoue M. (2002) Correlation of MR imaging findings and open exploration of medial patellofemoral ligament injuries in acute patellar dislocations. Knee 9 (2): 139-143.

Nummi J. (1971) Fractures of the patella: A clinical study of 707 patellar fractures. Annales Chirurgiae et Gynaecologiae Fenniae Sup 179: 1-85.

Patrick L, Kroell C, Mertz H. (1965) Forces on the human body in simulated crashes. Stapp Conf Proc 9: 237-259.

Powell W, Ojala S, Advani S, Martin R. (1975) Cadaver femur responses to longitudinal impacts. Stapp Conf Proc 19: 561-579.

Rice D, MacKenzie E, et al. (1989) Cost of Injury in the United States: A Report to Congress, Atlanta, GA.

Reynolds, H. (1996) Personal Communication. Ergonomics Research Laboratory, LLC. (See www.erlllc.com for details of the study.)

Rupp JD, Reed MP, Van Ee CA, Kuppa S, Wang SC, Goulet JA, Schneider LW. (2002) The tolerance of the human hip to dynamic knee loading. Stapp Car Crash Conf J 46:211-228.

Robinson SC, States JD. (1978) Epidemiology, treatment, and prevention of patellar fractures. In: Symposium on Reconstructive Surgery of the Knee: 11-120. St. Louis, C. V. Mosby Company.

Sallay P, Poggi J, Speer K, Garrett W. (1996) Acute dislocation of the patella: A correlative pathoanatomic study. Am J Sports Med 24 (1): 52-60.

Sandmeier RH, Burks RT, Bachus KN, Billings A. (2000) The effect of reconstruction of the medial patellofemoral ligament on patellar tracking. Am J Sports Med 28 (3): 345-349.

Schneider L, Robbins D, Pflug M, Snyder R. (1983) Anthropometry of motor vehicle occupants. USDOT NHTSA Publication (1): 33.

Thompson R, Oegema T, Lewis J, Wallace L. (1991) Osteoarthritic changes after acute transarticular load. J Bone Jt Surg 73-A (7): 990-1001.

Yamada H. (1970) Mechanical properties of locomotor organs and tissues. In: Strength of Biological Materials: 19-105. Ed by FG Evans. Baltimore, The Williams & Wilkins Company.

CHAPTER THREE

EXCESSIVE COMPRESSION OF THE HUMAN TIBIO-FEMORAL JOINT CAUSES ACL RUPTURE BEFORE BONE FRACTURE

ABSTRACT

The knee is one of the most frequently injured joints in the human body. A recent study suggests that axial compressive loads on the knee may play a role in injury to the anterior cruciate ligament (ACL) for the flexed knee, because of an approximate 10° posterior tilt in the tibial plateau (Li et al., 1998). The hypothesis of the current study was that excessive axial compressive loads in the human tibio-femoral (TF) joint would cause relative displacement and rotation of the tibia with respect to the femur, and result in isolated injury to the ACL when the knee is flexed to 60°, 90° or 120°. Sixteen isolated knees from eleven fresh cadaver donors (74.3±10.5 years) were exposed to repetitive TF compressive loads increasing in intensity until catastrophic injury. ACL rupture was documented in 14/16 cases. The maximum TF joint compressive force for ACL failure was 4.9 ± 2.1 kN for all flexion angles combined. For the 90° flexed knee, the injury occurred with a relative anterior displacement of 5.4±3.8mm, a lateral displacement of 4.1±1.4mm, and a 7.8±7.0° internal rotation of the tibia with respect to the femur.

INTRODUCTION

The knee is one of the most frequently injured joints in the human body. Epidemiological studies have shown there are approximately 80,000 anterior cruciate ligament (ACL) tears in the United States each year with a total cost near one billion dollars (Griffin et al., 2000). This study also reports that 70% of ACL tears are due to "non-contact" types of injury. In a study of high school soccer, volleyball and basketball players for one season, 6 of 8 serious ACL injuries were "non-contact" (Hewett et al., 1999). Many studies have investigated the loading mechanisms that cause injury to the ACL. Boden et al. (2000) suggests that ACL injuries frequently occur in landing from a jump on one or both legs. In jump landings the knee may be flexed 60-80° (Hewett et al., 1996). ACL injury is also common in skiing with 25% to 30% of all ski related knee injuries involving the ACL (Speer et al., 1995). These injuries are mainly associated with twisting or a hard landing from a jump with a flexed knee (Ettlinger et al., 1995).

The ACL functions as the primary restraint to limit anterior tibial displacements for both 30° and 90° of knee flexion (Butler et al., 1980, Fukubayashi et al., 1982, Torzilli et al., 1994). It provides approximately 85% of the total ligamentous restraining force during anterior tibial displacement. Fleming et al. (2001) confirm this notion by showing that normal, *in vivo* weight bearing in the knee induces tensile strain in the ACL during anterior neutral-position shift of the joint. This study also supports earlier investigations showing that tensile forces develop in the ACL under physiological levels of tibio-femoral (TF) joint compressive loading (Li et al., 1998, Markolf et al., 1981). Torzilli et al. (1994) show that physiological levels of compressive loading on the human TF joint generates anterior tibial translation with respect to the femur for all flexion angles greater than 15°. This response is

primarily thought due to an inherent posterior tilt of the tibial plateau of 10°-15° (Li et al., 1998) (Figure 1). This study further suggests "that excessive compressive loads caused by impact loads along the tibial shaft (e.g., load from a jump landing) may contribute to injury of the anterior cruciate ligament, especially when the knee is flexed."

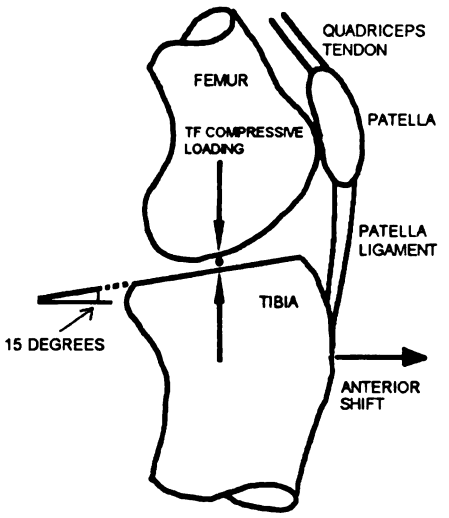

Figure 3.1. Anterior neutral-position shift, which is attributed to the inherent tilt of the tibial plateau, may cause an anterior translation of the tibia during TF joint loading.

The hypothesis of the current study was that the injury mechanism for a flexed, isolated human knee joint under excessive TF compression would be ACL rupture. The study will document the amount of relative joint displacement and rotation, and the compressive loads required to cause this injury in joints flexed 90°. Additional data showing the same injury in knees flexed to 60° and 120° will also be documented in the study.

METHODS

Experiments were conducted on 16 knees from 11 pairs of human TF joints (74.3 ± 10.5 years of age). The joints were procured through university sources (See Acknowledgement), stored at -20° C, and thawed to room temperature for 24 hours prior to testing. The joints were selected from donors with no known knee injuries. Five joint pairs

had been previously thawed and refrozen after another study. One knee from each of these five pairs was randomly selected for sequential TF joint loading with 60° of joint flexion (0° flexion for a straight leg), and the opposite joint was loaded with 120° of flexion. Six other knee specimens were loaded with 90° of joint flexion. In these 6 specimens motions of the femur were measured during axial loading of the tibia. Each joint preparation was sectioned approximately 15 cm proximal and distal to the center of the knee. The femur and tibia shafts were cleaned with 70% alcohol and potted in cylindrical aluminum sleeves with room temperature curing epoxy (Fibre Strand, Martin Senior Corp. Cleveland, OH), using a previously established protocol (Banglimaier et al., 1999).

A load transducer (Model #10101a-2500, Instron Corp. Canton, OH; load accuracy 0.5% of ±8896 N and resolution 0.004 N) was fixed to the actuator of a servo-hydraulic materials testing machine (Model 1331, Instron Corp. Canton, OH) (Figure 2). A rotary encoder (Model #RCH25D-6000, Renco Encoders Inc. Goleta, CA; accuracy ±0.01°) and stainless steel shaft were attached to the offset bar. The stainless steel shaft was connected to the potted tibia after passing through a sleeve bearing on a horizontal stabilizer bar. The rotary encoder allowed the internal-external rotations of the potted tibia to be measured with respect to the femur. The sleeve bearing and horizontal stabilizer bar allowed axial forces in the tibia to compress the TF joint with a minimal bending moment applied to the load transducer. The potted femur was secured to a fixture that allowed knee joint flexion angles of 60°, 90° and 120°. A bed of epoxy was added to the anterior surface of the femur to help distribute compressive loads over the proximal end of the femur. The fixture was attached to an X-Y translational plate that had linear encoders (Model #X00Z01A, Renishaw, Hoffman

Estates, IL; accuracy ±1 μm) attached to record anterior-posterior and medial-lateral motions of the femur relative to the tibia during tests

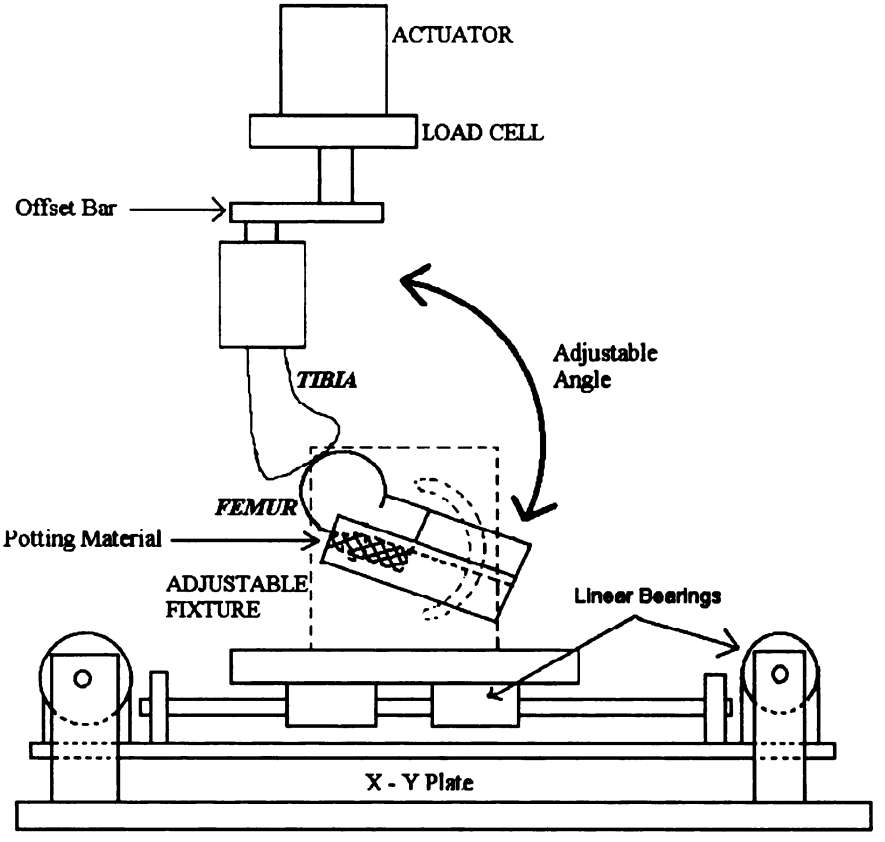

Figure 3.2. An adjustable fixture that recorded the motion of the femur in the X(anterior-posterior), Y(medial-lateral) plane and rotation of the tibia about its axis during TF joint loading.

on the 90° flexed joints. All joints were repeatedly loaded using a protocol in which a preload of 6-8 N was applied, followed by a single 10 Hz haversine load waveform that simulated the time to peak ground reaction loads in a typical jump landing (Richards et al., 1996). The load was increased by increments of 500 N in successive tests until catastrophic injury of the joint. The injury type and location were documented photographically for each specimen.

TF compression load and time to peak load were recorded in these experiments. In the 90° flexion experiments three additional variables; anterior-posterior femur displacement relative to the tibia, medial-lateral femur displacement relative to the tibia, and internal-external rotation of the tibia relative to the femur were also recorded. All data are given as mean ± one standard deviation.

RESULTS

Fourteen of sixteen knee joints at flexion angles of 60°, 90° and 120° suffered ACL rupture at a combined peak load of 4.9 ± 2.1 kN. ACL ruptures were mid-substance and occurred near its femoral insertion (Figure 3). Five of six tests with 90° flexion resulted in a torn ACL at a peak load of 5.6 ± 3.0 kN. Four of five 60° flexion tests and all five 120° flexion tests resulted in a torn ACL at peak loads of 4.9 ± 1.5 kN and 4.4 ± 1.0 kN, respectively (Table 1).

In the 90° test series the peak TF loads resulted in a posterior displacement of 5.4 ± 3.8 mm for the femur with respect to the tibia/fibula (Figure 4 A&B). There was also 4.1 ± 1.4 mm of medial motion of the femur with respect to the tibia/fibula, and 7.8 ± 7.0 degrees

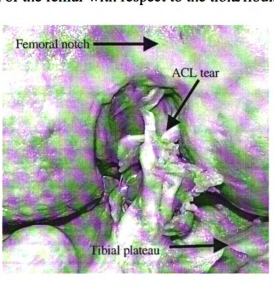

Figure 3.3. A typical injury in an unconstrained knee was rupture of the ACL.

of internal rotation of the tibia in these experiments (Table 2). Similar joint motions were observed in knees at 60° and 120° of flexion, but were not measured.

Specimen ID	Sex (Age)	Angle	Peak Load (kN)	Time to peak (ms)	Description
00524R	F (64)	60	4.2	56	ACL Tear
00524L	F (64)	120	3.7	51	ACL Tear, Meniscal Tear
00540L	M (69)	60	3.5	50	ACL Tear
00540R	M (69)	120	4.9	54	ACL Tear, Meniscal Tear
99535L	M (NA)	60	3.1	54	ACL Tear
99535R	M (NA)	120	2.9	53	ACL Tear
99750R	M (86)	60	5.9	60	ACL Tear, Femoral Condyle Fracture
99750L	M (86)	120	5.1	55	ACL Tear
99571L	M (74)	60	6.8	54	Tibial Plateau Fracture
99571R	M (74)	120	5.1	53	ACL Tear
		60 Average	4.9 (1.5)	55.0 (4.0)	
		120 Average	4.4 (1.0)	53.0 (1.0)	

Table 3.1. Experimental data for 60° and 120° flexed knee joint preparations in failure tests.

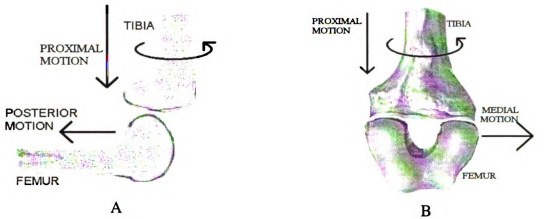

Figure 3.4. The application of TF loads resulted in proximal translation and internal rotation of the tibia, whereas the femur moved medial and posterior relative to the tibia.

Specimen ID	Sex (Age)	Angle	Peak Load (kN)	Time to peak (ms)	Femur AP Disp (mm)	Femur ML Disp (mm)	Tibial Rot (deg)	Description
00808L	F (78)	90	4.7	55	6.5	2	8.3	ACL Tear, Tibial Plateau Fracture
00882L	F (59)	90	5.5	57	4.1	5.4	6.4	ACL Tear
00886L	M (81)	90	5.4	54	4.6	4.2	7.3	ACL Tear
00894R	M (69)	90	11.3	55	12.6	5.4	20.9	ACL Tear, Femoral Condyle Fracture
00893R	F (89)	90	2.9	55	2.3	3	2.3	ACL Tear
00898L	M (70)	90	3.5	53	2.5	4.6	1.3	Tibial Plateau Fracture
		90 Average	5.6 (3.0)	54.8 (1.3)	5.4 (3.8)	4.1 (1.4)	7.8 (7.0)	

Table 3.2. Experimental data for 90° flexed knee joint preparations in failure tests.

DISCUSSION

The current study showed that rupture of the ACL occurred in 14/16 cases at 4.9 ± 2.1 kN of TF joint compressive loading. During compression the femur displaced posteriorly and medially with respect to the tibia, and the tibia rotated internally with respect to the femur. These motions would be similar to anterior and lateral motion of the tibia with respect to a fixed femur. Since the goal was to apply axial loads in the tibia, the femur was allowed to move in the current study.

Impulsive axial compressive loading of the knee occurs *in vivo* during landing from a jump with a flexed knee (Hewett et al., 1996). During landing ground forces are transmitted through the tibia to the TF joint. The ground reaction forces during a landing are approximately 4.2 and 6.1 times body weight for females and males, respectively (Hewett et al., 1996). These force levels are high enough to suggest that a typical individual may rupture an ACL, based on the current data from the aged isolated cadaver knee preparation. Additionally, the forces of contracting muscles, such as the quadriceps, could also produce significant compressive loads in the TF joint (Torzilli et al., 1994).

Although the line of action of the quadriceps muscle on the tibia is directed slightly posteriorly for flexion angles above 65° (Draganich et al., 1987), the effect of quadriceps loading on anterior-posterior tibial translation at 90° of knee flexion has been inconclusive (Li et al., 1999, Li et al., 2004, Torzilli et al., 1994). These studies document between 0.2 mm of posterior translation and 1 mm of anterior translation of the tibia for quadriceps loads between 133 N and 400 N. This may be due to the competing effects of the slight posterior vector of the quadriceps and the stronger proximal vector producing joint compression. A case study of elite skiers by McConkey (1986) suggests that extreme levels of quadriceps

force might be sufficient to produce ACL rupture. In the documented cases skiers strenuously attempting to recover from a falling-back position damaged their ACL. However, in at least 5 of 13 cases of ACL injury from that study a jump landing caused the large contractions of the quadriceps muscles. In light of data from the current study the mechanism of ACL injury in these cases may have actually been associated more with the combination of TF compression loads generated during the landing, and the joint compression due to quadriceps contraction.

In contrast, hamstrings muscle contraction produces a posterior directed force on the tibia (Pandy and Shelburne, 1997 and Li et al., 1999). This joint constraint force was documented in a previous study at 90° flexion for isolated joint specimens (Jayaraman et al., 2001). A mean load of 1.2 ± 0.5 kN is sufficient to prevent anterior motion of the tibia at fracture-causing load levels of TF joint compression (9.2 ± 2.6 kN, n=6) .

While previous studies have documented ACL injury loads from anterior shear loading (Aune et al., 1997) and quadriceps tension for the slightly flexed knee (DeMorat et al., 2004), the authors are not currently aware of previous studies that document the TF compressive loads that cause rupture of the ACL. Several knee joint compression studies have used a constrained knee joint model in which the tibia is only allowed to move in the proximal-distal direction relative to the femur (Hirsch and Sullivan, 1965, Kennedy and Bailey, 1968 and Banglmaier et al., 1999). The most recent study, Banglmaier et al. (1999), examines TF impact responses using 90° flexed, isolated human knee joints. The authors document fracture of the medial and/or lateral tibial plateau, or medial femoral condyle or notch at a maximum compressive load of 8.0 ± 1.8 kN. This load is significantly higher than the failure load documented in the current study. In fact, the lower extremity injury criterion

for TF joint loading used in the automotive industry is currently based on data from these constrained knee joint studies (Kuppa et al., 2002). The current study would suggest that the current injury criterion should be re-examined using unconstrained knee joint preparations.

A study by Woo et al. (1991) documents that approximately 6 mm of tensile deformation and 658 ± 129 N of load is required to rupture the 60-97 year old ACL mid-substance in its anatomic orientation. Since the ACL is oriented approximately 7° with respect to the tibial plateau in the 90° flexed knee (Herzog and Reed, 1993), it seems reasonable that tensile failure of the ACL occurred at 5.4 ± 3.8 mm of posterior translation of the femur in the current study. Yet, this does not take into account medial translation of the femur and internal rotation of the tibia that also occurred during TF joint compression. Because of differences in test methodologies between Woo et al., 1991 and the current study (tension versus compression) failure loads could not be directly compared.

There were a number of limitations in the current study that need to be addressed in the future. Since isolated knee preparations were used, the potential effects of muscle forces acting across the knee were not included. Since documented loads in jump landings may approach those causing ACL rupture in the current study with aged cadaver specimens, these data suggest muscle action is essential in preventing ACL injuries. Because of their ages these specimens only represent a small portion of today's population, and not that of the population active in sports. Additional studies are required on a younger population of human knees to address the potential for ACL injuries in sports related jump landings. Additionally, the repetitive nature of the tests in the current study may be a limitation. The potential consequence of accumulated microdamages in soft tissue structures, such as the

ACL, must be considered in future studies. Microdamages are known to occur prior to gross rupture in other ACL models (Yahia et al., 1990).

In summary, this study showed that ACL rupture occurred in the human knee via excessive TF compressive loading. Since the peak compressive loads were in the range that could regularly be generated during a jump landing, the role of muscle forces in preventing anterior translation, lateral displacement and internal rotation of the tibia are essential constraints and therefore must be investigated in future studies using younger human cadaver specimens that represent the population involved in sports today.

ACKNOWLEDGEMENT

This study was supported by a grant from the Centers for Disease Control and Prevention, National Center for Injury Prevention and Control (R49/CCR503607). Its contents are the sole responsibility of the authors and do not necessarily represent the official views of the Centers for Disease Control and Prevention. The authors wish to gratefully acknowledge Cliff Beckett, Vijay Jayaraman, Eric Sevensma, Masaya Kitagawa and Chris O'Neill for technical assistance during this study. We also thank Mr. R.S. Wade, Director of the Anatomical Services Division / State Anatomy Board, University of Maryland for help procuring these test specimens.

REFERENCES

Aune, A.K., Cawley, P.W., Ekeland, A., 1997. Quadriceps muscle contraction protects the anterior cruciate ligament during anterior tibial translation. Am J Sports Med. 25 (2): 187-190.

Banglmaier, R., Dvoracek-Driksna, D., Oniang'o, T., Haut, R.C., 1999. Axial compressive load response of the 90° flexed human tibio-femoral joint. 43rd Stapp Car Crash Conf., 127-140.

Boden, B.P., Dean, G.S., Feagen, J.A Jr., 2000. Mechanisms of anterior cruciate ligament injury. Orthopedics. 23 (6): 573-8.

Butler, D.L., Noyes, F.R., Grood, E.S., 1980. Ligamentous restraints to anterior-posterior drawer in the human knee. J Bone Jt Surg. 62A: 259-270.

DeMorat, G., Weinhold, P., Blackburn, T., Chudik, S., Garrett, W., 2004. Aggressive quadriceps loading can induce noncontact anterior cruciate ligament injury. Am J Sports Med. 32 (2): 477-483.

Draganich, L.F., Andriacchi, T.P., Anderson, G.B.J., 1987. Interaction between intrinsic knee mechanics and the knee extensor mechanism. J Orthop Res. 5: 539-547.

Ettlinger C.F., Johnson, R.J., Shealy, J.E., 1995. A method to help reduce the risk of serious knee sprains incurred in alpine skiing. Am J Sports Med. 23(5): 531-537.

Fleming, B., Renstrom, P., Beynnon, B., 2001. The effect of weight-bearing and external loading on anterior cruciate ligament strain. J Biomech 34: 163-170.

Fukubayashi, T., Torzilli, P.A., Sherman, M.F., Warren, R.F., 1982. An in vitro biomechanical evaluation of anterior-posterior motion of the knee, tibial displacement, rotation and torque. J Bone Jt Surg. 64A: 258-264

Griffin, L.Y., Agel, J., Albohm, M.J., et al. 2000. Noncontact anterior cruciate ligament injuries: Risk factors and prevention strategies. J Am Acad Orthop Surg. 8 (3): 141-150.

Hewett, T.E., Stroupe, A.L., Nance, T.A., Noyes, F.R., 1996. Plyometric training in female athletes: Decreased impact forces and increased hamstrings torques. Am J Orthop Soc Sports Med. 24 (6): 765-773.

Hewett, T.E., Lindenfeld, T.N., Riccobene, J.V., Noyes, F.R., 1999. The effect of neuromuscular training on the incidence of knee injury in female athletes: A prospective study. Am J Orthop Soc Sports Med. 27 (6): 699-705.

Herzog, W., Reed, L.J., 1993. Lines of action and moment arms of the major force-carrying structures crossing the human knee joint. J Anat. 182 (Pt 2): 213-30.

Hirsch, G., Sullivan, L., 1965. Experimental knee-joint fractures. Acta Orthop Scand. 36: 391-399.

Jayaraman, V.M., Sevensma, E.T., Kitagawa, M., Haut, R.C., 2001. Effects of anterior-posterior constraint on injury patterns in the human knee during tibio-femoral joint loading from axial forces through the tibia. Stapp Car Crash J. 45: 449-468.

Kennedy, J.C., Bailey, W.H., 1968. Experimental tibial-plateau fractures: studies of the mechanism and a classification. J Bone Jt Surg 50(A): 1522-1534.

Kuppa, S. 2002. An overview of knee-thigh-hip injuries in frontal crashes in the United States. 17th ESV

Li, G., Rudy, T., Allen, C., 1998. Effect of combined axial compressive and anterior tibial loads on in situ forces in the anterior cruciate ligament: a porcine study. J Orthop Res 16:122-127.

Li, G., Rudy, T.W., Sakane, M., Kanamori, A., Ma, C.B., Woo, S.L.-Y., 1999. The importance of quadriceps and hamstring muscle loading on knee kinematics and in-situ forces in the ACL. J Biomech 32: 395-400.

Markolf, K.L., Bargar, W.L., Shoemaker, S.C., Amstutz, H.C., 1981. The role of joint load in knee stability. J Bone Jt Surg. 63: 570-585.

McConkey, JP., 1986. Anterior cruciate ligament rupture in skiing: A new mechanism of injury. Am J Sports Med. 14 (2): 160-164.

Pandy, M.G., Shelburne K.B., 1997. Dependence of cruciate-ligament loading on muscle forces and external load. J Biomech. 30 (10): 1015-1024.

Richards, D.P., Ajemian, S.V., Wiley, J.P., Zernicke R.F., 1996. Knee joint dynamics predict patellar tendonitis in elite volleyball players. Am J Sports Med. 24 (5): 676-683.

Speer, K.P., Warren, R.F., Wickiewicz, T.L., Horowitz, L., Henderson, L., 1995. Obeservations on the injury mechanism of anterior cruciate ligament tears in skiers. Am J Sports Med. 23 (1): 77-81.

Torzilli, P., Deng, X., Warren, R., 1994. The effect of joint-compression load and quadreceps muscle force on knee motion in the intact and the anterior cruciate ligament-sectioned knee. Am J Sports Med. 22: 105-112.

Woo, S.L., Hollis, J.M., Adams, D.J., Lyon, R.M., Takai, S., 1991. Tensile properties of the human femur-anterior cruciate ligament-tibia complex: The effects of specimen age and orientation. Am J Sports Med. 19 (3): 217-225.

Yahia, L., Brunet J., Labella, S., Rivard C.H., 1990. A scanning electron microscopic study of rabbit

CHAPTER FOUR

THE EFFECT OF AXIAL LOAD IN THE TIBIA ON THE RESPONSE OF THE 90° FLEXED KNEE TO BLUNT IMPACTS WITH A DEFORMABLE INTERFACE

ABSTRACT

Lower extremity injuries are a frequent outcome of automotive accidents. While the lower extremity injury criterion is based on fracture of bone, most injuries are of less severity. Recent studies suggest microscopic, occult fractures may occur in the knee for impacts with rigid and deformable interfaces due to excessive levels of patello-femoral contact pressure. One method of reducing this contact pressure for a 90° flexed knee is to provide a parallel pathway for knee impact loads into the tibial tuberosity. Yet, blunt loads onto the tibial tuberosity can cause posterior drawer motion of the tibia, leading to injury or rupture of the posterior cruciate ligament (PCL). Recently studies have shown that axial loads in the tibia, which are measured during blunt loading on the knee in typical automobile crashes, can induce anterior drawer motion of the tibia and possibly help unload the PCL. The purpose of the current study was to explore the effect of combined anterior knee loading (AKL) and axial tibia loading (ATL), without muscle tension, on response and injury for the 90° flexed human knee.

In repeated impacts with increasing ATL the stiffness of the knee to an AKL impact increased. For a 3 kN AKL, the stiffness of the knee increased approximately 26% when the ATL was increased from 0 kN to 2 kN. For 6 kN and 9 kN AKL, the stiffness was increased approximately 17% and 20%, respectively, when the ATL was increased from 0 kN (uniaxial) to 4 kN (biaxial). The posterior tibial drawer was shown to increase

with increased AKL and decrease with increased level of ATL at an average of 0.3 mm per 1 kN ATL for both the 3 kN and 6 kN ATL scenarios. For 9 kN AKL this drawer displacement was significantly reduced for biaxial versus uniaxial impacts, from 7.4±1.4 mm to 5.8±0.6 mm, respectively. Additionally, the percentage of the load carried by the tibial tuberosity increased with an ATL. For AKL impacts of 3, 6, and 9 kN, the percentage of load carried by the tibial tuberosity increased from 2.1% (range 0-19%) to 4.9% (0-36%), 2.1% (0-15%) to 6.9% (0-36%), and 8.7% (0-25%) to 12.7% (0-33%), respectively, between uniaxial and biaxial tests. The biaxial loading scenario also resulted in a reduction of the patello-femoral contact force by approximately 11.2% versus uniaxial impacts. Ten knee impacts resulted in PCL tears at an average peak load of 12.7±2.4 kN in biaxial impacts (n=5) and 12.0±3.1 kN for uniaxial impacts (n=5). These PCL injured specimens had an average age of 62±11.3 years. The remaining specimens (78±12.9 years of age) had bone fractures at approximately 9.0±3.1 kN.

This study showed that combinations of compressive ATLs, whose peaks occur at nearly the same time and magnitude as AKL, have a stiffening effect on the response of the knee impacting a stiff but deformable interface. Furthermore, ATL can reduce the posterior drawer of the tibia, which is the basis for PCL injury in the knee. While the current injury tolerance criterion reflect the vulnerability of the PCL to injury by limiting tibial drawer to 15 mm, the current dummy design does not incorporate the stiffening effect of an ATL that may occur at the same time as knee contact into an instrument panel in a typical crash environment.

INTRODUCTION

The yearly medical cost of automobile accident injuries in the United States in 2000 was $32.6 billion (Blincoe et al., 2002). These injuries account for approximately 3.2% of the US total medical costs, second only to cancer (Miller et al., 1998). Lower extremity injuries are a frequent outcome of automotive accidents (Fildes et al., 1997). Kuppa (2002) documents that the comprehensive cost of lower extremity injuries is $7.64 billion annually, and it makes up a significant percentage of the total motor vehicle trauma. These injuries include 18% of all Abbreviated Injury Scale (AIS) 2+ injuries to front seat occupants in frontal collisions and 23% of the associated life years lost to injury. Injuries to the knee-thigh-hip complex account for 52%, or $4 billion, of these lower extremity injury costs.

The current injury threshold limit for the knee-thigh-hip complex prescribed by FMVSS 208 and used in NCAP is 10 kN of axial femur load for the 50^{th} percentile male. This level of femur load has been associated with a 35% probability of AIS 2+ injury in human cadavers (Morgan et al., 1990). Patella and distal femur fractures were the most common injuries in this data set. These data compare to those in a recent study of the 1993-1995 National Accident Sampling System (NASS) showing that 17% of knee injuries in automobile crashes for those years were patella fractures, which occurred at a frequency similar to that of femur fractures (Atkinson and Atkinson, 2000). In contrast, tendon and ligament injuries (AIS 2 and 3) account for approximately 2.5 % of all the knee injuries.

Much of the data reported in the Morgan et al. (1990) study documents experimental patella and distal femur fractures using rigid impact interfaces. Yet,

automotive interior contact points would more typically involve contact on the knee via a deformable interface. Early cadaver studies have shown that while rigid interfaces into the knee typically generate patella fracture, deformable interfaces more often produce femur fractures (Powell et al., 1975, Melvin et al., 1975, Patrick et al., 1965). Recent studies from this laboratory, using isolated cadaver knees, confirm the data of earlier studies on whole human cadavers. While 5 kN impacts, via a rigid interface, result in transverse patella fracture, no injuries have been documented in the patella or femur following 5.8 kN impacts via a deformable interface (1.4 MPa crush strength Hexcel) (Atkinson et al., 1997). In contrast, 5 kN impacts with a slightly stiffer, but deformable, interface (3.3 MPa crush strength Hexcel) produced occult microcracks underlying the retropatellar cartilage (Atkinson and Haut, 2001). A recent study shows that these types of occult microcracks are seen in automobile accident victims suffering hip fractures (Bealle and Johnson, 2000). The clinical literature suggests these occult microcracks (bone bruises) occur often in ligament injured sports patients and lead to early degradation of knee joint cartilage reminiscent of that which occurs in the early stages of osteoarthritis (Johnson et al., 1998).

Atkinson et al. (1997) also suggest that these occult microcracks of bone underlying the retropatellar cartilage in the joint are caused by excessive levels of patello-femoral (PF) joint pressure during blunt impact onto the knee, and they are precursors of a gross fracture of the patella. One method of reducing PF joint contact forces during a blunt impact is to provide a parallel pathway of load transmission across the knee, by increasing the contact area over the knee (Hering and Patrick, 1977). For a typical crash configuration of a 90° flexed knee this would involve contact on the tibial tuberosity

(Figure 1). Yet, blunt loads acting solely on the tibial tuberosity have been shown to present the possibility of damage to the posterior cruciate ligament (PCL) via rupture or avulsion from the tibia. Blunt loads of 7 kN onto the 90° flexed knee (contacting the patella and tibial tuberosity) of seated human cadavers resulted in five PCL avulsion fractures and one PCL tear out of eight knees (Viano et al., 1978). Isolated joint tests in the same study show partial tears of the PCL at a relative translation (drawer) of the tibia with respect to the femur of 14.4 mm and complete failure of this ligament at 22.6 mm. Based on these data Mertz (1993) recommends an injury threshold level of 15 mm of relative translation between the femur and tibia at the knee joint for a 50^{th} percentile male.

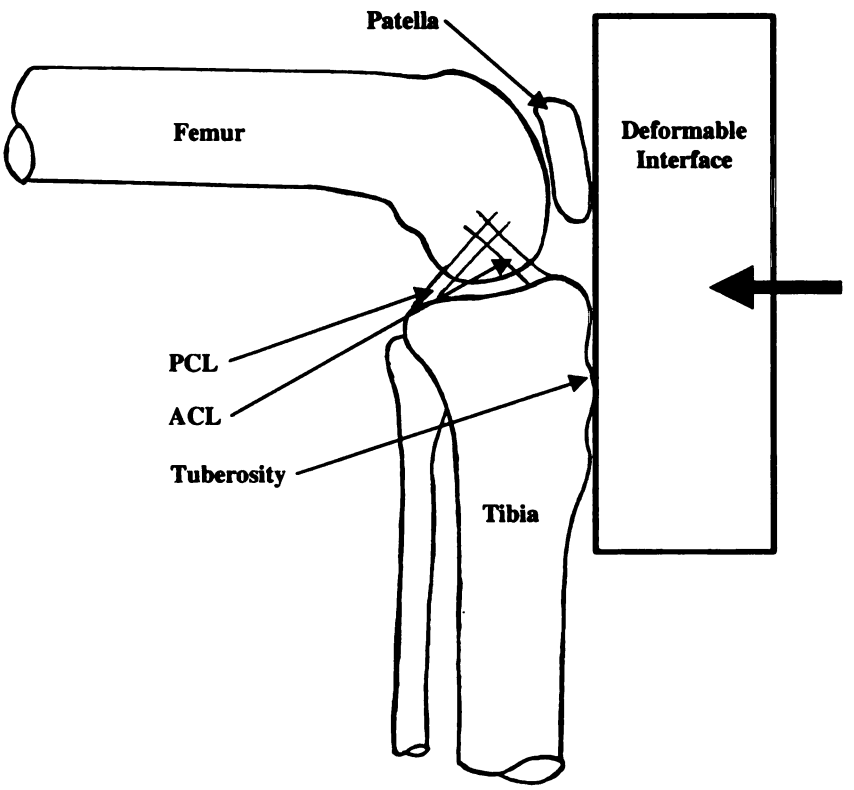

Figure 4.1. Orientation of anterior knee impact on the patella and tibial tuberosity.

Interestingly, while a blunt impact to the front of the knee via the tuberosity of the tibia can result in posterior translation (drawer) of the tibia relative to the femur, recent studies show that axial tibia loads can cause anterior translation of the tibia with respect to the femur (Torzilli et al., 1994, Fleming et al., 2001, Li et al., 1998, Markolf et al., 1981). In fact, a recent study has shown that approximately 5.8 kN of axial tibia load (ATL) is sufficient in a 90° flexed, isolated human knee to cause rupture of the anterior cruciate ligament (ACL) (Jayaraman et al., 2001). This response is primarily thought due to an inherent anterior-posterior tilt of the tibial plateau. While this type of injury has only been shown in a few experiments (Funk et al., 2000), the injury is not well documented in the NASS database per se. Crash simulation data suggests that the level of ATL needed for ACL rupture may be achieved (Bedewi and Diggs 1999). One possible explanation for the lack of field ACL injury data in auto crashes may be that when ATL peaks during a crash, the knee may also be in contact the instrument panel (knee bolster), and anterior loads in the knee (AKL) may also peak at nearly the same time and magnitude (Bedewi and Diggs, 1999) (Figure 2).

Figure 4.2. Combined loading scenario caused by instrument panel contact and floor pan intrusion.

The AKL may act to restrain anterior translation of the proximal tibia, preventing ACL injury. In effect, the knee may be "constrained". In this situation experimental data from isolated joints under flexion angles varying from 0-20° from a straight leg document tibial plateau fractures occurring at approximately 8 kN of ATL (Hirsch and Sullivan, 1965). Based on those tests, Mertz (1993) recommends a proximal tibia axial force limit of 8 kN to address tibial plateau and split femoral condyle fractures in the 50th percentile male. The Jayaraman et al. (2001) study documents fracture of the tibial plateau and femoral condyle at 9.2 kN of ATL for the 90° flexed, isolated tibio-femoral joint. Banglemaier et al. (1999) dynamically tested 90° flexed, isolated tibio-femoral joints and document fractures of the femoral notch, femoral condyles, tibial plateau and combination injuries at an average peak load of 8 kN delivered axially through the tibia.

The objective of the current study was to investigate the effects of combined axial loads in the tibia (ATL) and anterior knee loads to the patella and tibial tuberosity (AKL) via a stiff but deformable impact interface using isolated human knee joint preparations flexed at 90°. The hypotheses of the study were that; (1) ATL presented during blunt knee impacts would result in anterior translation of the tibia, thereby stiffening the knee's response during contact with a deformable interface. (2) The constraint of the knee with the deformable interface would prevent ACL rupture from ATL large enough to rupture the ACL in unconstrained tests. (3) The application of an ATL during blunt knee contact involving the tibial tuberosity would help unload the PF joint due to increased load being supported in the tibia via its anterior translation. (4) And, the AKL required to generate PCL rupture, via contact on the tuberosity of the tibia, would be increased by an anterior

directed resultant force coming from an axial load component generated by simultaneously applying an axial load in the tibia.

METHODS

Blunt impact was delivered to ten pairs and one single knee joint aged 71.7±14.6 years. The limbs were procured from university sources (see Acknowledgment) and stored at -20°C until testing. The joints were selected from donors with no known knee injuries or signs of surgical intervention during a postmortem evaluation. Twenty-four hours prior to testing the joints were thawed to room temperature. The preparations were sectioned 20 cm inferiorly and superiorly to the knee joint. Superficial muscle tissues were excised from each preparation leaving the articular joint capsule intact. Therefore, muscle tension was not simulated during the experiments. The femur and tibia/fibula were cleaned with alcohol and potted in 6.3 cm diameter cylindrical aluminum sleeves with room temperature curing epoxy (Fibre Strand #6371, Martin Senour Co. Cleveland, OH). Figure 3 shows that the tibia/fibula was centered and aligned axially within the 10 cm deep cylinder. The femur was also aligned axially, but the posterior surface was placed adjacent to the edge of a 14 cm deep cylinder and extra epoxy was placed between the anterior surface of the femoral condyle and an extended piece of the aluminum cylinder. This extra epoxy supported the femoral condyle under an ATL. Each test specimen was mounted in the fixture with 90° of flexion. This flexion angle was visually established by aligning the femur and tibia with a 90° square tool. The femur was oriented vertically with the knee joint facing up, and the tibia was positioned horizontally

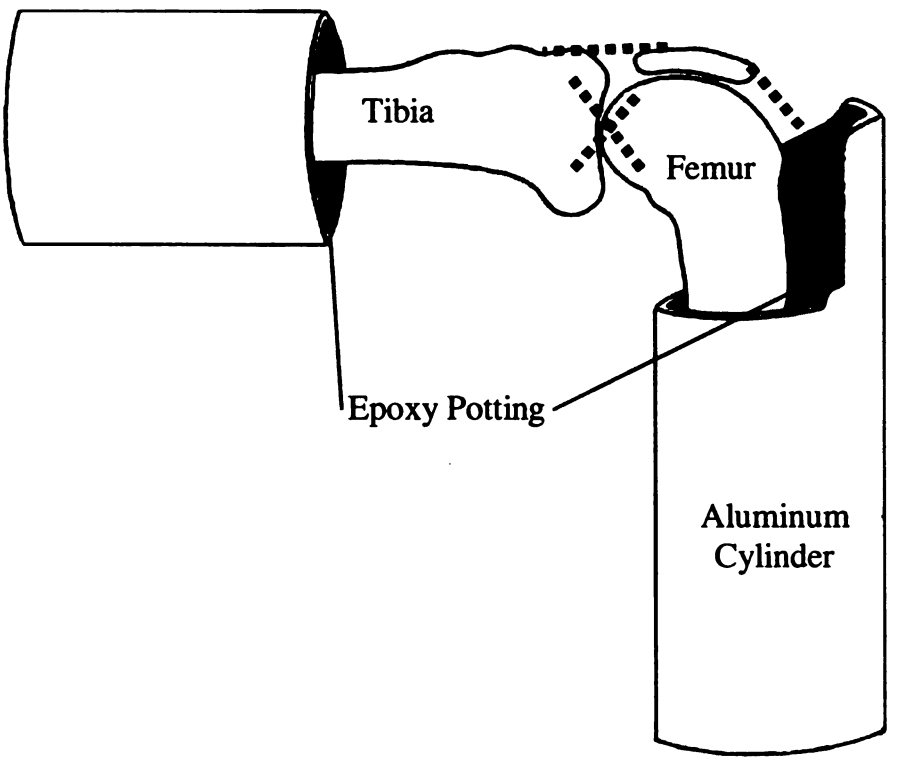

Figure 4.3. Two-dimensional schematic of the 90° flexed knee after dissection and potting in epoxy-filled aluminum cylinders.

in the fixture. The femur was not allowed to rotate axially, but axial rotation of the tibia was allowed via the horizontal hydraulic actuator of the testing machine (Figure 4).

Figure 4 shows how the impact loads were applied simultaneously in two directions with two servo-controlled hydraulic actuators that were oriented 90° to each other. This biaxial testing machine consisted of a vertically oriented 5.5 kip actuator (model #204.52, MTS Corp., Eden Prairie, MN) on a 22 kip (model #312.21, MTS Corp.) frame, and a horizontally oriented 11 kip actuator (model # 204.61, MTS Corp.) mounted to a custom designed frame. The actuators had separate electronic controls (model #458.2 Microconsole for the vertical actuator and a #448.82 Test Controller for the horizontal actuator, MTS Corp.). The actuators were programmed to run simultaneously with a

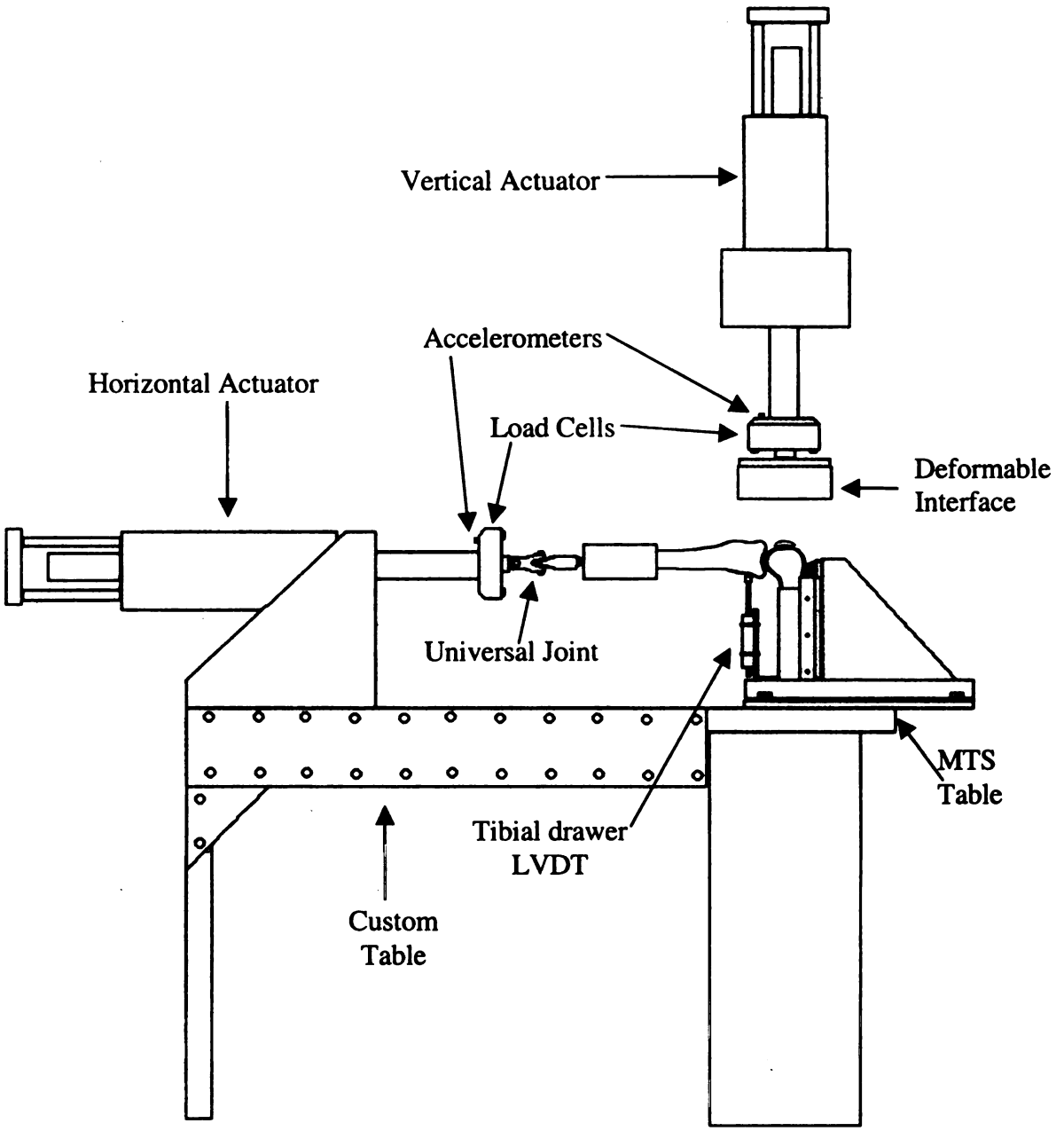

Figure 4.4. Biaxial impact machine and test set-up for simultaneous AKL and ATL impacts to the 90° flexed knee.

common source waveform generator (model #458.91 Microprofiler, MTS Corp.) that generated a haversine load waveform input with a 50 ms time to peak. Prior to each test a preload of approximately 50 N was applied to the joint in both actuators for biaxial impacts and only in the vertical actuator for uniaxial impacts.

A repetitive loading protocol was followed based on Table 1, with the programmed peak loads increasing for each impact until a gross failure was visualized in the joint. Specimen pairs followed identical impact protocols up to test 6. After test 6, one knee was randomly chosen from each pair to be loaded uniaxially, while the opposite knee was loaded with a sequence of biaxial impacts. The uniaxial knee from each pair was subjected to impacts consisting of only an AKL, which was increased by increments of 3 kN until joint failure. The biaxial knee was also impacted with an AKL increasing by 3 kN increments after test 6, however these impacts were in combination with an ATL of 4 kN.

	AKL (kN)	ATL (kN) 1st knee	ATL (kN) 2nd knee
Test 1	3	0	Same
Test 2	3	Preload	Same
Test 3	3	2	Same
Test 4	6	0	Same
Test 5	6	2	Same
Test 6	6	4	Same
Test 7	9	0	4
Test 8	12	0	4
Test 9	15	0	4
Test 10	18	0	4

Table 4.1. Impact sequence for biaxial knee tests.

Some specimens were loaded with slightly different impact protocols, as described next. The first two pairs of knees in the study did not follow the pattern established by Table 1 for test 1-6. Instead, the uniaxial knee from each pair was subjected to only an AKL, which started at 3 kN and increased by increments of 3 kN

until failure. The biaxial knee from each pair was also impacted with a 3 kN incremental AKL, but these were combined with an ATL which was increased by 2 kN increments up to 6 kN. Four additional knees were also loaded normally through test 6, however an additional impact with 6 kN of AKL and 6 kN of ATL was also applied. The biaxial knee in each of these pairs was loaded with 6 kN of ATL until failure. Finally, there were three supplementary knees that did not follow the normal protocol, but failure level data was documented and reported here.

All AKL impacts were delivered with a stiff but deformable interface (3.3 MPa crush strength aluminum honeycomb #CR III 5056, Hexcel Corp., Starnford, CT). The interface was attached to a 15 cm by 15 cm by 1.25 cm thick steel plate. The honeycomb was not precrushed. A 5 kip (thousands of pounds) load transducer (model #3210AF-5K, Interface, Scottsdale, AZ) was attached to the actuator behind the knee impact interface. ATL was applied to the tibia/fibula cylinder via the horizontal actuator through a universal joint. An 18 kip load transducer (model # FFL (18/±12)u-(3/±2)sp, Strainsert Co., West Conshohocken, PA) was attached to the actuator behind this universal joint. Load data from both transducers were inertially compensated with accelerometers (model #353B15,PCB Piezoelectronics, Depew, NY). A LVDT (model #1002 XZ-D, Shaevitz, Fairfield, NJ) was attached to the base of the femoral potting cylinder and measured the posterior displacement (drawer) of the tibia relative to the femur. Four channels of data (load and displacement) from the testing machine, two channels of compensated load data, and one channel of displacement data from the LVDT were collected at 1000 Hz and recorded on a personal computer with a 16-bit analog/digital board (model DAS 1600; Computer Boards, Mansfield, MA).

Prior to each sequential test, pressure sensitive film (Prescale; Fuji Film Ltd., Tokyo, Japan) was manually inserted under the quadriceps tendon into the patello-femoral joint to measure the magnitude and distribution of contact pressures generated in the joint during impact. The pressure film was placed to ensure that it covered the entire retropatellar surface. Low (0-10 MPa) and medium (10-50 MPa) range pressure films were stacked together and sealed between two sheets of polyethylene (0.04 mm thick) to prevent exposure of the film to body fluids (Atkinson et al., 1998). A new pressure film packet was placed under the quadriceps tendon and into the patello-femoral joint immediately prior to each test in the sequence. The film was later removed from the sealed polyethylene packet and digitally scanned at 150 dpi (ScanMaker E6, Microtek International Inc., Redondo Beach, CA). The film was converted to grey scale values using commercial software (Scion Image 4.0.2; Scion Corp, Frederick, MD). Calibration tests were performed on similar film packets prior to the cadaver tests. Briefly, a haversine, displacement-controlled waveform was used to generate calibration peak loads in approximately 50 ms. The calibration film packets were loaded between two polished stainless steel plates. This provided a dynamic calibration for the pressure film over the range of loads used in the current study. As described by Atkinson et al. (1998), the stacking order of the film and the rate of loading are important factors for accurate calibration of joint contact pressures.

After each impact in the repetitive series of tests, the specimen were examined for gross fracture of bone by visual inspection of the entire knee joint and palpation of the patello-femoral joint from under the quadriceps tendon. Ligaments were also inspected after each impact by a manual laxity evaluation performed on the joint after each test.

Following the failure test, each joint was carefully dissected and all injuries were documented photographically. After potting the knees in epoxy, but before impacting, medial-lateral radiographs were obtained with 90° of knee flexion. Subsequently, Figure 5 documents how these radiographs were used to approximate the anterior-posterior slope angle of the tibial plateau in each specimen.

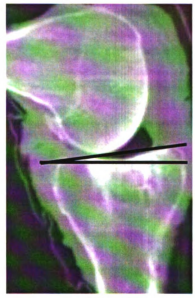

Figure 4.5. Lateral radiographic image of the 90° flexed knee showing the anterior-posterior tibial plateau slope angle.

Additionally, five knees (from 3 subjects, average age=65) were scanned by computed tomography (Light Speed C.T. 4, General Electric) at 1.25 mm resolution, with a 50% overlap for increased fracture imaging capability. The knees chosen for CT evaluation were from the younger specimens that appeared to have high tissue quality. CT scanning was done prior to impacting. CT scans were also taken following impacts in cases where load-displacement data appeared to suggest a ligamentous failure that was not obvious with gross examination of the joint. The focus of the CT scan was to search for occult microscopic fractures of bone in the tibial plateau or femur. Finally, one knee joint from

each pair was also scanned by dual energy X-ray absorptiometry (DEXA, QDR 4500 Hologic Inc., Bedford, MA) to measure the average bone mineral density for the entire knee (Figure 6). The femoral condyles and tibial plateau of each specimen were scanned in an anterior-posterior direction using an established technique (Murphy et al., 2001).

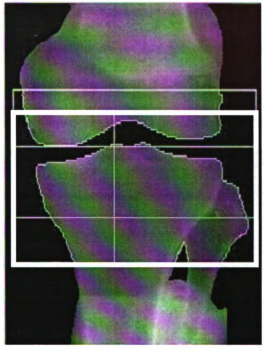

Figure 4.6. Knee joint BMD measurement region in a DEXA scan from a representative specimen. The scan area is represented by the trace within the thick rectangle.

The deformable impact interface (Hexcel) from each test and shown in Figure 7 was digitally scanned at 300 dpi. The areas of patella and tibial tuberosity contact were measured using image analysis software (SigmaScan, Systan Software Inc., Point Richmond, CA.). The percentage of tibia contact area to patella contact area was then computed and served as a reference to compute load sharing between the two bone surfaces.

The results (mean ± standard deviation) of peak load and peak displacement from the horizontal and vertical sensors, and the tibial drawer from the LVDT were

documented for each test in the study. Peak loads, displacements and stiffnesses for various test configurations were compared with one-way, repeated measure ANOVAs. The percentage of interface contact area on the tibia versus patella was compared (mean, range) between uniaxial and biaxial specimens with paired t-tests. Specimen age, bone mineral density and tibia slope angle were compared with unpaired t-tests. Multi-variate linear regressions were developed to show the relationship between tibial drawer or patello-femoral contact force and the applied loads (Sigma Stat v2.03, SPSS Inc., Chicago, IL). Statistical significance in all tests was set at $p<0.05$.

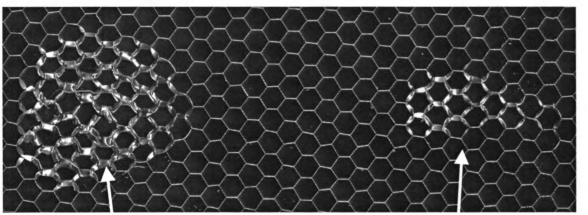

Figure 4.7. Hexcel deformation from a representative specimen (31382R6).

RESULTS

Sub-Injury Tests

The output load-time response curves for simultaneous AKL and ATL impacts showed similar loading and unloading regions as Figure 8 with an average time to peak load of approximately 50 ms. Figure 9 documents the overall shape for all load-displacement responses during the loading portion of the tests was linear with r^2 values

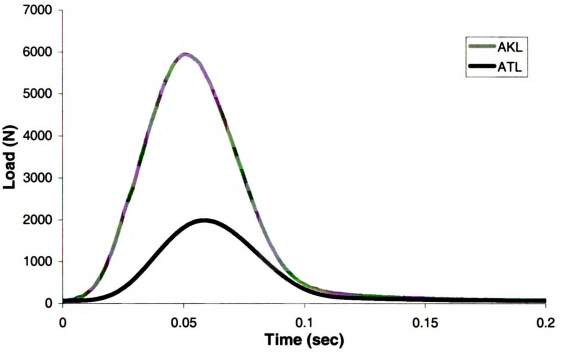

Figure 4.8. Load versus time curves for test 5 from a representative specimen.

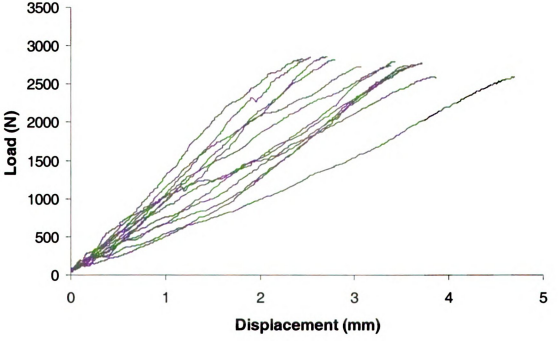

Figure 4.9. Load versus displacement loading curves for test 3.

above 0.95. The impact response of the isolated knee in biaxial tests produced an increasing stiffness with increasing ATL in the various sub-failure AKL tests. Comparisons were made between tests with similar AKL levels (tests 1-3, average AKL of 2.6±0.2 kN [Table 2] and tests 4-6, average AKL of 5.6±0.2 kN [Table 3]). Figure 10 shows that the AKL impact load-displacement response of test 3 (831±222 N/mm), the impact with the highest ATL in this group, was significantly stiffer than test 1 (659±208 N/mm, p=0.002) and test 2 (716±222 N/mm, p=0.009). The ATL stiffness in test 3 was 860±188 N/mm, but could not be calculated for tests 1 and 2 because no load was delivered in that direction. In the higher group, the AKL stiffness of test 6 (921±193 N/mm) was significantly stiffer than test 4 (786±155 N/mm, p=0.002), but not test 5 (850±188 N/mm, p=0.123). In this group there was also a significant difference between test 4 and 5 (p=0.018). However, there was no significant difference between the ATL stiffness responses for test 5 (1299±333 N/mm) and test 6 (1314±284 N/mm).

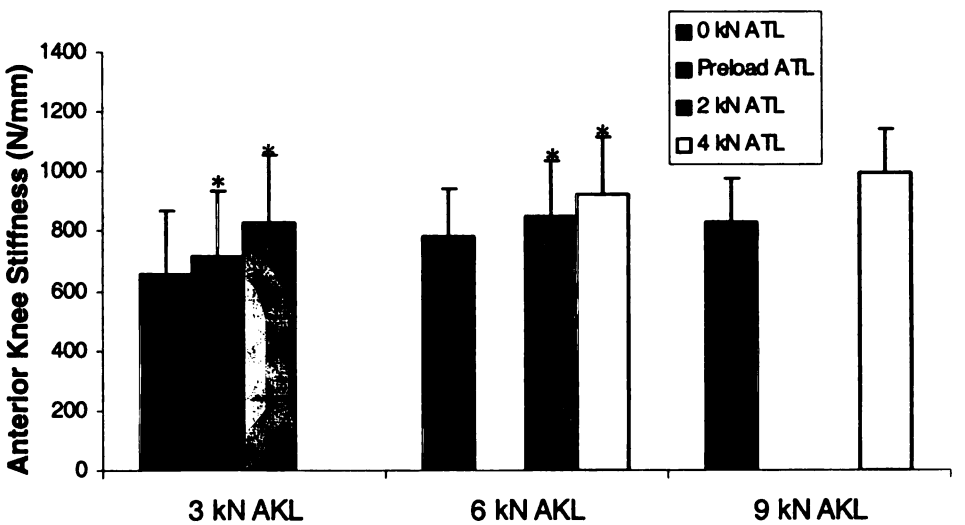

Figure 4.10. Bar graph of the anterior knee stiffness with increasing ATL at various AKL levels. * Significantly different from uniaxial impacts.

Specimen ID	Test Number	Anterior Knee			Axial Tibia			Tibia Drawer (mm)	Pressure Film Force (N)
		Load (N)	Disp (mm)	Stiffness (N/mm)	Load (N)	Disp (mm)	Stiffness (N/mm)		
31387R	1	1795	6.29	360.94	0	0		5.32	2523
31387L	2	2323	6.92	269.89	634	1.14		5.89	1577
31237R	1	2445	6.21	377.44	0	0		1.6	3418
31237L	2	2654	3.62	778.07	734	0.87		2.59	2115
30899R	1	2297	5.35	429.51	0	0		3.13	3623
	2	2465	5.15	477.65	393	-0.46		2.35	3709
	3	2592	4.78	536.99	1427	1.95	664.78	2.69	2972
30899L	1	2437	5.89	416.52	0	0		4.59	4292
	2	2465	5.85	414.49	564	-0.61		4.36	2853
	3	2619	5.41	466.15	1631	1.66	898.85	3.35	3254
31392R	1	2718	3.15	934.14	0	0		2.83	3044
	2	2781	2.84	1071.7	276	-0.25		2.6	3228
	3	2654	2.61	1148.7	1568	1.7	918.87	2.28	3772
31392L	1	2601	3.45	812.25	0	0		1.8	2544
	2	2706	3.63	766.78	255	-0.25		1.95	2619
	3	2736	3.42	820.76	1816	1.72	955.95	1.86	3153
31405L	1	2763	3.05	964.5	0	0		0.92	4000
	2	2794	2.73	1110.1	232	-0.25		1.4	3309
	3	2826	2.49	1220.5	1313	2.05	601.06	2.39	3662
31405R	1	2661	3.93	703.36	0	0		2.01	4377
	2	2725	3.32	900.73	397	-0.45		3.32	3233
	3	2801	2.9	1032.9	1478	1.98	673.09	3.32	3623
31378R	1	2583	4.41	594.14	0	0		3.05	3394
	2	2661	4.1	662	283	-0.12		2.34	3199
	3	2759	3.74	731.34	2086	1.57	1087.8	2.3	3122
31378L	1	2660	3.35	855.01	0	0		2.23	3428
	2	2579	3.6	772.89	394	-0.5		2.18	3368
	3	2730	3.15	926.78	2059	1.46	1189.7	1.75	3648
31383L	1	2430	4.33	569.01	0	0		2.45	3400
	2	2463	4.34	565.55	290	-0.33		2.16	3584
	3	2587	3.87	662.7	1478	2	670.12	2.09	3601
31383R	1	2609	4.06	651.12	0	0		3.03	4683
	2	2579	3.86	713.27	519	-0.68		3.12	4344
	3	2786	3.45	804.84	1583	1.72	833.2	2.45	4184
31382R	1	2623	4.75	560.08	0	0		3.92	2608
	2	2689	4.26	630.51	380	-0.39		3.19	2441
	3	2769	3.74	754.41	1981	1.37		2.47	2509
31382L	1	2680	4.19	631.97	0	0		2.35	3123
	2	2593	4.1	635.46	230	-0.2		1.38	3680
	3	2730	3.67	742.19	1836	1.75		1.45	1165
31390R	1	2760	2.88	991.24	0	0		1.83	3632
	2	2831	3.1	926.26	359	-0.39		1.75	3510
	3	2859	2.7	1061.9	1815	1.52	1035.4	1.48	2940
31390L	1	2538	3.78	708.24	0	0		3.09	3911
	2	2545	3.69	726.48	270	-0.25		3.39	3427
	3	2708	3.61	739.61	1705	1.79	788.16	2.18	3463
Average (SD)	1	2537 (237)	4.3 (1.1)	669 (208)*	0 (0)	0 (0)	-	2.8 (1.1)	3507 (652)
	2	2616 (141)	4.1 (1.1)	714 (222)*	388 (151)	-0.2 (0.5)	-	2.7 (1.2)	3174 (700)
	3	2740 (89)	3.5 (0.8)	831 (222)	1699 (243)	1.7 (0.2)	860 (188)	2.3 (0.6)	3257 (746)

Table 4.2. Load, displacement, stiffness and pressure film force for tests 1-3, 3 kN AKL with varying ATL. * Significantly different than test 3.

Specimen ID	Test Number	Anterior Knee			Axial Tibia			Tibia Drawer (mm)	Pressure Film Force (N)
		Load (N)	Disp (mm)	Stiffness (N/mm)	Load (N)	Disp (mm)	Stiffness (N/mm)		
31387R	4	5571	8.06	674.71	0	0		7.34	6919
31387L	5	5348	8.91	605.4	1939	1.54	1103.6		3676
31237R	4	5391	8.44	643.76	0	0		3.56	4625
31237L	5	5467	7.38	716.57	2170	2.62	774.2	4.12	6172
	6	5541	6.72	803.64	3580	5.58	633.96	3.2	1954
31392R	4	5729	5.25	1113.3	0	0		4.95	4252
	5	5916	4.64	1281.8	1968	1.23	1470.9	4.38	3866
	6	5984	4.33	1372.5	3789	2.55	1361.8	4.23	4080
31392L	4	5551	6.2	893.32	0	0		3.83	4795
	5	5793	5.89	938.33	1917	1.51	1120.9	3.56	4942
	6	5807	5.91	934.88	3908	2.77	1284.7	3.66	4814
31405L	4	5360	6.64	841.69	0	0		3.58	7326
	5	4981	7.24	700.53	1788	1.61	991.38	4.49	7229
	6	5389	7.42	694.53	3901	3.2	1025	4.81	7158
31405R	4	5549	6.31	896.44	0	0		5.49	6241
	5	5640	5.96	975.49	1774	1.49	1071	5.58	5942
	6	5807	5.38	1067.6	3765	3.01	1103.7	5.1	5775
31378R	4	5711	7.27	769.46	0	0		5.86	4844
	5	5884	5.74	1006.5	2294	1.33	1449.3	4.4	3641
	6	5970	6.14	925.24	4418	2.53	1536.6	4.35	4632
31378L	4	5390	7.07	768.2	0	0		5.63	5963
	5	5703	6.74	825.21	2250	1.14	1668.7	4.58	5841
	6	5676	6.1	923.25	4482	2.49	1571.5	3.89	5919
31383L	4	5222	8.44	608.69	0	0		6.54	5209
	5	5384	7.44	718.42	2194	1.34	1411.4	4.35	5813
	6	5580	7.03	765.44	4100	2.69	1322.5	3.73	
31383R	4	5009	8.66	576.12	0	0		6.54	5949
	5	5430	7.4	727.18	2232	1.3	1462.2	6.8	4864
	6	5604	6.7	822.05	4395	2.66	1405.4	5.72	4922
31382R	4	5361	7.13	795.76	0	0		5.23	5912
	5	5549	6.64	857.53	2486	1.01	2036.5	4.67	5600
	6	5699	6.35	911.79	4317	2.27	1733.21	2.28	5405
31382L	4	5408	7.13	762.29	0	0		4.58	5927
	5	5828	7.02	764.58	2116	1.14	1242.4	3.09	5966
	6	5734	6.62	839.3	4193	2.5	1460.4	3.4	4988
31390R	4	5641	5.67	1006.2	0	0		4.01	5861
	5	5766	5.37	1087.1	2043	1.21	1478.4	3.46	5774
	6	5767	4.95	1192.5	4221	2.53	1474.7	3.22	
31390L	4	5346	7.8	647.46	0	0		6.09	6405
	5	5346	7.6	682.87	1951	1.7	909.03	4.43	5905
	6	5490	7.42	718.02	3973	3.01	1151.3	4.77	6369
Average (SD)	4	5462 (202)	7.1 (1.1)	786 (155)*	0 (0)	0 (0)	-	5.2 (1.2)	5731 (886)
	5	5560 (255)	6.7 (1.1)	850 (188)#	2080 (204)	1.4 (0.4)	1299 (333)	4.5 (0.9)	5387 (1025)
	6	5696 (176)	6.2 (0.9)	921 (193)	4080 (284)	2.9 (0.8)	1314 (284)	4.0 (0.3)	5091 (1354)

Table 4.3. Load, displacement, stiffness and pressure film force for tests 4-6, 6 kN AKL with varying ATL.

* Significantly different than test 6. # Significantly different than test 4.

The amount of posterior translation (drawer) of the tibia relative to the femur was also measured in this study and is shown in Figure 11. There was a trend for decreasing tibial drawer with increasing ATL at both levels of AKL. Tibial drawer at both levels of AKL decreased an average of 0.3 mm per 1 kN of ATL. A multivariate linear regression analysis of these data yielded the following expression:

$$\text{Tibial drawer} = 0.886 + 0.76 * \text{AKL} - 0.31 * \text{ATL}, \qquad (1)$$

where both AKL (kN) and ATL (kN) were determined to be significant predictors of tibial drawer (mm) (Table 4).

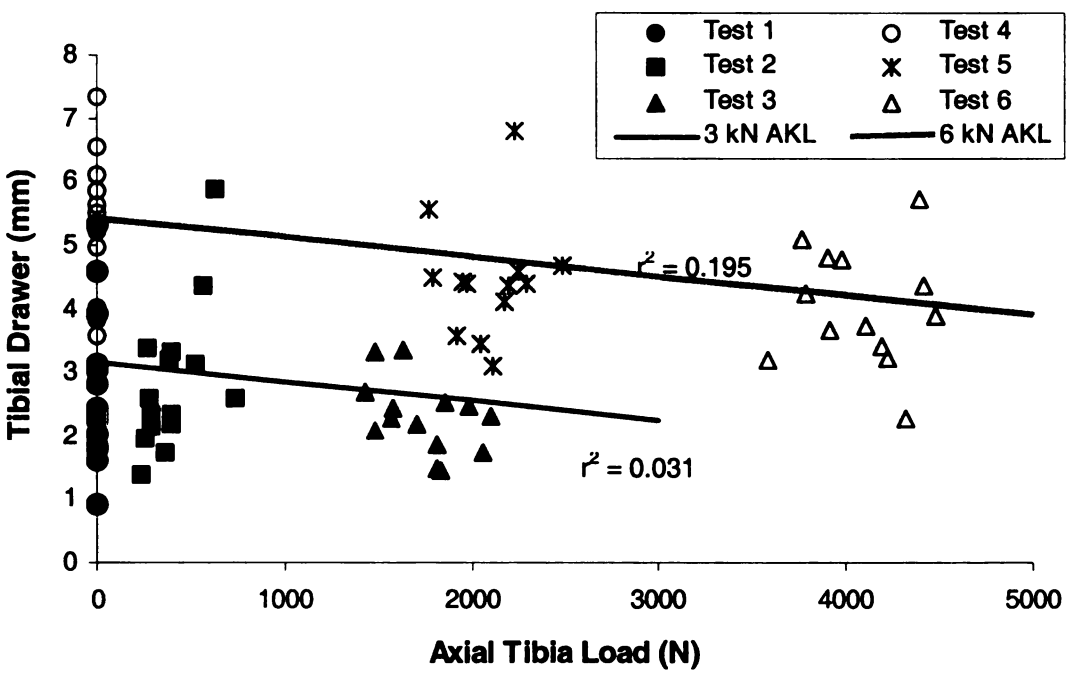

Figure 4.11. Tibial drawer displacement in tests 1-3 and 4-6 with increasing ATL.

	Y-intercept	AKL (kN)	ATL (kN)
Independent Variable	0.886	0.76	-0.31
Standard Error	0.33	0.09	0.09
P-value		<0.001	0.001

Table 4.4. Multiple linear regression variables for tibial drawer (Equation 1).

For test 7 the intent was that one knee from each pair was impacted uniaxially with 9 kN of AKL, while the opposite knee was impacted biaxially with a 9kN AKL and a 4 kN ATL. Statistically, the mean values of peak load and displacement for each protocol were not different (Table 5). Thus, the average peak AKL and displacement were 8.2±0.4 kN and 9.6±1.4 mm, respectively for the combined uniaxially and biaxially impacted knees. The stiffness responses of each group were also not statistically different (p=0.097), but on average the biaxial impacted knees tended to be stiffer (997.8±146 N/mm) than the uniaxial impacted knees (831.2±146 N/mm). There was, on the other hand, a statistically significant difference between the peak tibial drawers for the uniaxial (7.4±1.4 mm) versus the biaxial (5.8±0.6 mm, p=0.017) impacted knees.

Specimen	Anterior Knee			Axial Tibial		Tibia
ID	Load (N)	Disp (mm)	Stiffness (N/mm)	Load (N)	Disp (mm)	Drawer (mm)
31387R	8335	8.55	1025.9	0	0	7.03
31387L	7971	9.66	912.46	3157	2.09	5.93
31237R	8141	12.02	679.44	0	0	5.49
31392L	8570	8.48	1012.5	0	0	6.45
31378L	8353	9.8	837.37	0	0	8.37
31378R	8763	7.82	1151	4346	2.24	6.28
31383R	7235	11.78	653.14	0	0	9.4
31383L	8330	10.15	793.67	4529	2.33	6.44
31382L	8193	9.95	831.94	0	0	6.42
31382R	8517	8.54	1023.6	4853	1.87	5.67
31390L	7821	10.43	777.81	0	0	8.52 *
31390R	8342	7.9	1108.4	4511	2.3	4.97
0 ATL Ave (SD)	8093 (290)	10.1 (1.4)	831.2 (146.3)	0 (0)	0 (0)	7.4 (1.4)
4 kN ATL Ave (SD)	8384 (290)	8.8 (1.0)	997.8 (146.0)	4279 (654)	2.2 (0.2)	5.8 (0.6)

Table 4.5. Load, displacement and stiffness for test 7, 9 kN AKL with either 0 kN or 4 kN ATL in paired specimen. * Significantly different than biaxial impacts (4 kN ATL).

Contact Interface Deformation

The contact areas in the deformable interface were measured to estimate the relative loads applied to the PF joint and to the tibial tuberosity during each test (Figure

7). Figure 12 shows a significant difference in the percentage of load carried by the tibial tuberosity in biaxial tests (6.9%, range 0-36%) versus the uniaxial tests (2.1%, range 0-15%, p=0.034) for an AKL of 6 kN. At the 3 kN and 9 kN levels of AKL the percentages of tuberosity load in biaxial versus uniaxial tests were 4.9% (0-36%) versus 2.1% (0-19%) and 12.7% (0-33%) versus 8.7% (0-25%) respectively. However, these differences were not statistically significant.

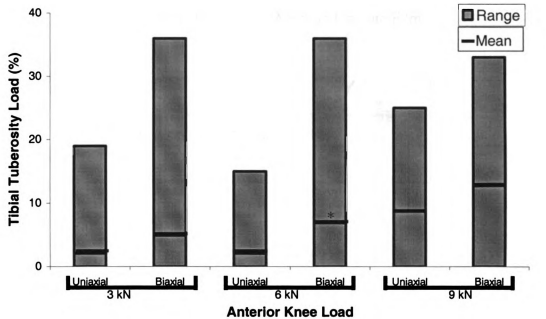

Figure 4.12. Bar graphs of the percentage of load carried by the tibial tuberosity for impacts at various AKL levels. * Significantly different from uniaxial impacts.

Pressure Film Force

The contact pressures and contact areas within the PF joint were documented using Fuji film in tests 1-6 on each specimen. Generally, the pressure distributions were

smooth with little or no apparent creasing of the film as shown by Figure 13. The PF force was determined by the merging data from the low and medium pressure films

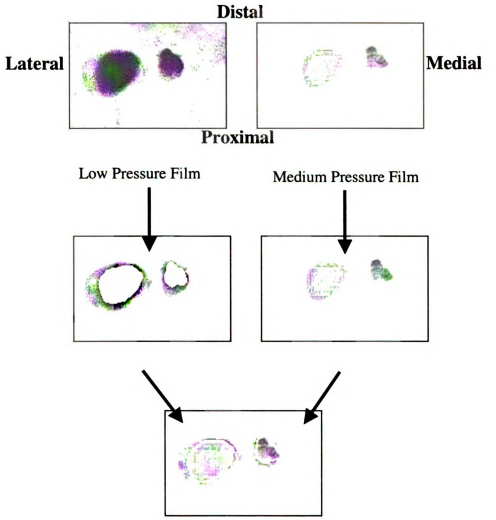

Figure 4.13. Pressure film from a representative specimen (31382L6).

(Tables 2 and 3). Figure 14 documents the trend for decreasing PF contact force with increasing ATL at both levels of AKL, which can also be shown by a multiple linear regression:

$$\text{PF Force} = 1.43 + 0.77 * \text{AKL} - 0.18 * \text{ATL}, \qquad (2)$$

where both AKL (kN) and ATL (kN) were determined to be significant predictors of PF contact force (kN) (Table 6):

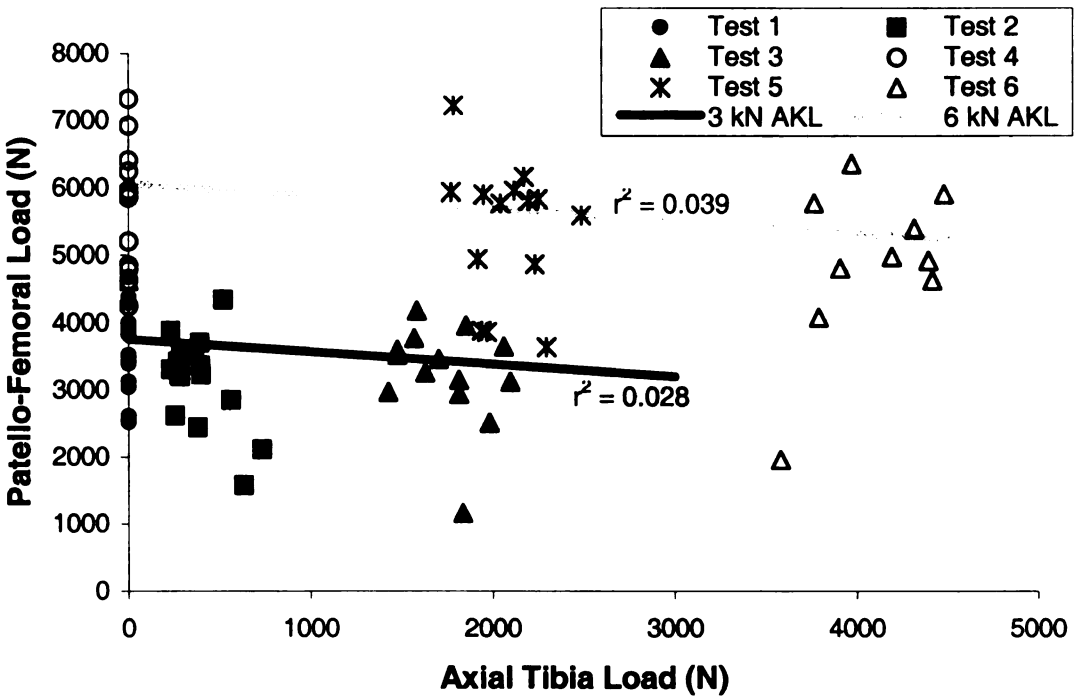

Figure 4.14. Patello-femoral force from pressure film in tests 1-3 and 4-6 with increasing axial tibia load.

	Y-intercept	AKL (kN)	ATL (kN)
Independent Variable	1.43	0.77	-0.18
Standard Error	0.29	0.08	0.08
P-value		<0.001	0.03

Table 4.6. Multiple linear regression variables for PF force (Equation 2).

Injury Tests

Gross injuries, seen in Figure 15, were in the form of a ligament tear or a bone fracture and occurred in or after test 8. Ten knee impacts resulted in a complete tear, partial tear or avulsion of the PCL at an average maximum AKL of 12.4±2.6 kN and displacement of 19.7±6.6 mm (Table 5). Among the knees that had PCL trauma, there was not a statistically significant difference between the failure AKL of biaxial (12.7±2.4

(A) PCL avulsion fracture from posterior tibia

(B) Split femoral condyle fracture

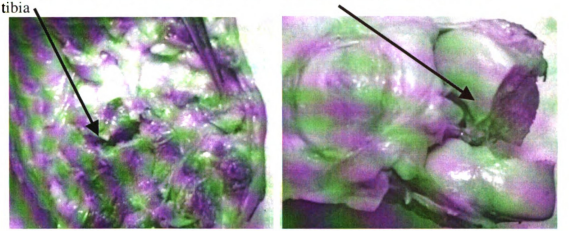

Figure 4.15. Representative photographs of injuries to paired human knees (31390).

Specimen ID	Sex	Age	BMD (g/cm^2)	Tibial Plateau Angle (deg)	Anterior Knee Load (N)	Anterior Knee Disp (mm)	Axial Tibia Load (N)	Axial Tibia Disp (mm)	Tibia Drawer (mm)	Injury Comments
31387R	M	71	0.818	13	13998	25.52	0	0	19.92	PCL Midsubstance Tear
31387L	M	71		11	13580	15.61	4052	5.29	14.48	PCL Avulsion
31237R	M	47		14	13031	19.43	0	0	17.9	PCL Avulsion
31237L	M	47	0.556	9.5	13216	23.19	5236	4.06	20.9	PCL Midsubstance Tear
30899L	F	92	0.148	10	3342	18.49	0	0	16.46	Split Femoral Condyle Fracture
30899R	F	92		7	3106	14.59	895	2.12	9.24	Split Femoral Condyle Fracture
31392L	M	59	0.631	8	12046	17.41	0	0	16.07	Partial PCL Tear, Patella Fracture
31392R	M	59		11	8107	6.78	4243	4.33	8.43	Tibial Plateau Fracture, Patella Avulsion
31405R	M	81		5	7920	15.75	0	0	15.6	Split Femoral Condyle Fracture, Patella Avulsion
31405L	M	81	0.344	7	7742	10.01	3684	6.06	8.8	Tibial Tuberocity and Plateau Fracture
31378L	F	81	0.714	8.5	11231	25.8	0	0	24.34	Split Femoral Condyle Fracture
31378R	F	81		8	11279	14.1	2945	3.59	7.28	Split Femoral Condyle Fracture, Lateral Tibial Plateau Fracture
31383R	M	89		7	10562	40	0	0	32	Split, Comminuted Femoral Condyle Fracture, Patella Avulsion
31383L	M	89	0.671	7	9898	21.4	3986	2.17	14.7	Split Femoral Condyle Fracture
31382L	F	58		6.5	13283	37.9	0	0	34.6	Split, Comminuted Femoral Condyle Fracture
31382R	F	58	0.795	10.5	10846	12.4	3624	1.89	9.46	Partial PCL Tear, Tibial Plateau Fracture
31390L	F	78		-	8954	29.5	0	0	31.17	Split, Comminuted Femoral Condyle Fracture
31390R	F	78	0.588	6	10063	12.47	4436	2.11	9.98	PCL Avulsion, Fibula Fracture
03952R	M	76	0.737	-	6793	24.4	0	0	-	PCL Midsubstance Tear
03844L	M	57		-	14374	32.6	0	0	-	PCL Midsubstance Tear
03844R	M	57	0.754	-	16000	14.1	5080	1.42	13.1	Partial PCL Tear
PCL Ave. (SD)		62.1 (11.3)	0.721 (0.11) *	10.3 (2.8) *	12395 (2610) *	19.7 (6.6)	2243 (2407)	1.5 (1.9)	15.2 (4.3)	Midsubstance n=5 Avulsion n=4
Fx Ave. (SD)		78.3 (12.9)	0.459 (0.26)	8.0 (1.9)	8856 (3093)	20.6 (4.5)	1615 (1878)	1.7 (2.1)	17.7 (10.2)	Tibia Plateau n=4 Femoral Condyle n=9

Table 4.7. Specimen properties, load, displacement, and injury comments for failure tests. * Significantly different than fractured specimens.

kN) versus uniaxial (12.0±3.1 kN) impacted knees. However, the peak displacement of the AKL actuator was significantly less for PCL failure in knees with an ATL (15.6±4.5 mm) versus without an ATL (23.9±5.9mm, p=0.018). Additionally, the peak tibial drawer decreased from 18.0±1.9 mm without ATL to 13.6±4.6 mm with an ATL in cases of PCL trauma, but this difference did not rise to the level of statistical significance. The remaining knees (n=11) had gross bone fracture. These were in the form of either a split femoral condyle fracture or a tibial plateau fracture. In four cases these injuries were combined with an avulsion fracture of the patellar tendon from the distal patella. The average maximum AKL generated in the fractured specimens was significantly lower (8.9±3.1 kN, p=0.004) than that for the PCL injured specimens. It should be noted that specimens that showed bone fracture had an average age of 78.3±12.9 years, while the PCL injured specimens had a statistically different average age of 62.1±11.3 years (p=0.001). This may have also been related to bone mineral density, which was significantly higher for PCL injured specimens (0.721±0.11 g/cm^2) than bone fractured specimens (0.459±0.26 g/cm^2, p=0.036) (Table 7). Additionally, the tibial plateau slope angle was 8.0±1.9 degrees for bone fractured specimens, while it was significantly different for PCL injured specimens, being 10.3±2.8 degrees (p=0.016).

The peak tibial drawer for all failure tests was significantly lower (11.6±4.2 mm) for biaxially loaded knees than for uniaxial knees (23.1±7.6 mm, p=0.002). Additionally, the AKL actuator displacement at peak load was lower for biaxial loaded knees (14.5±4.9 mm) than uniaxial loaded knees (26.1±8.2 mm, p=0.003). These data follow similar trends from tests 1-6 showing an increased joint stiffness in biaxial versus uniaxial impacts on the knee. Analysis of the interface deformation revealed that biaxially loaded

knees carried 12.7% (range 0-33%) of the AKL on the tibial tuberosity. In contrast, 7.7% (0-24%) of the AKL was carried by the tibial tuberosity for uniaxial impacts ($p=0.097$). Since the AKL was similar for both groups (10.3±3.6 kN biaxially and 10.5±3.4 kN uniaxially) in the failure tests, the load generated across the PF joint in these tests was likely reduced for biaxial versus uniaxial tests. There was a difficulty confirming these data from Fuji film in the PF joint because bone fractures within the knee appeared to create significant artifact (Figure 16).

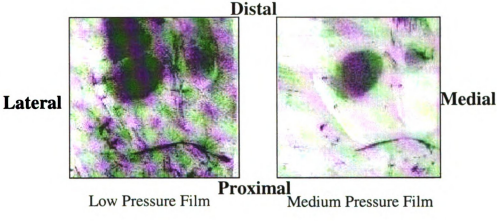

Figure 4.16. Pressure film for a fractured specimen (31382L).

Computed Tomography

Computed tomography (CT) imaging of five knees revealed two cases of particular interest. In both specimens CT scans were obtained before and after the impact sequence, but prior to dissection of the knee. Specimen 31390R had a gross injury consisting of a PCL avulsion which was observed through a laxity test between the tibia and femur (Figure 15A). A post-test CT scan, shown in Figure 17, documented occult microfractures in the subchondral bone of the anterior compartment of the tibial plateau in this specimen. While the gross injuries for specimen 31382R included a partial PCL

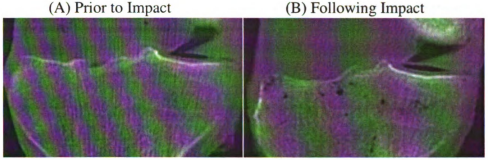

Figure 4.17. CT scan of specimen 31390R prior to and following impacting, documenting occult microfractures in the anterior compartment of the tibial plateau.

tear and a comminuted tibial plateau fracture shown in Figure 18, a CT scan conducted prior to the last impact on the joint indicated occult microfractures in the tibial plateau (Figure 19). The area of these occult microfractures was the location of gross bone fracture in the tibial plateau following the last impact.

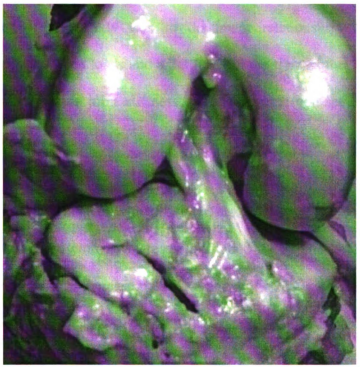

Figure 4.18. Photograph of specimen 31382R during dissection, showing gross fracture of the tibial plateau.

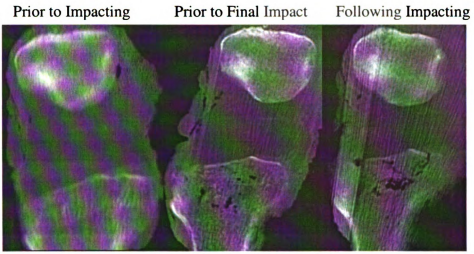

Figure 4.19. CT scans of specimen 31382R documenting occult microfractures progressing to gross fracture of the anterior tibial plateau.

DISCUSSION

The object of this study was to document relationships between various combinations of anterior knee loads and axial loads in the tibia of the 90° flexed human knee and the resulting knee joint stiffness, patello-femoral contact forces and injury patterns. Hypothesis (1) of the study was that ATL present during an AKL blunt impact by a deformable interface would result in less posterior translation of the tibia and stiffen the knee response during contact with this interface. In the current study the posterior tibial translation increased with an increase in applied AKL. On the other hand, tibial translation decreased with an increase in ATL at a rate of 0.3 mm per kN of ATL (Figure 11). While both load variables were shown to be significant predictors of tibial translation, it should be noted that there was a high level of variation between samples and therefore r^2 values were low. This variation was likely caused by other variables not considered in the multiple linear regression, such as age, BMD and anatomical geometry.

The stiffness of the knee for an AKL impact was increased between 17% and 26% when an ATL was applied simultaneously (Table 2, 3 and 5). The effect was likely due to an anterior directed force component that tended to displace the tibia anteriorly under an ATL. This was largely suggested due to an average tibial plateau slope of approximately 9° among the specimens (Figure 5). Table 7 shows individual specimen tibial plateau slope values. Previous measurements based on lateral radiographs have shown the tibial slope of the average knee to be 10±3° (DeJour et al., 1994, Gevien et al, 1993, Giffin et al., 2004). Hypothesis (2) of the study was that constraint of the knee with a deformable interface would prevent ACL rupture due to anterior translation of the tibia for an ATL previously documented to injure the ACL in an unconstrained knee. While a previous study documented rupture of the ACL with 5.8±2.9 kN of ATL (Jayaraman et al., 2001), no such injuries were documented in the current study for an ATL of as much as 6 kN. Hypothesis (3) of the study was that application of an ATL during blunt knee impacts involving the tibial tuberosity would help reduce the patello-femoral joint force due to increased load supported by the tibial tuberosity. The current study showed that for an AKL of 6 kN and an ATL of 4 kN the PF contact force was reduced by approximately 11.2% versus specimens with no ATL. And lastly, hypothesis (4) of the current study was that the AKL needed to cause rupture of the PCL would be increased due to an anteriorly directed force component generated by an ATL. In specimens that had PCL trauma, the average maximum AKL was 12.7 kN for biaxial versus 12.0 kN for uniaxial tests, but these AKL's were not statistically significant in the study.

Knees were impacted at 90° of flexion to simulate the flexion angle during contact with the IP in simulated car crashes (Atkinson et al., 1999). Additionally, this

flexion angle facilitates comparisons with previous experiments using the 90° flexed human cadaver knee. AKLs were directed parallel with the axis of the femur to simplify the bending moments in the bones. However, while this loading scenario is comparable to a majority of previous studies, it may not simulate all occupant orientations in real world frontal crashes, due to the possibility of abduction or adduction of the hip (Meyer and Haut, 2003 and Rupp et al., 2003).

Early impacts on the PF joint with a rigid impact interface (Haut, 1989) document split femoral condyles and transverse and comminuted fractures of the patella in the knees of 9 human subjects aged 72±11 years at a maximum contact force of 8.5±3.0 kN. The maximum load was increased to 9.5±4.0 kN when a 25 mm thick foam (Rub-A-Tex R310V) was applied to the interface. Using a similar experimental set-up and impact protocol with a rigid interface, a later study documented femoral condyle and patella fractures at approximately 6.7±1.7 kN (n=10) and 6.7±2.1 kN (n=10) for two groups of specimens aged 48±9 years and 71.7 years, respectively (Atkinson and Haut, 1995). In the current study bone fractures (split femoral condyle, n=9 or tibial plateau, n=4) occurred at a maximum AKL of 8.9±3.1 kN (n=11) in a group of specimens aged 78.3±12.9 years. In contrast, the bone fracture loads presented in the current study were, on average, slightly lower that those documented for blunt patellar impacts using a 25 mm thick foam (Haut, 1989). The effect may be due to yet unknown differences in the impact characteristics of the Hexcel (pressure limiting) and foam interfaces used in each study and contact of this interface with the tibial tuberosity in the current study.

The characteristics of padded impact interfaces against the 90° flexed knee have indicated the bone fracture limiting nature of various interfaces (Hayashi et al., 1996). In

that study 10 isolated human knees were flexed 90° and impacted by a 20 kg pendulum with a rigid surface, a 3.1 MPa and a 0.7 MPa crush strength aluminum honeycomb padding (Hexcel), and a 0.35 MPa crush strength paper honeycomb. Patella and split femoral condyle fractures were reported with the rigid interface at 17.4 kN. A split femoral condyle fracture was reported at 15.5 kN for the stiffest, deformable interface. Subchondral injury of the patella and intercondylar regions of the femur were documented in 4 knee joints at 10.1±0.3 kN (subject age 61 and 68 years) for the 0.7 MPa interface. Based on analysis from a 3-D finite element human knee model and the experimental data of the study, the optimal interface for protecting the knee against bone fracture was hypothesized to be 0.62 MPa. No ATL however, was included in the analysis. The current study would suggest that ATLs could help unload the PF joint to possibly limit patella and split condylar fractures of the femur. Importantly, the Hayashi et al. (1996) study did not document any injuries to the PCL, in contrast to the current study.

A study by Herring and Patrick (1977) impacted the anterior knee similarly to the current study, but used relatively low forces and compliant interfaces and did not document fracture or PCL trauma in any tests. In these tests loads were measured biaxially in both the femur and in the distal tibia. Interestingly, for an AKL above a significant load component was generated along the axis of the tibia in the cadaver. For an AKL of approximately 4 kN there was a resultant ATL of 536±86 N. This compares well to data in the current study for test 2 where a slightly lower AKL of approximately 2.6 kN produced a resultant ATL of 388±151 N, when the tibia was constrained with an intial preload of 50 N. The previous study also documented that the amount of force

required to constrain the tibia in Part 572 dummy knee impacts was unexpectedly lower (174±31 N) than in the cadaver. This indicates that the Part 572 dummy knees were not accurately predicting the response of human knees to AKLs.

The maximum ATL applied in the current study was 6 kN. However, after this load level caused tibial plateau fracture in two biaxially impacted specimens (31392R and 31405L), the maximum ATL was reduced to 4 kN or 50% of the average fracture load documented in the Banglmaier et al. (1999) study. Initially, 6 kN of ATL was sought, to simulate load levels from Jayaraman et al. (2001) where ACL rupture was documented at 5.8 ± 2.9 kN of ATL for an unconstrained TF joint. In this study, the authors document that a force of 1.2 ± 0.5 kN is required to constrain anterior drawer of the tibia. With a static analysis of the knee (assuming a slope of 10° and an ATL of 6 kN) we anticipate the maximum anterior resultant force to be approximately 1.1 kN. For biaxial impacts with an ATL of 4 kN, as in the current, study we anticipate a resultant force of 0.71 kN would available to counteract the AKL applied to the tibial tuberosity (Figure 20). In fact, in failure experiments the difference between biaxial and uniaxial impacts for PCL rupture was approximately 0.7 kN. While close to what we expected, the difference between uniaxial and biaxial experiments was not statistical because of specimen variations using 4 kN in the current study.

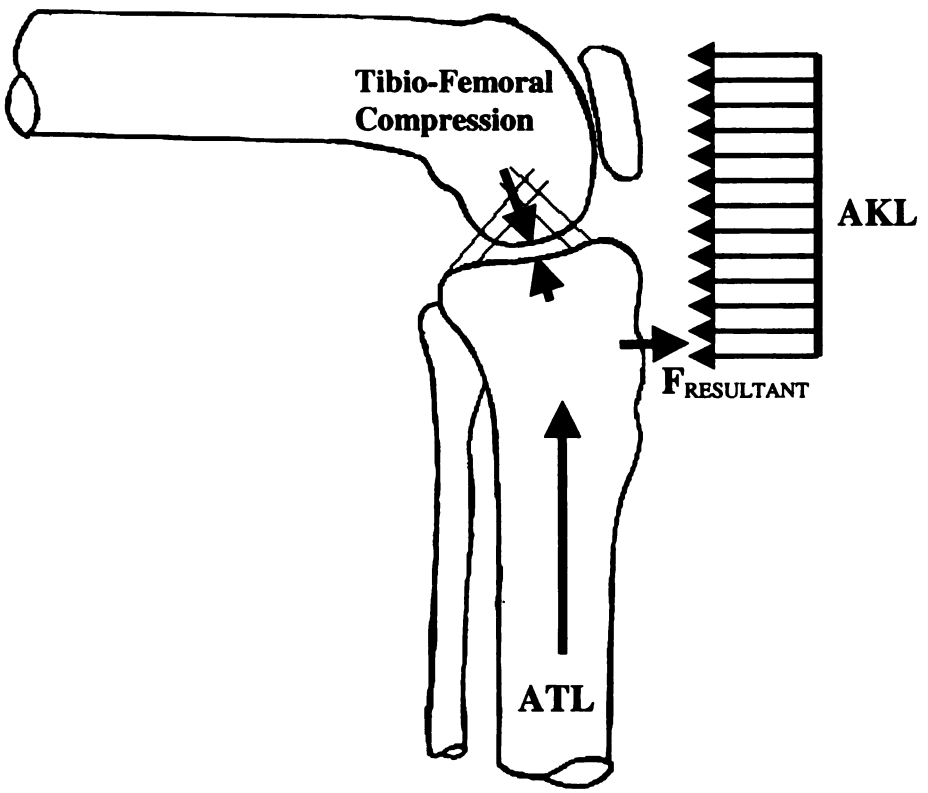

Figure 4.20. Orientation of applied and resultant forces for a 90° flexed human knee.

The current study also supports the earlier report by Viano et al. (1978) indicating injury to the PCL in numerous cases of blunt impact to the 90° flexed knee when contact occurs with the tibial tuberosity. In this previous study two isolated human knee joint preparations had PCL rupture for a peak load of 2.6±0.6 kN and posterior directed tibial drawer of 18.1±2.2 mm. These isolated knee joint tolerance tests involved controlled translation (subluxation) of the tibia across the femur at 90° flexion until complete joint failure. Combination PCL and tibial plateau fracture tests (n=5) yielded a peak force of 2.48±0.54 kN and 22.0±10.2 mm (cadaver age 68.8±15.1 years). In comparison to these isolated joint tolerance tests, blunt impact tests in the same study with a heavily padded interface (3.2 kN/cm) on the knees of seated human cadavers (63.7±16 years) resulted in

various combinations of PCL tears, avulsions, and tibial plateau and intercondylar femur fractures at 7.0±0.9 kN. In the current study with a 3.3 MPa aluminum honeycomb interface, PCL injuries occurred in tests having a peak AKL of 12.0±3.1 kN without an ATL (n=5, aged 62.1±11.3 years). The reason for the differences between these studies is unclear. The higher rate of loading in the Viano et al. (1978) study (26.3±4.8 ms primary pulse duration) would suggest that PCL injury may be via central (midsubstance) rupture and at higher loads than for the current study (Crownshield et al., 1976, Noyes et al., 1974). Yet, the predominant mode of PCL failure in the Viano et al. (1978) study using seated cadavers was avulsion fractures of bone from the tibial plateau. Furthermore, any inertial motions of the seated cadaver would have tended to increase failure loads for PCL injury compared to the current study using an isolated knee preparation. For yet unexplained reasons the differences in peak contact forces between these studies may have related to the differences in the stiffness of the impact interfaces. Importantly, PCL injury occurred at 18.1±2.2 mm (n=2) of posterior drawer in the isolated knee joint studies of Viano et al. (1978). This compared to 15.2±4.3 mm (n=10) in the current study.

The current study also noted that the total knee bone density was significantly higher in subjects with PCL injury than a bone fracture. This total knee bone density considers the density of the distal femur and the proximal tibia/fibula (Figure 6). These data suggest that younger versus older subjects, in general, may be more susceptible to ligamentous injury. Although BMD values are particularly relevant in comparing fracture to non-fracture type injuries within this study, it should be noted that the average bone mineral densities of all the impacted specimens in this study were generally lower than

previous data on healthy, non-osteoporotic, female patients ages 21-48 years (Murphy et al., 2001).

The natural progression of a PCL injury is the long-term development of degenerative changes in the medial compartment and patello-femoral joint of the knee (Li et al., 2002). Long-term degeneration of the knee after PCL injury occurs in 20-60% of patients, even after posterior stability is improved by PCL reconstruction. One explanation for the development of chronic disease in the knee may relate to the appearance of occult microcracks in bone underlying articular cartilage (Johnson et al., 2000). These compression injuries of the bone have been associated clinically with early changes in the overlying articular cartilage reminiscent of the disease osteoarthritis (Johnson et al., 1998, Vellet et al., 1991). A study by Rangger et al. (1998) indicates that these occult fractures, which are seen in histological sections from patients in automobile crashes, exist in areas identified by magnetic resonance imaging (MRI) as "bone bruises". In the current study occult microfractures were identified in the anterior compartment of the tibial plateau by CT scans in some cases of PCL injury. Examples of automotive injury cases show similar injuries (Sanders et al., 2000). The author documents cases of partial and complete PCL rupture due to a dashboard impact and corresponding "bone bruises" in the anterior compartment of the tibial plateau via MRI. These data may suggest the potential for a chronic disease in cases where the PCL is excessively tensed, or ruptured, following an automobile accident. A limitation of the current study, however, is that the above concern cannot be investigated using the human cadaver subject.

The cadaver model also does not currently incorporate the potential effects of muscle tensions that may exist in the lower extremity during an automobile crash (Figure

20). The potential combination effect of quadriceps and hamstrings muscle tensions on stiffness and strength of the knee during blunt impact loadings needs further investigations using cadaver subjects that incorporate various levels of simulated muscle contractions. Muscle tensions may well show increased stiffness of the knee that could help explain the relatively low frequencies of knee ligament injuries documented in the NASS automotive accident databases.

CONCLUSION

The study showed that axial compressive loading of the tibia, which may occur at nearly the same time and magnitude as anterior knee loads during a frontal automotive crash, has a stiffening effect on the response of the knee. Furthermore, ATL can also act to reduce the relative translation between the tibia and femur generated by contact between a deformable interface and the tibial tuberosity for the 90° flexed knee. The effect of an ATL is also to carry more load in the tibial tuberosity, helping to unload the patello-femoral contact forces. This effect can increase, if only slightly, the tolerance of the knee to PCL injury. Current injury tolerance criteria reflect the vulnerability of the knee to shear displacements by limiting tibia-femur translation to 15 mm. This level of tibia drawer for PCl injury compared well to the current study. Finally, ACL injury was not documented in any biaxial specimens, suggesting that instrument panel contact and the generation of an anterior knee load will help constrain the tibia from moving forward relative to the femur.

ACKNOWLEDGEMENT

This study was supported by a grant from the Centers for Disease Control and Prevention (R49/CCR503607). Its contents are solely the responsibility of the authors and do not necessarily represent the official views of the Centers for Disease Control and Prevention. The authors wish to gratefully acknowledge Cliff Beckett for technical assistance in this study, Dr. Todd Fenton for providing the radiographs, Glenn Miller and Alexis King for assistance with the CT scans and DEXA. We also thank Dean Mueller, Coordinator of the Anatomical Donations Program, University of Michigan for procuring human test specimens for this research project.

REFERENCES

Atkinson PJ, Haut RC, (1995) Subfracture insult to the human cadaver patellofemoral joint produces occult injury. J Orthop Res 13:936-944.

Atkinson PJ, Garcia JJ, Altiero NJ, Haut RC. (1997) The influence of impact interface on human knee injury: Implications for instrument panel design and the lower extremity injury criterion, Stapp Conf Proc 41: 167-180.

Atkinson PJ, Newberry WN, Atkinson TS, Haut RC. (1998) A method to increase the sensitive range of pressure sensitive film. J Biomech 31: 855-859.

Atkinson PJ, Benny J, Sambatur K, Gudipaty K, Maripudi V, Hill T. (1999) A parametric study of vehicle interior geometry, delta-v, and instrument panel stiffness on knee injury and upper kinetic energy. Stapp Conf Proc 43: 203-215.

Atkinson T, Atkinson P. (2000) Knee injuries in motor vehicle collisions: A study of the National Accident Sampling System database for the years 1979-1995. Accid Anal Prev 32 (6): 786.

Atkinson P, Haut R.C. (2001) Impact responses of the flexed human knee using a deformable impact interface. J Biomech Egr 123 (3): 205-211.

Banglmaier R, Dvoracek-Driksna D, Oniang'o T, Haut R. (1999) Axial compressive load response of the 90° flexed human tibiofemoral joint. Stapp Conf Proc 43: 127-139.

Bealle D, Johnson D. (2000) Subchondral contusion of the knee caused by axial loading from dashboard impact. J Southern Orthop Assoc 9(1): 13-18.

Bedewi PG, Diggs KH. (1999) Investigating ankle injury mechanisms in offset frontal collisions utilizing computational modeling and case study data. Stapp Car Crash Conf 42: 217-242.

Blincoe L, et al. (2002) The economic impact of motor vehicle crashes 2000. NHTSA, DOT HS 809 446.

Crowninshield RD, Pope MH. (1976) The strength and failure characteristics of rat medial collateral ligaments. J Trauma 16:99-105.

Daniel D et al. (1994) Fate of the ACL–injured patient: A prospective outcome study. Am J Sports Med 22: 632-644.

Dejour H, Bonnin M. (1994) Tibial translation after anterior cruciate ligament rupture. Two radiological tests compared. J Bone Joint Surg Br. 76 (5): 745-749.

Ewers BJ, Jayaraman V, Banglmaier R, Haut R. (2000) The effect of loading rate on the degree of acute injury and chronic conditions in the knee after blunt impact. Stapp Conf Proc 44: 299-314.

Fildes B, Lane L, Vulcan P, Seyer K. (1997) Lower limb injuries to passenger car occupants. Accid Anal Prev 29: 789-795.

Fleming, B., Renstrom, P., Beynnon, B., and et al., 2001. The effect of weight-bearing and external loading on anterior cruciate ligament strain. J Biomech 34: 163-170.

Funk JR, Tourret LJ, Crandall JR. (2000) Experimentally produced tibial plateau fractures. IRCOBI Conf: 171-182.

Genin P, Weill G, Julliard R. (1993) The tibial slope. Proposal for a measurement method. J Radiol. 74: 27-33.

Giffin J, Woo S, Harner C. (2004) Effects of increasing tibial slope on the biomechanics of the knee. Am J Sports Med 32 (2): 376-382.

Haut RC. (1989) Contact pressures in the patellofemoral joint during impact loading on the flexed human knee. J Orth Res 7: 272-280.

Hayashi S, Choi HY, Levin RS, Yang KH, King AI. (1996) Experimental and analytical study of knee fracture mechanisms in a frontal knee impact. Stapp Car Crash J 40: 160-171.

Hirsch G, Sullivan L. (1965) Experimental knee-joint fractures. Acta Orthop Scand 36: 391-400.

Hering WE, Patrick LM. (1977) Response comparisons of the human cadaver knee and a Part 572 dummy knee to impacts by crushable materials. Stapp Car Crash Conf 21: 1017-1053.

Jayaraman, V.M., Sevensma, E.T., Kitagawa, M., Haut, R.C., 2001. Effects of anterior-posterior constraint on injury patterns in the human knee during tibio-femoral joint loading from axial forces through the tibia. Stapp Car Crash J. 45: 449-468.

Johnson D, Bealle D, Brand J, Caborn D. (2000) The effect of a geographic lateral bone bruise on knee inflammation after acute anterior cruciate ligament rupture. J Orth Soc for Sports Med 28: 152-154.

Johnson DL, Urban WP, Caborn DN, Vanarthos WJ, Carlson CS. (1998) Articular cartilage changes seen with magnetic resonance imaging-detected bone bruises associated with acute anterior cruciate ligament rupture. Am J Sports Med 26 (3): 409-414

Kuppa S. (2002) An overview of knee-thigh-hip injuries in frontal crashes in the United States. 17th ESV

Li, G., Rudy, T., Allen, C., 1998. Effect of combined axial compressive and anterior tibial loads on in situ forces in the anterior cruciate ligament: a porcine study. J Orth Res 16:122-127.

Li G, Gill T, Defrate L, Zarins B. (2002) Biomechanical consequences of PCL deficiency in the knee under simulated muscle loads-an in vitro experimental study. J Orth Res 20: 887-892

Markolf, K.L., Bargar, W.L., Shoemaker, S.C., Amstutz, H.C., 1981. The role of joint load in knee stability. J Bone Jt Surg. 63: 570-585.

Melvin J, Stalnaker R, Alem N, Benson J, Mohan D. (1975) Impact response and tolerance of the lower extremities. Stapp Car Crash Conf Proc 19: 543-559.

Mertz H. (1993) Anthropomorphic Test Devices. Accidental Injury, Biomechanics and Prevention edited by Nahum A, Melvin J. Springer-Verlag.

Meyer EG and Haut RC. (2003) The effect of impact angle on knee tolerance to rigid impacts. Stapp Car Crash J 47: 1-19.

Miller M, Osborne J, Gordon W, Hinkin D, Brinker M. (1998) The natural history of bone bruises: A prospective study of magnetic resonance imaging: detected trabecular microfractures in patients with isolated medial collateral ligament injuries. Am J Sports Med 26: 15-19.

Morgan RM, Eppinger RH, Marcus JH, Nichols H. (1990) Human cadaver and hybrid III responses. International Conference on the Biomechanics of Impacts.

Murphy E, Bresnihan B, FitzGerald O. (2001) Validated measurement of periarticular bone mineral density at the knee joint by dual energy x ray absorptiometry. Ann Rheum Dis 60: 8-13.

Noyes FR, Delucas J, Torvik P. (1974) Biomechanics of anterior cruciate ligament failure: An analysis of strain-rate sensitivity and mechanisms of failure in primates. J Bone Jt Surg 56 (2): 236-253.

Patrick L, Kroell C, Mertz H. (1965) Forces on the human body in simulated crashes. Stapp Car Crash Conf Proc 9: 237-259.

Powell W, Ojala S, Advani S, Martin R. (1975) Cadaver femur responses to longitudinal impacts. Stapp Car Crash Conf Proc 19: 561-579.

Rangger C, Kreczy A. (1998) Bone bruise of the knee, Acta Orthop Scand 69 (3): 291-294.

Rupp JD, Reed MP, Jeffreys TA, Schneider LW. (2003) Effects of hip posture on the frontal impact tolerance of the human hip joint. Stapp Car Crash J 47: 20-34.

Sanders T, Lawthorn K. (2000) Bone contusion patterns of the knee at MR imaging: Footprint of the mechanism of injury. J Radiographics 20: S135-S151.

States JD. (1986) Adult occupant injuries of the lower limb. Proc Symp Biomech: 97-107.

Torzilli, P., Deng, X., Warren, R., 1994. The effect of joint-compression load and quadriceps muscle force on knee motion in the intact and the anterior cruciate ligament-sectioned knee. Am J Sports Med. 22: 105-112.

Vellet AD, Marks PH, Fowler PJ, Munro TG. (1991) Occult posttraumatic osteochondral lesions of the knee: Prevalence, classification, and short-term sequelae evaluated with MR imaging. J Radiology 178: 271-276.

Viano DC, Culver CC, Haut RC, Melvin JW, Bender M, Culver RH, Levine RS. (1978) Bolster impacts to the knee and tibia of human cadavers and an anthropomorphic dummy. Stapp Car Crash Conf Proc 22: 403-428.

CHAPTER FIVE

THE CHRONIC POST-TRAUMATIC EFFECT OF A SINGLE BLUNT IMPACT IN TISSUES OF THE RABBIT KNEE

ABSTRACT

Blunt joint trauma is a major burden to our society because of its potential for initiating post-traumatic osteoarthritis (OA), which is associated with chronic debilitation of patients and long-term medical costs. Clinically, degenerative changes have been documented in joints two to five years following severe fractures. In contrast, less severe injuries may require ten years to manifest changes. To most effectively study the mechanisms of this disease, *in vivo* animal models are needed, one of which is the rabbit. The hypothesis of this study was that blunt trauma to the rabbit TF joint, would result in accelerated cartilage and subchondral bone changes from those in the non-impacted knee. The average peak load applied to a group of ten short-term (12 weeks or less) was approximately 470 N. There were no gross injuries observed at the time of impact or dissection. Impacted 12 week knee joints had significantly less organized calcified cartilage layer and subchondral bone morphology than non-impacted joints on the medial side. Additionally, the subchondral plate thickness was increased on both sides for impacted joints and there was slightly more horizontal splitting of the articular cartilage. The results of the current study provide insight on how rapidly pathogenesis may develop in a traumatized joint. However, long-term data is necessary to understand the mechanics leading up to an end-stage clinical disease in the joint.

INTRODUCTION

The number of automotive fatalities is decreasing due to mandated use of seat belts and airbags (Lund & Ferguson 1995, Viano 1995), however more occupants are reporting musculoskeletal injuries (Burgess et al. 1995, Dischinger et al. 1992). While the current lower extremity injury criterion for automotive accidents is based on fracture of bone (Viano et al. 1977), most injuries are of less severity (Atkinson & Atkinson 2001). Many clinical studies have revealed a high percentage of patients with early post-traumatic pain, which eventually can lead to the development of osteoarthritis without a documented bone fracture (Chapchal 1978, Rassmussen 1972, States 1970). A direct relationship between trauma and osteoarthritis has been difficult, as diagnosis usually occurs when the disease reaches its end-stage: complete loss of the articular cartilage covering a joint. The most common clinical evidence of the disease is radiographic loss of joint space. Clinically, these changes have been observed in human joints two to five years following severe fractures (Wright 1990). In contrast, less severe fractures may require ten years to manifest changes and may take even longer if the impact does not generate gross bone fracture.

The ability to diagnose degenerative joint disease in its earliest stages would be useful in learning to delay or mitigate the development of post-traumatic OA (Kerin et al., 2002). Animal studies are necessary to help understand some of the mechanisms of early joint degeneration. Recent studies have provided more information about the relationship between a single blunt insult and the pathogenesis of osteoarthritis (Newberry et al., 1997). It is well documented that a severe, blunt impact will cause fissures on the surface of articular cartilage (Thompson et al. 1991, Haut et al. 1992).

This damage of the cartilage then accumulates over time and seems to show early signs of osteoarthritis at six months. Similarly, Donohue et al. (1983) indicated early histological changes in the articular and calcified cartilage after a blunt impact. They attempted to show that these changes signify softening of the cartilage, and increased stress in the underlying bone, producing microcracks and sclerosis that would lead to osteoarthritis.

Radin et al. (1978) investigated another possible mechanism by using low-level cyclic loading of the rabbit tibiofemoral (TF) joint. They showed changes in the bone preceding changes in the overlying cartilage, and at six months documented significant degradation of the joint. In the current study, a blunt force trauma model has been developed using a rabbit TF joint, which, without generating gross bone fracture may be used to document early changes in the cartilage, and underlying bone. Based on similar studies by this laboratory dealing with the patello-femoral joint (Ewers et al. 2000) the hypothesis of the current study was that a single blunt impact would produce significant changes in the bone and calcified cartilage layer, and be similar to those produced by Radin following low intensity, cyclic loading of the TF joint.

METHODS

Animal Model

The animal model selected for study was the mature (8 month old) Flemish Giant rabbit. This model has been used for many impact studies in this laboratory (Ewers et al. 2000). A total of 30 animals were used in this study comprising three groups; controls (non-impacted), low speed, short duration animals and high speed, one year animals. All animals were exercised for a least two weeks before the impact and throughout the entire study post impact, except for a one week period following the impact. Exercise consisted of treadmill hopping for 10 minutes, five days a week at 0.3 mph. The "short duration" animals were euthanized between one and 12 weeks post-impact. The results section for this chapter contains all data collected from the short duration animals. However, one year and control animals are currently being exercised so there is currently no chronic data available for these groups. After the one year post impact period expires similar data will be collected for one year animals. This study has been approved by the Michigan State University All-University Committee on Animal Use and Care.

Low Speed (Instron) Impact Protocol

A single blunt impact was delivered to one randomly chosen leg of the ten rabbits in this group. Animals were maintained at a surgical plane of anesthesia using 2% isoflurane. The randomly chosen knee was shaved and the foot wrapped in foam athletic pre-wrap. A clamp secured the leg while a metal plate connected to a bolt was attached to the bottom of the foot with fiberglass casting tape (J&J Delta-Lite 'S'). The cast covered the entire foot except for the ends of the toes and continued proximally to the mid-calf.

The rabbit was laid on its back on a raised platform attached to the table of the servo-hydraulic testing machine (model # 1331, Instron Corp. Canton, OH). The bolt attached to the foot was fixed through a hole in the table so that the knee was flexed 90° and the femur was approximately parallel with the table (Figure 5.1). The knee was positioned so that it was directly beneath the hydraulic actuator. Then a custom fitting interface was created with fast drying epoxy to distribute the force over a large area of the knee (Figure 5.2).

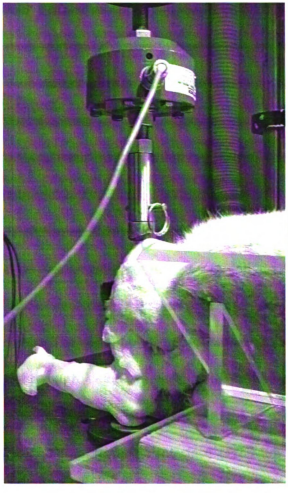

Figure 5.1. Positioning of the rabbit's 90° flexed knee directly beneath the actuator.

Figure 5.2. Custom epoxy interface in position on the knee.

A single load-controlled haversine waveform impact was delivered to each animal with a programmed load of 2000 N. The load was programmed to peak in 50 ms, but due to this fast rate and the relatively compliant response of the tissue actual loads were much lower than the input value. The average value of the actual load was approximately half the load required for bone fractures in a pilot study on animal carcasses from another study. Actual loads were measured with a load transducer (model # 10101a-2500, Instron Corp. Canton, OH) and data was collected at 1000 Hz and recorded on a personal computer with a 16-bit analog/digital board (model DAS 1600: Computer Boards, Mansfield, MA). Peak load and the time to peak were recorded for each animal. After impact, the animals were extracted from the testing machine and checked for gross fracture or trauma. The cast was removed with an autopsy saw with care not to cut the skin. Then the animal was revived from anesthesia and returned to its cage.

High Speed (Gravity Drop) Impact Protocol

A single blunt impact was delivered to the right leg of ten rabbits using a gravity accelerated mass. Animals were anesthetized and shaved, as described for the previous group. The plate, however, was attached to the foot with leather straps that were secured tightly with Velcro, rather than using casting material. The body and leg positioning was similar to the previous group with the knee flexed to 90°. Impacts were delivered with a 4 cm square deformable interface (1.2 MPa Hexcel) that insured the impact was equally distributed over the knee (Figure 5.3). A 1.33 kg mass was dropped from a height of 70 cm to induce a severe level of load to the tibiofemoral joint without causing bone fractures (Figure 5.4).

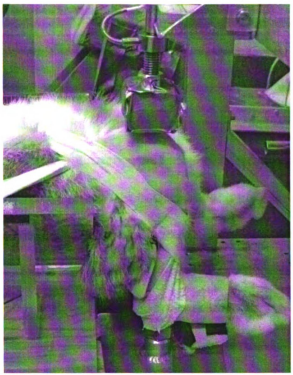

Figure 5.3. Rabbit knee flexed 90° and secured with Velcro straps positioned beneath a deformable interface.

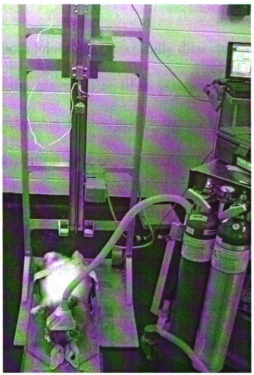

Figure 5.4. Anesthetised rabbit positioned for a gravity-accelerated mass impact.

The impacting mass was arrested electronically to prevent multiple impacts. A load transducer (model 31/1432 Sensotec, Columbus, OH) with a 500 lb capacity was attached behind the impact interface to record the actual load applied to the knee. Experimental data was collected at 10 kHz on a personal computer. Peak load and time to peak were recorded for all but 4 animals (electronic problem in triggering of data collection software). The animal was extracted from the impact fixture and checked for gross injuries before it was revived from anesthesia and returned to its cage.

Tissue Quality Quantification

Following euthanasia of each animal both knees were surgically dissected and all gross joint trauma was recorded. Additionally the retropatellar, tibial plateau and anterior and posterior femoral surfaces were stained with India ink and photographed at 25x using a Wilde microscope and digital camera. The control and impacted tibia plateaus were placed in phosphate buffered saline and the cartilage on the medial and lateral sides was mechanically tested in a materials testing machine (Figure 5.5). The structural integrity of the cartilage was determined with stress-relaxation indentation tests (Newberry et al., 1997). Briefly, each tibia was placed in a clamp attached to a camera mount (Bogen, Ramsey, NJ) that was secured to an x-y translational base plate. These features allowed the tibiae to be positioned so that the indentation tests were perpendicular to a flat location on the surface. Indentations were performed with a computer controlled stepper motor (model M-168.30 Physik Instruments, Waldbrom, Germany). A flat, rigid, non-porous, 0.5 mm diameter probe was pressed 0.1 mm into the cartilage in 30 ms and maintained for 150 seconds. The resistive loads were recorded from a load transducer (model JP-25 Data Instruments, Acton, MA) attached between the probe and the actuator. Data was collected with a personal computer at 1000 Hz for the first second and 20 Hz for the remainder of the test. The response to indentation was a sharp spike in load followed by a period of load relaxation. Five minutes following the indentation test the thickness of the site was measured by depressing a needle into the cartilage.

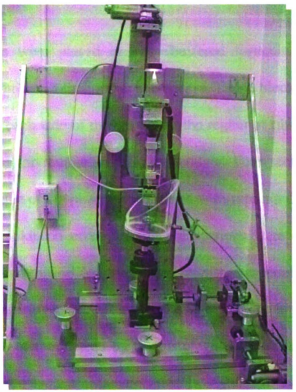

Figure 5.5. Indentation material testing machine.

The stiffness of the cartilage was determined from the results of the indentation and thickness tests by a calculation of a shear modulus from an assumed elastic layer bonded to a rigid half space (Hayes et al. 1972) The instantaneous (Gu) and relaxed (Gr) moduli were calculated based on the load at 80 ms and 150 s, respectively, using equation 1. These moduli were then normalized to the opposite, non-impacted control joint to minimize variation between animals.

$$G = \frac{P(1-\nu)}{4aKw} \qquad (5.1)$$

Where P is the measured load, ν is Poisson's ratio (assumed to be 0.5 for Gu and 0.4 Gr), a is the indenter radius, w is the penetration depth, and K is a scaling factor that depends on the thickness and Poisson's ratio.

Histological analysis

Tibial plateaus were placed in 10% buffered formalin for seven days and decalcified in 20% formic acid for another seven days. Tissue blocks were cut in a medial to lateral direction on each side of the plateau in the region of tibiofemoral contact. The blocks were processed for routine paraffin embedding. Four sections, eight μm thick, were cut across each side of the plateau and stained with safranin O and fast green, using standard techniques (Atkinson et al. 1998). The sections were examined under light microscopy at 25-400 magnification, and scored by histomorphometric analysis. A table of the categories and scoring system is given in Table 5.1. The highest quality slide was chosen from each side of the plateau by the histological technician (J. Walsh) and this slide was blindly scored by the technician and two graduate students (E. Meyer, A. Meram) in all categories. The thickness of the cartilage, calcified cartilage and subchondral bone were also measured at 40x with a calibrated eyepiece.

Surface Geometry	Normal	0	**Tide Mark**	Present/Distinct	0
	Slightly Irregular	1		Multiple (not all across)	1
	Moderately Disrupted	2		Focal Loss	2
	Focally Disrupted	3		Diffuse Loss	3
	Extensively Disrupted	4		Total Loss	4
Articular Cartilage Fissures	None	0	**Calcified Cartilage Thickness**	_____	units
	1-3 Surface	1	**Calcified Cartilage Spikes**	Normal	0
	1-2 Midzone	2		Slight	1
	3-4 Midzone	3		Moderate	2
	4+ Midzone	4		Focally Excessive	3
	1+ Deep Zone	4		Excessive	4
Proteoglycan Stain	Normal	0	**Calcified Cartilage Stain**	Normal	0
	Slight Loss	1		Slight	1
	Moderate Loss	2		Moderate	2
	Focally	3		Dark	3
	Total Loss	4	**Subcondral Bone Thickness**	_____	units
Articular Cartilage Cells	Normal	0	**Subcondral Bone Morphology**	Dense	0
	Some Clones	1		Some Small Spaces	1
	Many Clones	2		Moderate Spaces	2
	Some Clusters	3		Some Splits	3
	Many Clusters	4		Numerous Splits	4
	Path Cells	4	**Red Cells/Patches**	None	0
Articular Cartilage Disruptions	None	0		Few	2
	Compression Ridges	2		Numerous	4
	Horizontal Splits	4			
	Vertical Splits	4			
Articular Cartilage Thickness	_____	units			

Table 5.1. Histomorphometric scoring table

Following histomorphometric scoring the slides were digitally photographed at 25x and trabecular bone porosity was measured in a standard area with an image analysis software package (SigmaScan, Jandel Scientific, San Rafeal, CA) for each picture by dividing the area of the pores by the total area (Figure 5.6).

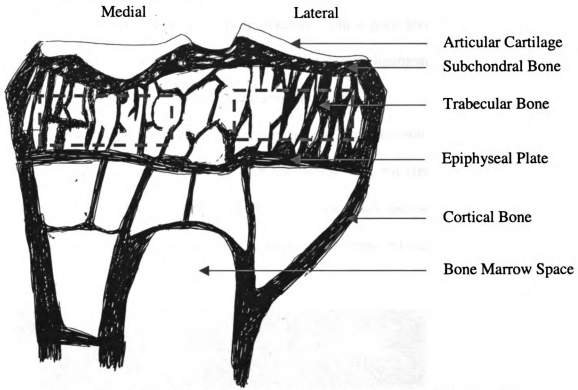

Figure 5.6. Schematic of a histology slide of the rabbit tibial plateau with regions for porosity measurement of the trabecular bone.

Statistics were performed by paired t-tests (data passed test for normality) to determine significant differences between the groups of impacted and non-impacted joints (significance for $p<0.05$). All data shown as mean ± one standard deviation.

RESULTS

Low speed impacted animals were divided into two groups based on the time duration after impact when they were euthanized. The first group consisted of all animals

euthanized before 12 weeks, and the second group were euthanized at exactly 12 weeks. The average peak load achieved in all the impacts was 469.6 ± 123 N, and there was not a statistical difference between the peak loads applied between groups (<12 week animals 429 ± 75 N, 12 week animals 510 ± 156 N). This load was approximately 50% of the peak load required to cause gross bone fracture from a pilot study on rabbit cadavers (Appendix). There were no gross injuries (bone fracture or ligament tears) observed at the time of impact or dissection in any of the animals.

Gross examination after dissection of the tibio-femoral joint revealed more cartilage fissures on the medial side then the lateral side, but similar amounts between impacted and non-impacted knees. There were a few small meniscal tears on the lateral plateau, however since these were not always on the impacted side, they were probably not caused by the impact (Figure 5.7).

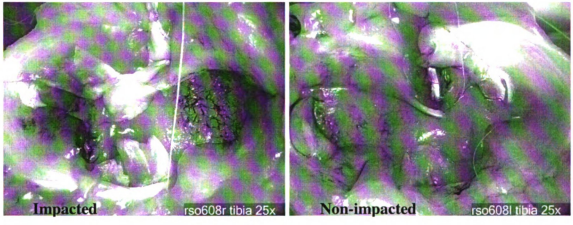

Figure 5.7. Specimen RSO608 gross dissection photographs of cartilage fissures and small meniscal tears on the tibia plateau.

The cartilage on the medial and lateral sides of the tibia plateau was mechanically indented to measure the instantaneous and relaxed moduli, as well as the cartilage thickness. For the 12 week group the impacted and nonimpacted data was combined in a

ratio, to eliminate variations between animals (Figure 5.8). Both the medial and lateral sides of the impacted joints showed a slight increase in cartilage thickness over controls, while the mechanical properties of the lateral side decreased and the medial side increased slightly. There were no statistical differences between medial and lateral sides or for impacted versus controls, probably due to the small sample size of only five animals in this group.

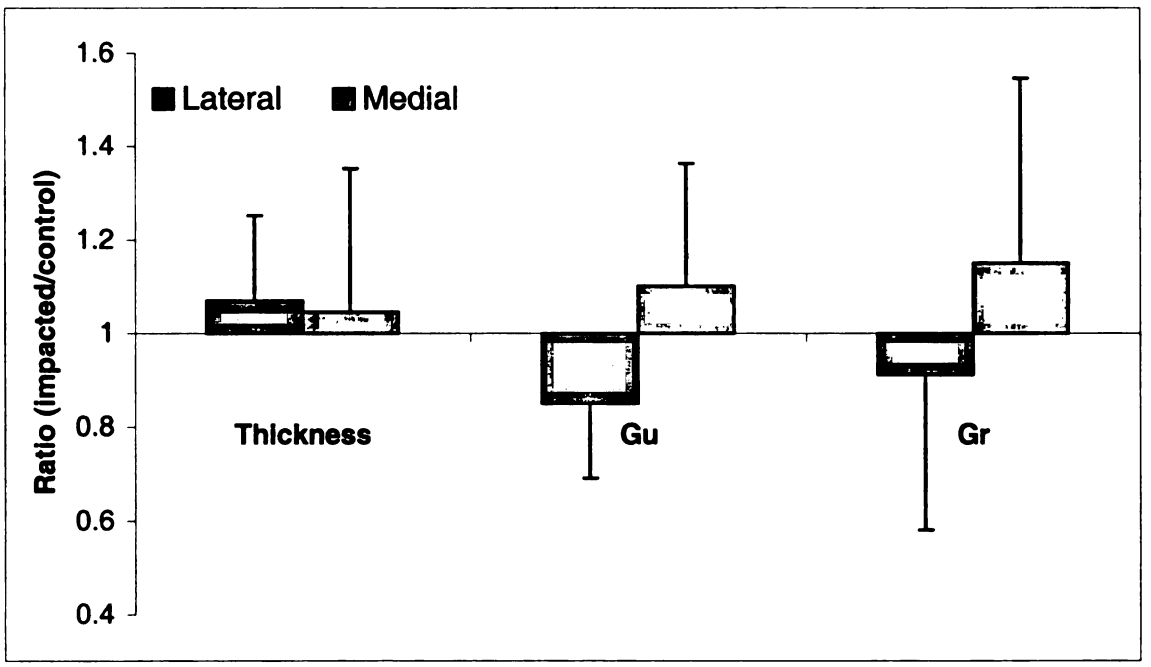

Figure 5.8. Results from mechanical indentation testing of the tibial plateaus of 12 week animals.

Histologically, there were significantly more fissures ($p<0.001$) and geometry irregularities ($p=0.014$) in the cartilage on the medial side than the lateral side. The articular cartilage was also thicker on the medial side in both impacted and non-impacted knees. In addition, impacted 12 week animals had a less distinct tidemark and less organized subchondral bone morphology on the medial side ($p=0.012$) (Figure 5.9). The subchondral bone plate thickness was statistically increased on the medial ($p=0.02$) and

lateral (p=0.01) impacted sides (Figure 5.10). These animals also had slightly more horizontal splitting of the articular cartilage in the impacted rabbit joints. The histomorphometric scoring system showed statistically more pathologic cells in the articular cartilage on the medial impacted side by the presence of excessive clones and clusters (p=0.024).

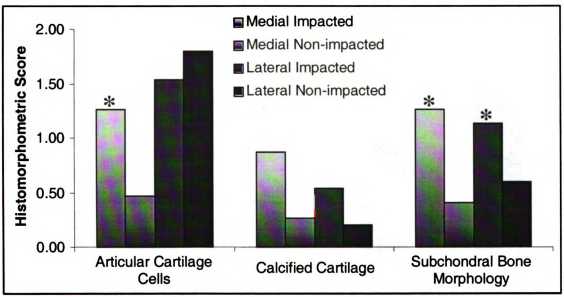

Figure 5.9. Results of histomorphometric scoring of 12 week rabbits.
* Indicates there was a statistical difference from the non-impacted knees.

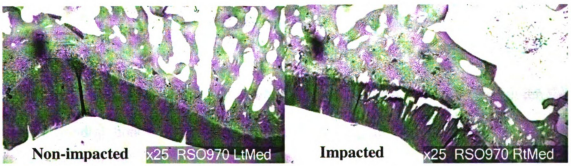

Figure 5.10. Increased subchondral bone plate thickness and horizontal splitting in the articular cartilage following impact.

Trabecular bone porosity was measured for a constant area in all 12 week animals (Figure 5.11). While there was not a significant difference between impacted and non-

impacted knees on either the medial or lateral side, the impacted medial side had the highest porosity of 47.7 ± 5.9% and the non-impacted side was lower with 39.7 ± 3.2% (p=0.06). In contrast, the porosity of the impacted lateral side was lower (36.9 ± 7.5%) than the non-impacted side (43.3 ± 12.9%), but these data were not statistically significant.

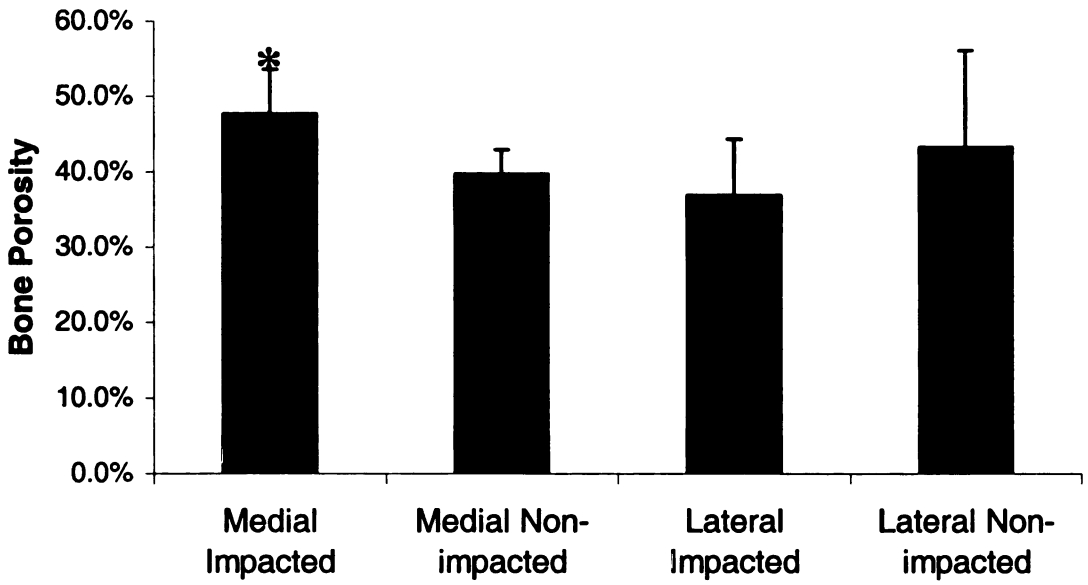

Figure 5.11. Trabecular bone porocity of 12 week impacted and non-impacted knees.
* Statistically different than Non-impacted

DISCUSSION

Blunt trauma to the TF joint resulted in an accelerated disease process in the joint by subchondral bone remodeling, horizontal splitting in the deep layer of articular cartilage, and the presence of chondrocyte clusters. This study provides evidence that a single impact may induce degenerative changes similar to those seen by Radin et al. (1984) with low level, cyclic TF compression. The previous study of Radin et al., documented a slight trend for decreased subchondral bone porosity with time, which they

concluded resulted in an increase in the stiffness of this region underlying the articular cartilage. Another study (Dedrick et al. 1997) that investigated OA progression in a canine model showed the opposite effect, documenting an increase in the subchondral bone porosity. Our study showed that the impacted subchondral bone became denser and thickened at 12 weeks. Subchondral bone plate thickening was also documented in the impacted patellofemoral (PF) joint by Ewers et al. (2002) at 7.5 months and Mazieres et al. (1987) by the third month. This is in agreement with the results of the current study. However, in contrast to the Radin et al. (1984) and Mazieres et al. (1987) studies, the animals in our experiment were regularly exercised. Exercise has been shown to have a beneficial effect on the impacted joint in the PF model (Weaver, 2001). In the previous study degenerative changes in the impacted PF joints were mitigated (or slowed) in the exercise group versus a cage-activity group.

In the current study degenerative changes were also present in the articular cartilage on the medial side of the TF joint by the presence of chondrocyte clones and clusters, a phenomenon indicative of early OA. The results of the current study provide insight on how rapidly pathogenesis may develop in a traumatized TF joint. However, data must be collected from the long-term animals after one year to understand the mechanics leading up to an end-stage clinical disease in the joint. Future studies should also investigate the effect of other variables such as exercise and various drug therapies on long-term degradation of diarthrodial joints following a single blunt impact.

REFERENCES

Atkinson PJ, Walsh JA, Haut RC. (1998) The Human Patella: A Comparison of Three Preparation Methods. J Histotechnology 21: 151-153.

Burgess A, Dischinger P, O'Quinn T, Schmindhauser C. (1995) Lower Extremity Injuries in Drivers of Airbag-equipped Automobiles: Clinical and Crash Reconstruction Correlations. J Trauma 38: 509-516.

Chaphal G. (1978) Post-traumatic Osteoartritis After Injury of the Knee and Hip Joint. Reconstr Surg Trauma 16: 87-94.

Dedrick DK, Goulet RW, O'Connor BL, Brandt KD. (1997) Preliminary Report: Increased Porosity of the Subchondral Plate in an Accelerated Canine Model of Osteoarthritis. Osteo and Cart 5: 71-74.

Dishinger P, Cushing B, Kerns T. (1992) Lower Extremity Fractures in Motor Vehicle Collisions: Influence of Direction, Impact and Seatbelt Use. AAAM 36: 319-326.

Donohue JM, Buss D, Oegema TR, Thompson RC. (1983) The Effects of Indirect Blunt Trauma on Adult Canine Articular Cartilage. J Bone Jt Surg 65-A: 948-957.

Ewers BJ, Weaver BT, Haut RC. (2002) Impact Orientation Can Significantly Affect the Outcome to the Rabbit Patellofemoral Joint. J Biomech 35: 1591-1598.

Haut RC, Ide TM, Walsh JC, Robbins JL, DeCamp CW. (1992) Studies on the Blunt Impact Response of Articular Cartilage: Animal Experiments, Human Cadaver Experiments, and Mathematical Modeling. IPTBS 1: 13-26.

Kerin A, Patwari P, Kuettner K, Cole A, Grodzinsky A. (2002) Molecular Basis of Osteoarthritis: Biomechanical Aspects. Cell Mol Life Sci 59: 27-35.

Lund A, Ferguson S. (1995) Driver Fatalities in 1985-1993 Cars with Airbags. J Trauma 38: 469-475.

Mazieres B, Blankaert A, Thiechart M. (1987) Experimental Post-contusive Osteoarthritis of the Knee: Quantitative Microscopic Study of the Patella and the Femoral Condyles. J Rheum 14: 119-122.

Newberry WN, Zukosky DK, Haut RC. (1997) Subfracture Insult to a Knee Joint Causes Alterations in the Bone and in the Functional Stiffness of Overlying Cartilage. J Orthop Res 15: 450-455.

Radin EL, Parker HG, Pugh JW, Steinberg RS, Paul IL, Rose RM. (1973) Response of Joints to Impact Loading III: Relationship Between Trabecular Microfractures and Cartilage Degradation. J Biomech 6: 51-57.

Radin EL, Martin RB, Burr DB, Caterson B, Boyd RD, Goodwin C. (1984) Effects if Mechanical Loading on the Tissues of the Rabbit Knee. J Orthop Res 2: 221-234.

Rasmussen PS. (1972) Tibial Condylar Fractures as a Cause of Degenerative Arthritis. Acta Orthop Scand 43: 566-575.

States JD. (1970) Traumatic arthritis- A Medical and Legal Dilemma. AAAM Proc 14: 21-28.

Thompson RC, Oegema TR, Lewis JL, Wallace L. (1991) Osteoarthritic Changes After Acute Transarticular Load: An Animal Model. J Bone Jt Surg 73-A: 1990-1001.

Viano DC. (1977) Considerations for a Femur Injury Criterion. Stapp Conf Proc 21: 445-473.

Viano DC. (1995) Restraint Effectiveness, Availability and Use in Fatal Crashes: Implications to Injury Control. J Trauma 38: 538-546.

Weaver BT. (2001) The Analysis of Tissue Response Following A Single Rigid Blunt Impact in an in vivo Animal Model: Regular Exercise is Beneficial in a Stable Joint After Trauma. MS Thesis: 33-50.

Wright V. (1990) Post-traumatic osteoarthritis- A medico-legal minefield. J Rheum 29: 474-478.

CONCLUSION

This thesis continues the efforts of the Orthopeadic Biomechanics Laboratory to understand mechanisms of osteoarthrosis and investigate methods of diagnosis, intervention, and prevention of this disease. Other investigators have shown that post-traumatic joint degradation is a significant problem in our society. However, the progression mechanisms are not very well understood, especially in cases with no gross fracture of bone.

Current automotive industry standards for crash tests of new vehicles require that femur load not exceed 10 kN. This injury criterion is based on gross bone fracture that was documented in human cadaver biomechanical experiments (Melvin et al. 1975, Patrick et al. 1965, Powell et al. 1975) similar to Chapter 1 in the current study. The purpose of doing experiments similar to previous studies is that one injury mechanism, which was suggested in those early, broad studies, may be isolated and investigated in higher detail. Another motivation is to look for additional occult injuries that may occur before gross bone fracture, but were not documented previously. These occult injuries such as cartilage fissures and microfractures of the underlying bone are thought to be precursors to chronic joint degradation. If a explicit correlation was revealed between these occult injuries and development of osteoarthritis then it would suggest that the automotive industry should reevaluate their injury criterion for one that could better protect passengers against this disease.

Chapter 2 documented that the patella is more vulnerable to fracture with a rigid interface when the knee was impacted obliquely versus axially with respect to the femur. Additionally, the orientation of the fracture pattern changed from a horizontal linear or

comminuted fracture for axial impacts to a vertical fracture across the patella for oblique impacts. In two cases of oblique impact on the knee the patella dislocated laterally prior to fracture. Since clinical studies often show an association of patella fractures and dislocations with the onset of chronic disease in the knee and a large portion of drivers have been shown to sit with their legs abducted, these patients appear to have increased long-term risk from oblique than axial impacts on the knee.

Chapter 3 documented that ACL rupture could occur in the human knee prior to gross bone fracture for axial tibia load when displacement between the tibia and femur is not constrained. Anterior and lateral displacements of the tibia with respect to the femur as well as internal rotation of the tibia were recorded at the time of ACL failure. Since the compressive loads in the tibia were in the range of what could be generated during a jump landing, this may be a mechanism in many "non-contact" ACL tears.

Chapter 4 documented that axial tibia load, similar to what was investigated in Chapter 3, has a stiffening effect on the response of the knee to anterior knee impacts. At subfracture level loads the translation between the tibia and femur and the patello-femoral contact force were reduced. At failure level loads it took a slightly higher anterior knee load to cause PCL trauma for knees with a simultaneous axial tibial load. This load increase was comparable to the load that was required to constrain TF motion in a previous study (Jayaraman et al. 2001). Since axial compressive loads in the tibia are documented in crash simulations at the same time and magnitude as anterior knee loads, the knee may actually have a stiffer response than previously thought.

Chapter 5 documented the short-term degenerative changes of a rabbit tibio-femoral joint to blunt impact. Histologically, chondrocyte clones and clusters were seen

in the medial articular cartilage of impacted knees by 12 weeks. There was also degeneration of the calcified cartilage layer and subchondral bone morphology in both medial and lateral sides. Additional studies are in progress for one-year post impact. These will better document the mechanics of chronic joint degradation leading up to an end-stage clinical disease of the joint.